

Politecnico di Torino



Tesi di Laurea Magistrale

Relatore: Dr. Andrea Mazza

Correlatori: prof. Ettore Bompard, prof. Enrico Pons, Dr. Abouzar Estebansari

Modelling of Lithium and flow batteries for micro-grid energy management

Candidato: Lorenzo Esteban de la Iglesia

Laurea Magistrale in Ingegneria Meccatronica

Master thesis summary in Spanish

Introducción

Las baterías representan una solución prometedora para integrar las fuentes de energía renovables como puede ser eólica y solar y cuyas instalaciones se han visto incrementadas en los últimos años. Su coste y eficiencia han ido mejorando convirtiéndolas en una tecnología accesible.

El siguiente TFM plantea dos modelos de batería: una de flujo de vanadio y otra de iones de litio. El objetivo es desarrollar un modelo termo-químico-eléctrico de ambas para poder simular con precisión su funcionamiento en tiempo real en una microgrid. Se pretende demostrar que gracias a esta tecnología se puede reducir el intercambio de energía entre esa microgrid y la red de distribución a través del punto común de acoplamiento.

La división del trabajo en capítulos es la siguiente:

- 1) Introducción explicando los principales puntos de esta tesis.
- 2) Una descripción de los distintos tipos de modelos de batería que existen entre los artículos especializados, las causas por las cuales algunos modelos son preferidos antes que otros, las diferentes variables que son de importancia y diferentes estructuras de estos modelos.
- 3) El desarrollo de un modelo de batería de flujo de vanadio. Esta es elegida tras comparar en un estudio previo diferentes modelos de este tipo de batería que aparecen en la literatura especializada. Tras lo cual se selecciona un modelo dividido en tres bloques claramente diferenciados:
 - i) La reacción electroquímica
 - ii) El balance de masa entre los tanques y el paquete de células
 - iii) El balance de energía entre los tanques, el entorno y el paquete de células.
- 4) El desarrollo de un modelo de batería de iones de litio. Al igual que con la batería de vanadio, esta es elegida tras un estudio y comparación de distintos modelos que aparecen en artículos académicos. Se desarrolla el modelo escogido, el cual está dividido en dos partes:
 - i) La reacción electroquímica, que está basada en un circuito equivalente
 - ii) El balance de energía
- 5) El caso de estudio de una microgrid es desarrollado con datos obtenidos de una zona residencial apoyada con generación fotovoltaica, unida por un punto de acople a una red de distribución.

- 6) La estrategia de control implementada para la batería, de manera que se reduzca el intercambio de energía desde la zona residencial hacia la red de distribución.
- 7) La integración de todas las partes explicadas y la puesta de resultados.
 - i) Primer caso: Se plantea el caso de estudio, junto a una batería de vanadio dimensionada para el caso propuesto, aplicando la estrategia de control planteada
 - ii) Segundo caso: Se plantea el caso de estudio, junto a una batería de iones de litio dimensionada para el caso propuesto, aplicando la estrategia de control planteada.
- 8) Finalmente, hay un último apartado con las conclusiones de este TFM y aspectos que podrían mejorarse de cara a futuros trabajos.

Tipos de modelos

El desarrollo de ambas baterías se ha realizado mediante un estudio previo de diferentes modelos descritos en artículos especializados. Los diferentes tipos de batería pueden clasificarse como **caja blanca** o **caja negra**.

En el caso de la caja blanca se busca mediante los distintos parámetros físicos de la batería tratar de modelarla. Todos estos parámetros que pueden ser viscosidad, concentración o temperatura, por ejemplo, explican de acuerdo a las leyes físicas el comportamiento de la batería y la evolución de sus distintas variables. El caso más costoso a nivel de computación sería un **modelo numérico**, que dividiría cada celda de la batería en porciones más pequeñas y calcularía en cada periodo la evolución de cada una de estas. Ejemplos de modelos numéricos son Lattice-Boltzmann o una versión simplificada como son los modelos de una sola partícula. Los **modelos analíticos** serían otro caso de modelo de caja blanca, en el cual se reduce el coste de computación, al tratar de quedarse con las variables principales que puede tener el modelo. Ejemplo de este tipo se puede encontrar en el trabajo Dynamic control strategy for the electrolyte flow rate in Vanadium redox.

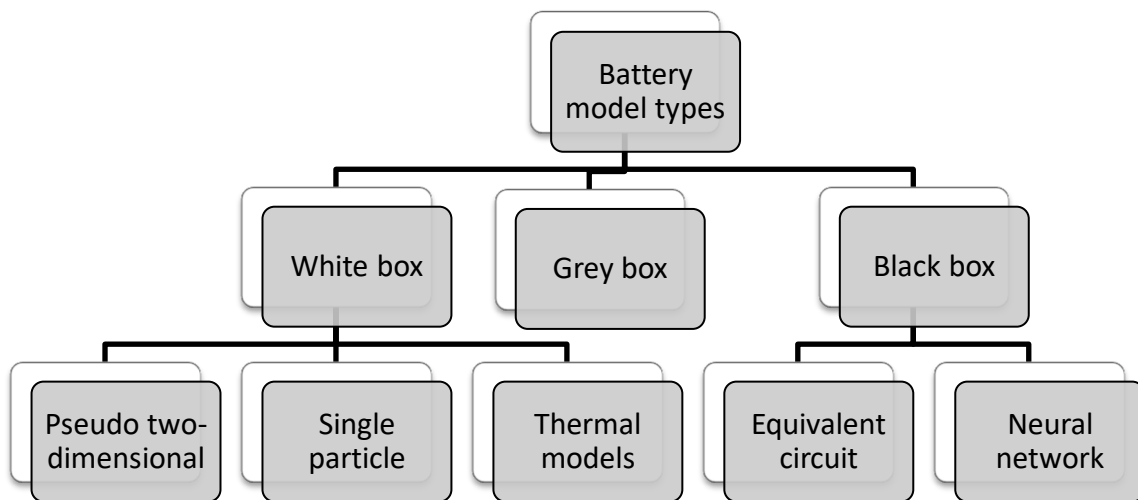
En el caso de la caja negra, la batería se modeliza a partir de datos experimentales, de tal forma que tras una muestra de las distintas entradas que pueda esta tener (es el caso de la corriente) y de las salidas que son respuesta de esas entradas (es el caso del voltaje de salida o del estado de carga) se busca identificar un sistema que se aproxime lo más fielmente posible a esos datos experimentales. El procedimiento para los modelos de caja negra, sería el siguiente:

1. Recopilación de datos de entrada y salida a partir de valores obtenidos en la realidad.
2. Elegir el tipo de estructura de modelo que más se pueda adecuar a las características del mismo.
3. Determinación de la complejidad que se requiera del modelo.
4. Ajuste de los parámetros del modelo de manera que las salidas se acerquen lo máximo posible.
5. Comprobación de la validez del modelo mediante datos de otro ensayo.

El ejemplo más conocido de caja negra es el **modelo de circuito equivalente**, en el cual se modeliza una corriente de entrada y un voltaje de salida mediante los valores que adquieren un circuito RC cuya complejidad puede variar desde un primer orden hasta circuitos de varios órdenes.

Existen otros modelos con estructuras más complejas, por ejemplo, basados en **redes neuronales**. No tienen tano desarrollo debido a su complejidad.

Por último se ha de indicar que los modelos más detallados suelen ser combinaciones de diferentes modelos. Estos **modelos grises** explican diferentes variables utilizando para cada una el modelo que reporte unas mejores características. Así, por ejemplo, es frecuente utilizar un modelo de circuito equivalente para explicar el comportamiento electroquímico y un modelo analítico para calcular la temperatura.



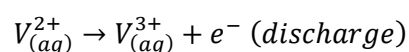
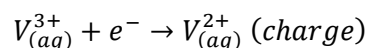
Batería de vanadio

Descripción

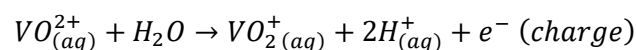
Las baterías de flujo de vanadio son un tipo de batería conocidas por su bajo mantenimiento y alta expectativa de vida. Su principal diferencia con otros tipos de baterías es que contiene dos electrolitos diferentes realizados con vanadio, un elemento común en la Tierra.

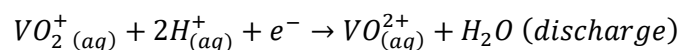
Es una batería de flujo, lo que significa que reaccionan dos electrólitos, separados por una membrana. La batería de vanadio, además, se caracteriza por utilizar el mismo elemento metálico en ambos electrolitos, utilizando diferentes valencias (+2, +3, +4, +5). La reacción REDOX, se puede representar por las reacciones siguientes:

Subreacciones del electrodo negativo

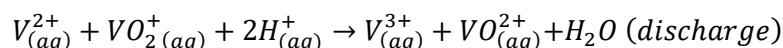
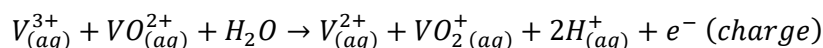


Subreacciones del electrodo positivo





Reacción total que se produce



La principal ventaja que se obtiene al utilizar el mismo elemento en ambos electrolitos reside en que esta no envejece y no pierde capacidad de almacenar energía ante cualquier posible mezcla que pueda darse entre ambos cuando los electrolitos atraviesan accidentalmente la membrana que los separa. Gracias a la estructura de este tipo de baterías, es muy fácil desacoplar potencia (proporcional al número de células) y capacidad de almacenamiento (proporcional al volumen almacenado en los tanques).

Esta batería funciona gracias a bombas que permiten el transporte del material reactivo entre los tanques en donde se almacena y los paquetes de células que es donde se llevan a cabo las correspondientes reacciones. Sus diferentes partes se resumen en las siguientes:

Tanques: Su función es almacenar ambos electrolitos. Una mitad de ellos almacenaran los iones de valencia +5 y +6, mientras que la otra mitad almacena los iones de valencia +3 y +4.

Células: Está dividida en dos medias partes mediante una membrana. Cada una de estas partes interactúa con uno de los electrolitos que contiene. Aunque la membrana mantenga separados ambos electrolitos, permite la difusión de iones H⁺ y con ello la reacción REDOX. Dentro de cada media celda se encuentra un material poroso que actúa como electrodo y es en donde se produce la reacción.

Las células acostumbran a encontrarse unidas entre ellas formando paquetes. Esto permite lograr una gran flexibilidad para obtener diferentes voltajes y potencias nominales.

Sistema de tuberías: Conectan tanques y células. Suelen estar hechas, al igual que los tanques de materiales polímeros, para evitar su corrosión.

Bombas: Funcionan gracias a motores eléctricos y permiten mover los electrolitos entre tanques y células.

Es un candidato prometedor a ser el futuro sistema de grandes cantidades de energía. Entre sus ventajas se puede citar:

*Alta eficiencia energética.

*Largo ciclo de vida.

*No se producen pérdidas de capacidad al mezclarse los electrodos.

*Flexibilidad a la hora de cambiar los requisitos de potencia y capacidad.

*Fácil mantenimiento.

Por el contrario plantea los siguientes problemas:

*Es más complejo que las baterías convencionales

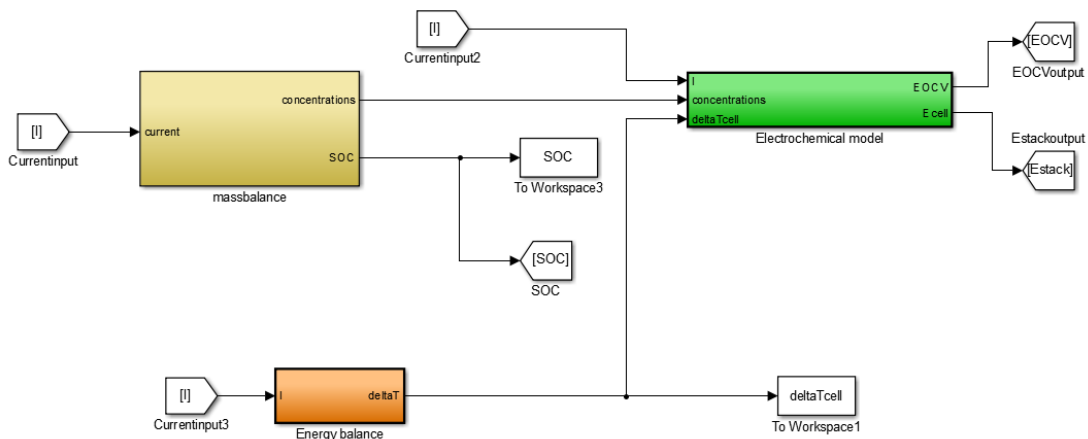
*La inclusión de un sistema hidráulico implica pérdidas de rendimiento.

*Tiene muy baja densidad de energía.

Desarrollo del modelo

Se ha realizado un estudio de los distintos tipos de modelos de esta batería que han sido encontrados en diferentes artículos especializados, seleccionando aquel que se ha considerado más adecuado a nuestro campo de aplicación. Se ha procedido a su desarrollo mediante Matlab Simulink. Este modelo se divide en tres partes claramente diferenciadas:

- i) La reacción electroquímica (en verde) que calcula el voltaje de salida del paquete de células. Utiliza la ecuación de Nernst y un pequeño circuito equivalente.
- ii) El balance de masas (en beis) que computa las diferentes concentraciones de las diferentes especies de vanadio en las distintas partes de la batería.
- iii) El balance energético (en naranja) que realiza dos funciones. En una primera parte, se calcularía el calor generado dentro de las células y en una segunda parte se calcularía la variación de temperatura tanto en el paquete de células como en los tanques de almacenamiento.



Posteriormente, se añade un último bloque cuya es dimensionar tanto la batería como las pérdidas de potencia en el convertidor electrónico, que esta pueda tener y que se incluyen en el modelo.

Con el modelo ya terminado se realizan dos simulaciones. Una de carga de la batería y otra de descarga de esta con el objetivo de observar cómo evolucionan las distintas variables del modelo realizado. Estas variables son comparadas con variables que aparecen en otras baterías en la literatura especializada para comprobar si existen desviaciones significativas.

Batería de iones de litio

El litio es el material con la mayor proyección dentro del almacenamiento de energía. Su uso es bien conocido tanto en la pequeña electrónica de consumo como en el vehículo eléctrico. También existen aplicaciones dentro del consumo eléctrico de gran escala en redes de distribución.

Su producción aparece esquematizada en la figura de abajo y puede representarse como una larga cadena que va desde la extracción de sus materias primas hasta la fabricación del producto final. Abarca diferentes tipos de industria como son la minería, la industria orgánica, la industria inorgánica, la industria metalúrgica, la industria de polímeros o la industria electrónica encargada del BMS (unidad de gestión de la batería).



Como puede observarse, diferentes tipos de compañías trabajan en la producción de esta batería, como puede ser Tesla, que abarca una amplia parte de esta cadena u otras empresas más pequeñas, encargadas de alguno de los procesos más específicos.

En cuanto a la localización geográfica de su industria, cabe destacar que con la excepción de compañías norteamericanas como Tesla, se encuentran principalmente empresas asiáticas (Japón, Corea del Sur y China) como pueden ser Panasonic, GS Yuasa, LG Chem, Samsung, Kokam, BYD Company o ATL.

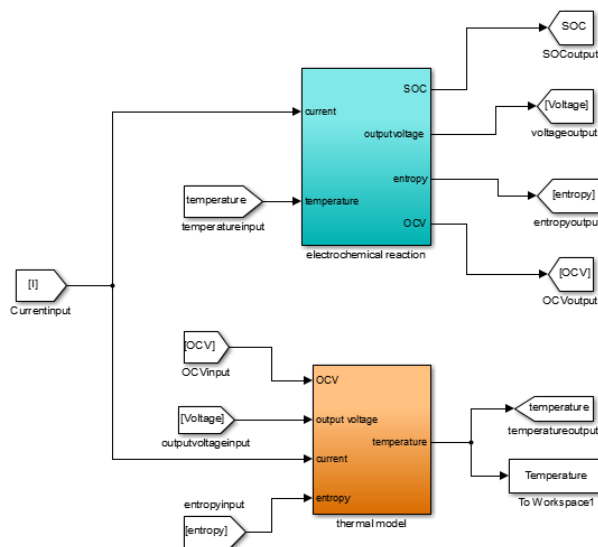
Esta batería aparece en un amplio espectro de aplicaciones, algunas de ellas emergentes en los últimos años. Su principal mercado viene por parte de ordenadores portátiles y de teléfonos inteligentes, aunque el transporte por carretera empieza a aparecer como uno de sus usos principales. Tiene su aplicación en el sector aeroespacial dentro de satélites y en la aviación. Es utilizado en el almacenamiento de energía en redes eléctricas. Tiene su mercado dentro de la industria médica, debido a la madurez de su industria, pues ofrecen propiedades como la robustez su reducido tamaño o su alta densidad de energía, útiles en aplicaciones que van desde audífonos hasta sensores de los niveles de glucosa.

Su uso para almacenamiento de energía en redes, se encuentra limitado por los costes de esta tecnología. Mientras estos sean superiores a 0.15€/kWh. No es competitivo en aplicaciones conectadas a red. A partir de 0.10€/kWh empiezan a aparecer casos de aplicación, almacenando energía en redes con gran diferencia en el precio de la energía para el usuario final. No obstante se debe indicar que su posible implementación para almacenamiento energético de gran escala se ve amenazado por la fuerte competencia que realizan otros tipos de baterías, como es el caso de la batería de vanadio, que aunque posean menor capacidad de almacenamiento de energía específica o

requieran de más apoyo y mantenimiento, sus costes parecen decantarse más a favor de este segundo tipo en grandes sistemas de almacenamiento eléctrico.

Se ha realizado un estudio de los distintos tipos de modelos de esta batería que han sido encontrados en diferentes artículos especializados, seleccionando aquel que se ha considerado más adecuado a nuestro campo de aplicación. Se ha procedido a su desarrollo mediante Matlab Simulink. Este modelo se divide en dos partes claramente diferenciadas:

- i) La reacción electroquímica (en azul), que calcula el voltaje de salida a partir del voltaje en circuito abierto y un modelo de circuito equivalente formado por un circuito eléctrico de primer orden.
- ii) El balance energético (en naranja) que tiene un diseño más sencillo que su homólogo en la batería de vanadio. Se resume en un balance de energías que entran y salen en forma de calor y la capacitancia térmica de cada una de las celdas que conforman la batería.



Se incluye, además, un capítulo en el que se dimensiona tanto la batería como las pérdidas de potencia que esta pueda tener y que se incluyen en el modelo.

Se desarrollan los modelos en el entorno de Matlab Simulink y se procede a una simulación de prueba, viendo la evolución de sus variables tras una carga y descarga completa realizada con potencia nominal. El objetivo de observar cómo evolucionan las distintas variables del modelo realizado. Estas variables son comparadas con variables que aparecen en otras baterías en la literatura especializada para comprobar si existen desviaciones significativas.

Caso de estudio

Se propone un caso de estudio formado por una microgrid que abastece de energía a una zona residencial. Se plantea el caso más sencillo posible, que consiste en un nodo, un pequeño grupo de casas que realizan un determinado consumo, una planta de generación solar capaz de compensar

en los dos meses en que los generadores fotovoltaicos producen menos energía eléctrica, por lo que parece que los generadores fotovoltaicos también están bien adaptados a los requisitos de la microgrid.

Es posible ver que las dos baterías pueden contribuir a reducir el consumo de energía que cruza el punto de acoplamiento común. La capacidad de alimentación de ambos se ha elegido para una batería que puede almacenar solo los requisitos de alimentación de un día completo porque es lo que se ha considerado como una buena compensación entre el tamaño y el soporte de energía. Los resultados de ambas baterías se presentan a continuación:

i) La caja de la batería de vanadio-redox tiene un flujo de potencia de 18,52 MWh. De la red de distribución a la microgrid y un flujo inverso de 2,23 MWh. Significa que la energía requerida de la microgrid es menos de la mitad de la que necesitaría si esa batería no existiera. Es importante mencionar que esta batería tiene algunos requisitos de potencia operativa (bombas de potencia) que podrían aumentar los sistemas de pérdidas si no están bien adaptados a los requisitos de la aplicación.

ii) La caja de la batería de ion litio tiene 13,73 MWh. del flujo de energía de la red de distribución a la microgrid y un flujo de energía inverso de 5,10 MWh. Significa una reducción de potencia del 75%. Esa batería también tiene una eficiencia mejor que la de vanadio.

Futuros trabajos

Ha sido un arduo trabajo de casi un año hacer este MFT, por lo que se ha considerado interesante poner énfasis en algunas de las dificultades que se han encontrado trabajando en él, por lo que si alguien continúa trabajando en el futuro, algo relacionado podría saber qué problemas Debería tener que enfrentarse. Aquí se presentan algunos de ellos:

Modelo de batería vanadio-redox: una de las principales ventajas de este tipo de batería es que se refrigera al mover sus electrolitos. No tiene sentido poner tanto esfuerzo en los balances de energía como se ha hecho en ese trabajo y no poner nada en la gestión de bombas que contribuye tanto a la eficiencia y las variaciones de voltaje de esa batería como a la temperatura por sí sola. Es una batería que parece difícil de modelar porque requiere algo más que un circuito equivalente.

Modelo de batería de iones de litio: hay muchos tipos diferentes de iones de litio y esa batería tiene una diferencia principal en comparación con el vanadio, que es que la potencia y la capacidad no se pueden desacoplar, lo que significa que el caso de la aplicación debe conocerse antes de elegir una precisa Modelo para no sobre dimensionado una de estas características de la batería. La curva de voltaje de histéresis podría ser interesante incluir para ajustar algunas pérdidas de energía que tiene la batería.

Estudio de caso: se ha incluido un diagrama de fasores del transformador. Parece que complica el modelo, mientras que la única variable importante son las pérdidas de potencia del transformador que podrían obtenerse con la resistencia nominal del mismo.

Simulaciones: para que los trabajos futuros se centren más en los aspectos eficientes de esa batería que en las dinámicas de tiempo que este modelo ha elegido. Las simulaciones de estudios de caso cubren dos meses con un segundo paso de tiempo. Algunas variables cambian en períodos de segundos como es el caso de OCV y algunas variables toman períodos de minutos u horas; Este es el caso del SOC. Es importante saber en cuál de estas variables se debe poner el enfoque de este trabajo. Si el efecto de los transitorios sobre el voltaje y las otras variables no son interesantes, es posible que los pasos de tiempo de un minuto se consideren aceptables y más fáciles de modelar.

Nomenclature

Vanadium flow battery

A	<i>A matrix of Linear Time Invariant System utilized in mass balance</i>
B	<i>B matrix of Linear Time Invariant System utilized in mass balance</i>
E^0	<i>Reference voltage</i>
E_{OCV}	<i>Open circuit voltage</i>
C_{ped}	<i>Specific heat of electrolyte</i>
c_{H^+}	<i>Protons concentration</i>
c	<i>Vector that represents concentration states</i>
c_{acell}	<i>Concentration of active species inside cell</i>
c_{atank}	<i>Concentration of reactive species inside tank</i>
c_{rcell}	<i>Concentration of reactive species inside cell</i>
c_{rtank}	<i>Concentration of reactive species inside tank</i>
$c_{V(V)}$	<i>Concentration of V^{5+}</i>
$c_{V(III)}$	<i>Concentration of V^{3+}</i>
$c_{V(IV)}$	<i>Concentration of V^{4+}</i>
$c_{V(II)}$	<i>Concentration of V^{2+}</i>
d_f	<i>Effective surface of electrode</i>
F	<i>Faraday constant</i>
H_{tank}	<i>Coefficient of heat transfer between tank and environment</i>
I	<i>Current</i>
k	<i>Permeability of porous electrode</i>
K	<i>Kozeny-Carman constant</i>
L	<i>Cell length</i>
M	<i>Number of cells that are part of the stack</i>
q	<i>step position</i>

\dot{q}_f	<i>Pressure losses</i>
q_{total}	<i>Total power losses</i>
\dot{q}_{losses}	<i>Resistive power losses</i>
q_r	<i>Reversible heat</i>
Q	<i>Electrolyte flow</i>
R	<i>Inert gas constant</i>
R_{eq}	<i>Equivalent resistance</i>
t	<i>time</i>
t_s	<i>time step</i>
T	<i>Temperature</i>
V_{cell}	<i>Cell volume</i>
V_{out}	<i>Cell voltage output</i>
ε	<i>Porosity coefficient</i>
Δp_{drop}	<i>Pressure drop inside cell</i>
ΔS_r^0	<i>Standard reaction entropy variation</i>
ΔT_{tanks}	<i>Temperature difference between tank and environment</i>
ΔT_{stack}	<i>Temperature difference between stack and environment</i>
P	<i>Electrolyte density</i>
μ	<i>Viscosity</i>

Lithium-ion battery

C	<i>Capacitor capacitance</i>
$\frac{dV}{dt}$	<i>Entropy variation</i>
E_{OCV}	<i>Open circuit voltage</i>
E	<i>Activation energy of R</i>
E_{ct}	<i>Activation energy of Rct</i>

hA	<i>Heat transfer coefficient of each single cell</i>
I	<i>Cell current</i>
MCp	<i>Heat capacitance of single cell</i>
q	<i>step position</i>
$\dot{q}_{exchange}$	<i>Heat exchanged between a cell and the environment</i>
\dot{q}_{losses}	<i>Cell resistive losses</i>
\dot{q}_r	<i>Reversible heat generation</i>
Q_{max}	<i>Cell capacity</i>
R	<i>Resistance value</i>
R_0	<i>Resistance value reference</i>
R_{Ct}	<i>Parallel resistance value</i>
R_{ct0}	<i>Resistance value reference</i>
R_g	<i>Inert gas constant</i>
t	<i>time</i>
t_s	<i>time step</i>
T	<i>Cell surface temperature</i>
T_A	<i>Environment temperature</i>
V_{out}	<i>Voltage output</i>
V_1	<i>Capacitor voltage</i>
x	<i>State of charge position</i>

Microgrid

I_N	<i>Nominal current of distribution transformer</i>
I	<i>Effective value of current that crosses transformer</i>
P_{distr}	<i>Power that enters in the distribution grid</i>
P_N	<i>Nominal power of distribution transformer</i>
P_{req}	<i>Powerflow that enters in the microgrid</i>

Q	<i>Reactive power injection in transformer</i>
R_n	<i>Distribution transformer resistance</i>
V_{\cosmic}	<i>Microgrid voltage projection over distribution grid voltage</i>
V_L	<i>Line voltage of distribution grid</i>
$V_{\text{microgrid}}$	<i>Voltage microgrid</i>
V_{\sinmic}	<i>Voltage perpendicular projection over distribution grid voltage</i>
X_n	<i>Distribution transformer impedance</i>
Z_{pu}	<i>Impedance expressed in pu units</i>
Z_n	<i>Distribution transformer total impedance</i>
$\alpha_{\text{microgrid}}$	<i>Angle difference between distribution grid and microgrid voltages</i>

Index of figures

- Figure 1: Equivalent circuit first order model [7]4
- Figure 2: Third order equivalent circuit of a Lithium-ion battery [8].....4
- Figure 3: Diagram representation of different battery models.....6
- Figure 4: Schematic representation of a Vanadium flow battery [11].10
- Figure 5: Vanadium battery block with its three subsystems14
- Figure 6: Electrochemical reaction subsystem block15
- Figure 7: Nernst equation part in electrochemical reaction block16
- Figure 8: Equivalent circuit utilized in VRB model16
- Figure 9: Block representation of equivalent circuit17
- Figure 10: Mass balance subsystem block divided into parts18
- Figure 11: Mass balance LTI system block18
- Figure 12: Concentration bus of stack Vanadium species20
- Figure 13: Blocks utilized to calculate SOC.....21
- Figure 14: Energy balance subsystem blocks21
- Figure 15: Heat generation subsystem block22
- Figure 16: Block that represents pump power heat generation23
- Figure 17: Electrochemical dissipative losses.....24
- Figure 18: LTI system that represents energy balance25
- Figure 19: Ratio between inverter power losses and inverter nominal power.....27
- Figure 20: electronic converter and pump losses block28
- Figure 21: Heat generation of Vanadium stack while it is charging29
- Figure 22: State of charge variation while Vanadium stack is charging.....30
- Figure 23: Grid power and stack power while Vanadium battery is charging30
- Figure 24: Vanadium temperature variation during a charge.....31
- Figure 25: Vanadium stack concentrations during a charge operation31
- Figure 26: OCV and voltage stack compared during charge operation32
- Figure 27: SOC of Vanadium battery under discharge operation33
- Figure 28: Battery power and grid power under a discharge condition.33
- Figure 29: OCV and stack voltage comparative under a discharge condition in Vanadium battery34
- Figure 30: Vanadium battery model species concentration under a discharge situation34
- Figure 31: Stack and tanks temperature variations under a discharge operation conditions35
- Figure 32: Heat generation of the Vanadium stack under discharge conditions35
- Figure 33: Lithium-ion schematic representation [16]37
- Figure 34: Lithium-ion industry [17]38
- Figure 35: Lithium-ion cell subsystem representation42
- Figure 36: electrochemical reaction subsystem block43
- Figure 37: Equivalent circuit schematic representation [19]44
- Figure 38: Different parts of equivalent circuit model of Lithium-ion battery.....45
- Figure 39: Subsystem block that computes OCV values in Lithium-ion model.....45
- Figure 40: Internal structure of Figure 39 block46
- Figure 41: Graphic representation of OCV as a variable SOC dependant as in (30)46
- Figure 42: Lithium-ion LiFePO4 entropy as a function SOC dependant (31).....47

Figure 43: Function Block of $R(T, x)$. Figure 44: Function Block of $R_{ct}(T, x)$.	47
Figure 45: V1 block representation in Lithium-ion battery model	48
Figure 46: Vout sum block in Lithium-ion battery model	48
Figure 47: SOC block integrator in Lithium-ion battery model.	49
Figure 48: Thermal balance block representation in Lithium-ion battery model	50
Figure 49: Thermal balance subsystem of Lithium-ion. Energy balances are marked.	51
Figure 50: Convection exchange with the environment in Lithium-ion.	51
Figure 51: Electrochemical dissipative losses in Lithium-ion equation (39) (39).	52
Figure 52: Reversible heat equation (40).	52
Figure 53: Heat sum and temperature integrator in Lithium-ion (37).	53
Figure 54: Battery, inverter and microgrid distribution [20].	55
Figure 55: Ratio between power dissipation inside the inverter and power movement between the battery and the microgrid [20]	55
Figure 56: A subsystem block that gives dimensions to the rack and include inverter dissipation losses	56
Figure 57: OCV and voltage output of each cell of Lithium-ion model while it is discharging.	57
Figure 58: SOC variation in lithium-ion battery while it is charging	58
Figure 59: Surface temperature variation while Lithium-ion battery is discharging.	58
Figure 60: Heat generation by the battery while it is discharging.	59
Figure 61: Resistance value variance while Lithium-ion battery is discharging	59
Figure 62: Power generated by the battery and power absorb by the microgrid while it is discharging	60
Figure 63: Cell current of Lithium-ion while it is discharging	60
Figure 64: Cell OCV and output voltage while Lithium-ion is charging	61
Figure 65: SOC variation while Lithium-ion rack is charging	62
Figure 66: Heat generation while charging Lithium-ion battery	62
Figure 67: Resistance values variation during charging process	63
Figure 68: battery power generated by the battery and power absorb by the grid	63
Figure 69: Cell current during Lithium-ion charge	64
Figure 70: Temperature variation on Lithium-ion cell	64
Figure 71: Single line diagram with microgrid elements (designed with AutoCad)	67
Figure 72: Catalogue of small distribution transformers of ABB [21]	67
Figure 73: Distribution transformer equivalent circuit (designed with AutoCad).	68
Figure 74: Example of one day power demand.	69
Figure 75: Power microgrid requirements on these two months.	70
Figure 76: Power consumption of these two months divided in levels of power demand.	70
Figure 77: Phasor diagram of current and voltages in CCP	71
Figure 78: Current, microgrid voltage components and power consumed calculated from power that is demand from the microgrid side.	72
Figure 79: Subsystem that computes power flow across distribution transformer.	73
Figure 80: Power management strategy of UpNa [22].	74
Figure 81: Simple Average Power requirements that is used as power reference by the control strategy	75
Figure 82: Power reference subsystem control block	76
Figure 83: Current regulator	76

Figure 84: Security margins in current regulator.....	77
Figure 85: Current regulator closed loop	78
Figure 86: Control + battery model validation	79
Figure 87: Power levels required in three different scenarios. Without battery, with vanadium one and with lithium-ion.	80
Figura 88: Power required using the control strategy selected and power required by the residential load and PV generators.....	81
Figure 89: Power flow between microgrid and distribution grid in Vanadium battery case in January the first.....	81
Figure 90: Voltage value of microgrid node in Vanadium flow case on January the 9 th	82
Figure 91: Angle difference between microgrid node and distribution node in rad in Vanadium case in January the 9 th	83
Figure 92: Battery power injection in Vanadium case on January the 9 th	84
Figure 93: Heat generation in Vanadium case on January the 9 th	84
Figure 94: Temperature variation in Vanadium case on January the 9 th	85
Figure 95: SOC variation on Vanadium case on January the 9 th	85
Figure 96: Stack and tank concentrations in Vanadium case on January the 9 th	86
Figure 97: OCV and output voltage comparative in Vanadium case on January the 9 th	86
Figure 98: Cell voltage in Lithium-ion on January the 9 th	87
Figure 99: SOC for Lithium-ion on January the 9 th	88
Figure 100: Power flow in Lithium-ion on January the 9 th	88
Figure 101: Heat generation in Lithium-ion on January the 9 th	89
Figure 102: Temperature variation in Lithium-ion on January the 9 th	90
Figure 103: Battery power generation in Lithium-ion on January the 9 th	90
Figure 104: MIcrogrid node voltage in Lithium-ion on January the 9 th	91
Figure 105: Voltage angle phase in microgrid node in Lithium-ion on January the 9 th	91

Index of tables

Table 1: Different types of battery models7
Table 2: Comparative of different VRB models12
Table 3: VRF battery model validation.....36
Table 4: Lithium-ion stack distribution explained54
Table 5: Validation of Lithium-ion cell65
Table 6: Power reference limits calculated in Figure 84.77

Index of contents

Master thesis summary in Spanish	iii
Nomenclature.....	xiii
Vanadium flow battery	xiii
Lithium-ion battery	xiv
Microgrid	xv
Index of figures.....	xvii
Index of tables	xx
1. Introduction.....	1
2. Battery model types.....	3
2.1. Introduction	3
2.2. White box models.....	3
Numerical	3
Analytical.....	3
2.3. Black box models.....	4
2.4. Grey models.....	5
2.5. Characteristics of different models	6
3. Vanadium-redox battery model.....	8
3.1. Main characteristics	8
3.2. Comparative of different Vanadium redox flow battery models.....	12
3.3. Vanadium battery model development	14
3.3.1. Description	14
3.3.2. Electrochemical reaction.....	15
3.3.3. Mass balance	18
3.3.4. Thermal model	21
3.3.5. Sizing Vanadium battery model.....	26
3.4. Results of the model.....	29
3.4.1. Charge operation	29
3.4.2. Discharge operation.....	32
3.5. Vanadium battery model validation.....	36
4. Lithium-ion battery models	37
4.1. Lithium-ion battery description	37
4.2. Different Lithium-ion comparative models	40

4.3. Lithium-ion model	41
4.3.1. Cell description	41
4.3.2. Electrochemical reaction.....	43
4.3.3. Thermal model	50
4.3.4. Integration of all the cell stacks.....	54
4.4. Results of Lithium-ion model	57
4.4.1. Discharge of a Lithium-ion cell	57
4.4.2. Charge of a Lithium-ion cell.....	60
4.5. Validation of the model	65
5. Case study.....	66
5.1. Description	66
5.2. Distribution transformer.....	67
5.3. Dynamic load and PV generator.....	68
5.5. PCC voltage and power flow	71
6. Control strategy	74
6.1. Power control strategy	74
6.2. Current regulator.....	76
7. Simulation and results.....	79
7.1. Simulation description	79
7.2. Results in Vanadium-flow battery simulation.....	80
7.3. Results in Lithium-ion battery simulation	87
Conclusions and future works	92
Bibliography.....	94

1. Introduction

Batteries represent a promising solution that can help to integrate renewable resources as wind and solar energy whose installations have been increased in recent years. Their electrical efficiency and costs have been improved making it a relievable technology.

This document will study two different types of batteries: a lithium-ion battery and a vanadium redox battery working in a micro-grid case study. It shows how these two batteries can reduce the power exchange at the Point of Common Coupling (PCC) between the microgrid and the main grid.

It is structured in the following chapters:

- 1) An introduction explaining the main topics of that thesis.
- 2) A description of the different types of battery models that exist in literature, the reasons why some models are developed, the different types of models, the different variables and different model structures.
- 3) A Vanadium redox flow battery model development. This chapter is divided in a research of different models developed in academic papers. An electrochemical thermal cell model is selected and it is divided into three points:
 - i) Electrochemical reaction.
 - ii) Mass balance between tanks and stack.
 - iii) Energy balance.

This model is tested in a full charge and discharge simulation and validated through comparing the ones speeding with other different Vanadium battery models found in literature.

- 4) A lithium-ion LiFePO₄ cell model development. It is also dimensioned and divided into two points:
 - i) Electrochemical reaction that is based on equivalent circuit model.
 - ii) Energy balance to supervise temperature fluctuations.

Those results are compared with the other models as it has been made for the Vanadium battery.

- 5) A micro-grid case study development based on data taken from a single node connected to a residential load and a renewable photovoltaic energy source.
- 6) A control strategy that could help to reduce reverse power flow in PCC.
- 7) An integration of all the elements explained showing results:
 - i) First case: Single node connected to grid, a dynamic load and the battery model developed for Vanadium with its control strategy.
 - ii) Second case: Single node connected to grid, a dynamic load and the battery model developed for Lithium-ion with its control strategy.

Introduction

- 8) Finally, there is a chapter of conclusions that tries to synthetized what could be improved and explains the results.

If anything on that TFM requires clarification, I include my e-mail:

loren.1994@hotmail.com

2. Battery model types

2.1. Introduction

There are three balances that appeared inside every battery that explained all physical phenomena.

- **Conservation of fluid flow and mass transport:** species that are inside electrolyte can only move by convection and mass dissipation effects.
- **Electrochemical reaction:** It is related with all physical phenomena that take part in chemical reaction.
- **Conservation of Energy:** It is related with energy dissipation phenomena that appear in that battery, how that heat generated moves inside battery and how it affects to temperature.

2.2. White box models

These models are calculated using exclusively the physical knowledge of batteries. Physical phenomena are described by equations that could be more or less detailed depending on the purpose. Their behavior is possible to explain knowing materials parameters as viscosity, conductivity, diffusion and others. These kinds of models could be divided into numerical models and parametrical models.

Numerical

Cells are divided into small portions and all the variables (temperature, species concentrations) of every block are updated based on electrochemical, thermal and mass equations in every time step.

Vanadium redox flow battery numerical models try to explain dynamics employing methods such as Lattice-Boltzmann and Stack level [1].

For Lithium-ion battery pseudo 2-dimension models [2] and single particle models [3] are employed. Those methods simplify the model to allow the computation in real time applications. There are some simplified models that are mixes between these two [3].

Analytical

This type of model reduce quite enough the complexity by using the most important variables such as state of charge (SOC) and open circuit voltage (OCV). Kinetic Battery Model [4] is an example of this type of model.

Another example of analytical model is presented in Dynamic control strategy for the electrolyte flow Vanadium redox [5]. It assumes some good simplifications (concentration and temperature is uniform inside tank, as example) and divides battery in its different balances.

2.3. Black box models

Black box models or Box-Jenkins models only take into account input and output variables and do not require any physical variable. They work around system identification techniques based on [6]:

1. Collection of the data set.
2. Choosing of the model set or the model structure, so that is suitable for the aims.
3. Determination of the suitable complexity level of the model.
4. Tuning of the parameters to pick the best model in the set, guided by the data.
5. Performing a model validation test.

Equivalent circuit model

A popular choice is the equivalent circuit model because it can simplify the model using a RC electrical model. Battery dynamics could easily be explained with a first (Figure 1), second or even a greater order electrical circuit (Figure 2).

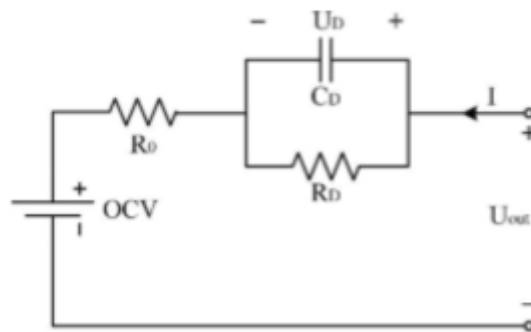


Figure 1: Equivalent circuit first order model [7]

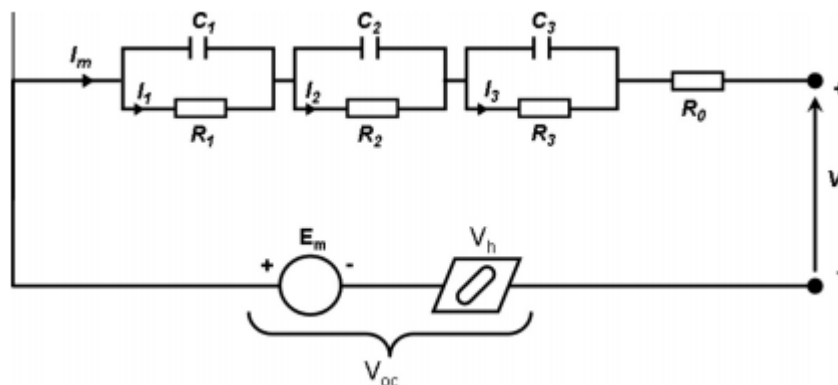


Figure 2: Third order equivalent circuit of a Lithium-ion battery [8]

Capacitors are used to explain polarization effects and resistors represent internal resistances of the battery.

Specialized literature explains that this model has as main disadvantage that it does not explain capacity loss and age battery effects [9]. Difficulties of that model are related with some non-linear relations that it does not explain.

An important variable in that model is the open circuit voltage (OCV) that is a value related with SOC and temperature through Nernst equation. It represents the voltage that battery would have under no load conditions. Values of the equivalent element of the electrochemical circuit are obtained using system identification methods that are easier and well known to model different electrical components that explain battery behavior.

Other black box models that use neural networks have problems on estimations that are due complexity of the relations that makes it difficult to train [10].

In conclusion, black box models could use RC elements that have a linear behavior and they give a simple and easy to compute but accurate approach. They give an answer to polarization effects and dynamics that happen inside battery. Black box models are chosen for system identification methods to avoid cost-computing numerical differential equations and battery elements properties. These models are considered accurate complemented with some electrochemical variables. They could work with accuracy if combines a good measurement of non-linear variables as OCV.

2.4. Grey models

This family collects the models that have parts based on physical world knowledge and parts that are made by system identification methods. They combine models explained in white box models and black box models chapters. A good example is a battery model that combines an equivalent circuit model and a thermal model. Equivalent circuit model could explain ion diffusion and electrochemical effects and thermal model could be constructed by knowledge of physical variables such as cell surface and heat coefficient.

2.5. Characteristics of different models

All the previous models are classified in Figure 4. A table with the different types of models and its advantages and disadvantages is included in Table 1.

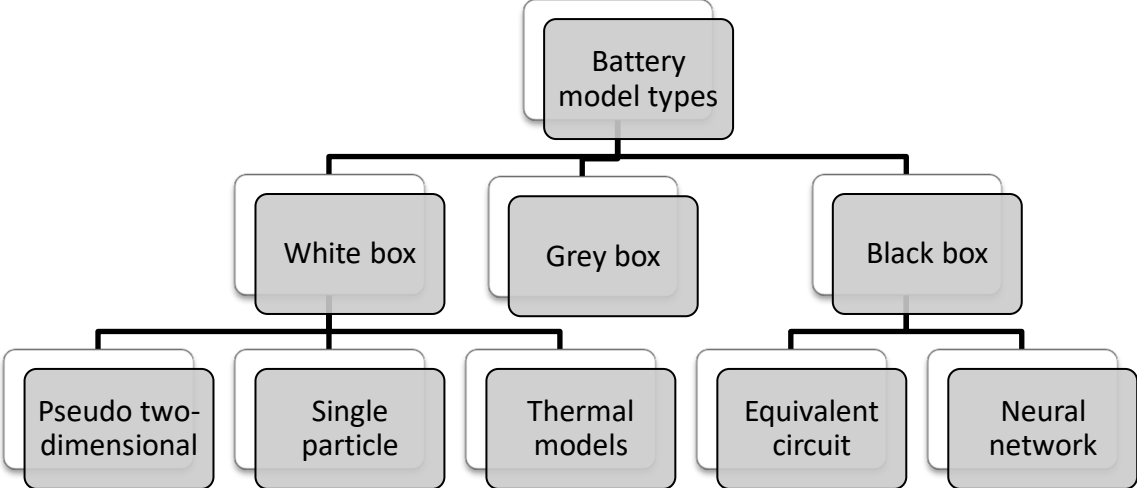


Figure 3: Diagram representation of different battery models

Table 1: Different types of battery models

Model	Type	Advantages	Disadvantages	Description
Equivalent circuit based	Black box	Easy to compute	Battery use and age could make that model inaccurate	A 1 or 2 order RC electrical circuit model that explains polarization effects and OCV
Neural Network	Black box	Once model is obtained is easy to compute.	Use and age could make that model inaccurate. It could be hard to train if battery dynamics are complex.	A trained Neural Network that tries to explained battery dynamics
Pseudo two-dimensional	White box	A detailed and accurate model	Hard to compute for real time operations	It includes mass transport and chemical kinetics to provide a detailed model
Single particle	White box	Accurate model in most of the situations that could occur.	It is inappropriate under large discharge currents	It is a simpler electrochemical model than pseudo 2 dimensional one.
Thermal	White box	It provide details related	It is a model that should be complemented with other one	Based on heat transfer equations
Simplified	White box	Some different mixes of different models and methods looking for an intermediate approach between pseudo two-dimensional accuracy and single particle easier computes.	It could be complex to improve. It could be quite cost computing.	Polynomial profile Transfer function Residual grouping

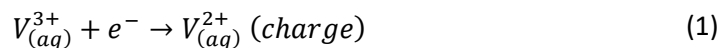
3. Vanadium-redox battery model

3.1. Main characteristics

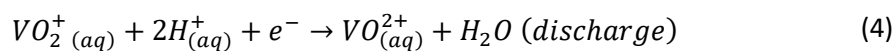
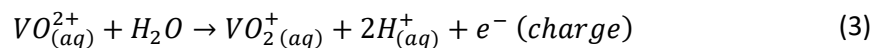
Vanadium redox flow battery is a type of technology that is known for low maintenance costs and high life performance. Its main difference with other types of batteries is that is made with two electrolytes of vanadium, a common Earth element.

It is a flow battery, a battery type made with two different electrolytes. It uses the same element in both redox reactions. Vanadium is famous for a great number of valence states (+2, +3, +4, +5). The REDOX reaction is these equations. Equations (1) and (2) represent the negative subreactions in negative electrode. Equations (3) and (4) represent the positive subreactions that occur in positive electrode. Finally, equations (5) and (6) represent the overall reaction.

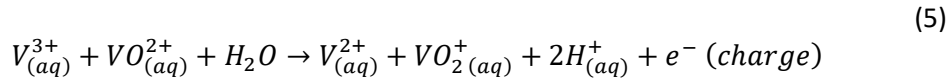
Negative electrode reaction



Positive electrode reaction



Overall reaction



One of the advantages of using the same element in both sides is that there are no capacity losses when electrolytes are mixed and that allows high life expectancy.

Reactions happen in cells that are communicated with the tanks by pipelines. Electrolytes are moved in a close circuit from the tanks where they are stored to the cells and vice versa. Its main components are:

Tanks: They storage two different electrolytes separated.

Cells: Every cell is divided into two half parts by a membrane. Each of these half parts includes one of the electrolytes that this battery has. They both are separated by a membrane that allows H⁺ ion diffusion but it doesn't lend electrolytes mixes. Each of those half cells includes a porous electrode where the reactions of (1), (2), (3) and (4) happen.

Cells used to be clustered in stacks to improve performance. That gives a lot of flexibility to obtain different voltage and power values.

Pipelines: Tubes that connects tanks with cells.

Pumps: It is moved by an electrical motor that moves electrolyte between tanks and cells.

Tanks and cells are separated elements so capacity and power are decoupled properties of that battery and can be easily modified in case of future demand changes. Any secondary reaction that occurs could be removed easily changing electrolyte solutions.

Vanadium battery model

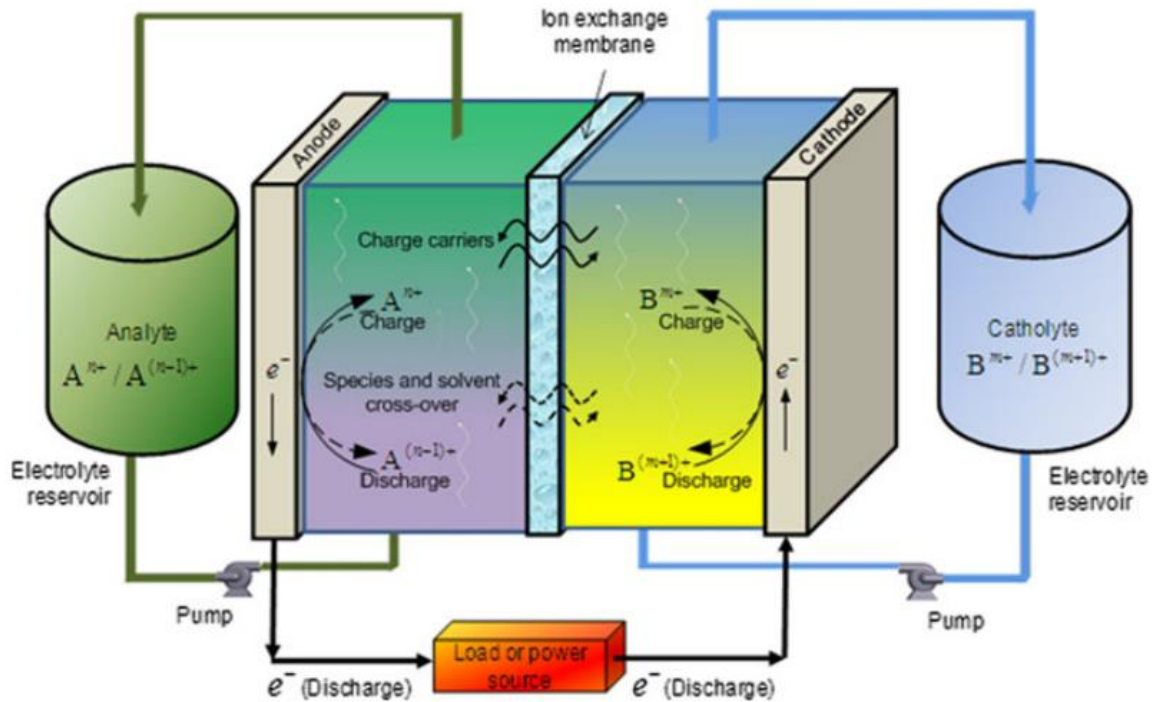


Figure 4: Schematic representation of a Vanadium flow battery [11].

Advantages

Flow vanadium battery is a promising candidate as future large energy storage system because of its multiple advantages:

- High energy efficiencies
- Long cycle life
- No capacity losses when electrolyte is mixed
- Flexibility for varying power and energy requirements (modular design)
- Simple electrolyte maintenance
- Readily available raw material

Disadvantages

On the other side, these are the main problems that this battery faces:

- It is more complex than conventional batteries.
- Its hydraulic system includes energy losses on it.
- It has low energy density.

3.2. Comparative of different Vanadium redox flow battery models

Table 2: Comparative of different VRB models

Name	Model type	Advantages	Disadvantages	Description
Thermal modelling and simulation of the all-vanadium redox flow battery [12]	Thermal-model	Easy to compute Simple	It only includes a thermal model. It needs a block for electrochemical reaction. It assumes simplifications as uniform stack temperature.	Three temperature states with their thermal dynamic equation
Fundamental models for flow batteries [1]	Electrochemical models	Really detailed models that explains by numerical methods different concentrations in each part of the battery	Many equations to compute. They are not practical at real time simulations. It requires some simplifications.	On Lattice Boltzmann method Molecular dynamics and density function simulations Stack level network model
Online monitoring of SOC and capacity loss for vanadium redox flow battery based on autoregressive exogenous modeling [9]	Equivalent circuit model	Accurate for Real-time applications. Easy to compute. It includes loss of capacitance. Adaptive control that corrects age changes.	It doesn't include temperature as a variable. It needs time to be initialized if state of battery is unknown.	A VRB model that try to estimate SOC and loss capacitance. It uses a RLS algorithm to estimate any change that could be
State of charge estimation of Vanadium redox flow battery based on sliding mode observer and dynamic model including capacity fading factor [13]	Equivalent circuit model	It includes all states variables: SOC, polarization, temperature and capacity loss. It works under non-linearity conditions.	It needs to include chattering effect. A fast observer will have chat a slow observer will not convergence in time to the desired value.	It includes changes states as temperature and battery age. A complete example is presented.

<p>Dynamic control strategy for the electrolyte flow rate of vanadium redox flow batteries [5]</p>	<p>Electrochemical model and a thermal model</p>	<p>It includes the three balances explained. A detailed model.</p>	<p>It concludes that is recommended to add side reactions and some improve on transient behavior.</p>	<p>It contains a thermal model and a flow model. It takes into account overpotentials using formulas</p>
---	--	--	---	--

3.3. Vanadium battery model development

3.3.1. Description

It is used a Vanadium battery model based on that scientific paper [5] of a laboratory experimental battery. It consists of a pair 900 l. tanks contain their own electrolytes solutions. The stacks are made by 25 Vanadium cells which have a 1.08 l. capacity and it is where reaction occurs. It is nominal power is 0.2 kWh per each cell and its storage capacity of 31.65 kWh.

As it is said, there are three different balances that appeared in the selected model, so the model is made by three blocks clearly identified, one for each of the different parts that battery is divided:

- i) Electrochemical reaction
- ii) Mass balance
- iii) Thermal balance.

Figure 5 represents the Vanadium battery model divided into three points marked previously.

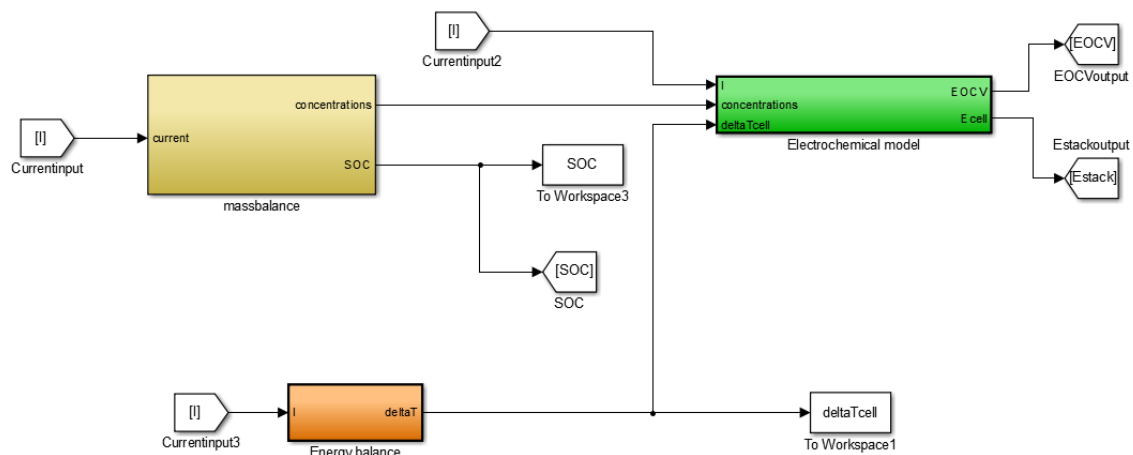


Figure 5: Vanadium battery block with its three subsystems

3.3.2. Electrochemical reaction

It is a subsystem block that computes stack output voltage. It has as input current, cell concentrations of vanadium valences and temperature. It calculates OCV by Nernst equations and output voltage by an equivalent circuit. Figure 6 represents subsystem block parts.

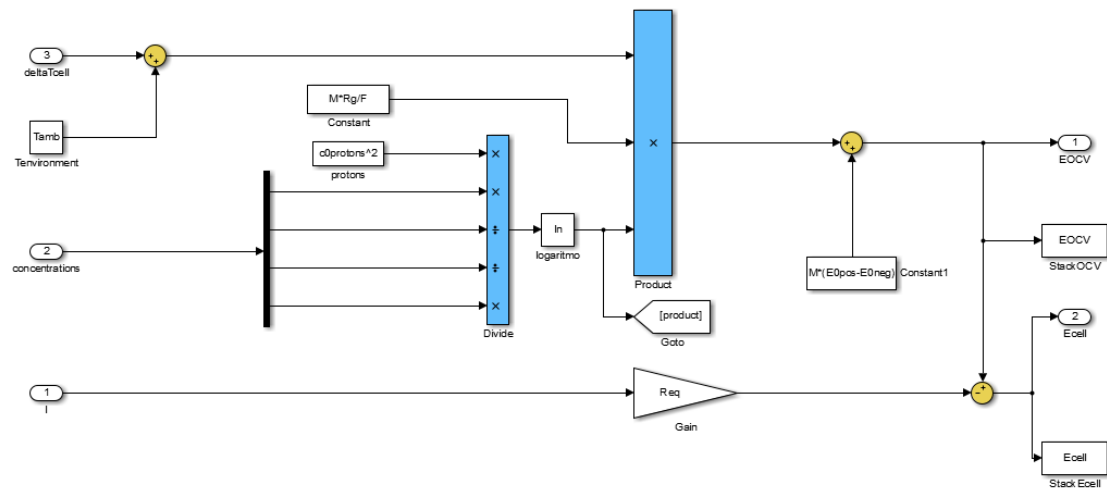


Figure 6: Electrochemical reaction subsystem block

Nernst equation

Nernst equation calculates OCV based on electrolytes composition and temperature. Equation (7) calculates OCV E_{OCV} where E^0 represents standard cell potential, R represents inert gas constant, T represents temperature, F represents Faraday constant, c_{H^+} represents proton concentration in both electrolytes and $c_{V(V)}$, $c_{V(III)}$, $c_{V(IV)}$, $c_{V(III)}$ represents molar concentration of the different vanadium species that are inside battery cell.

$$E_{OCV} = E^0 + \frac{RT}{F} \ln \left(\frac{c_{V(V)} c_{V(III)} c_{H^+}^2}{c_{V(IV)} c_{V(III)}} \right) \quad (7)$$

Figure 7 shows Nernst equation blocks representation. Inputs are temperature, current and concentration bus from mass balance block. It calculates OCV based on previous equation.

Vanadium battery model

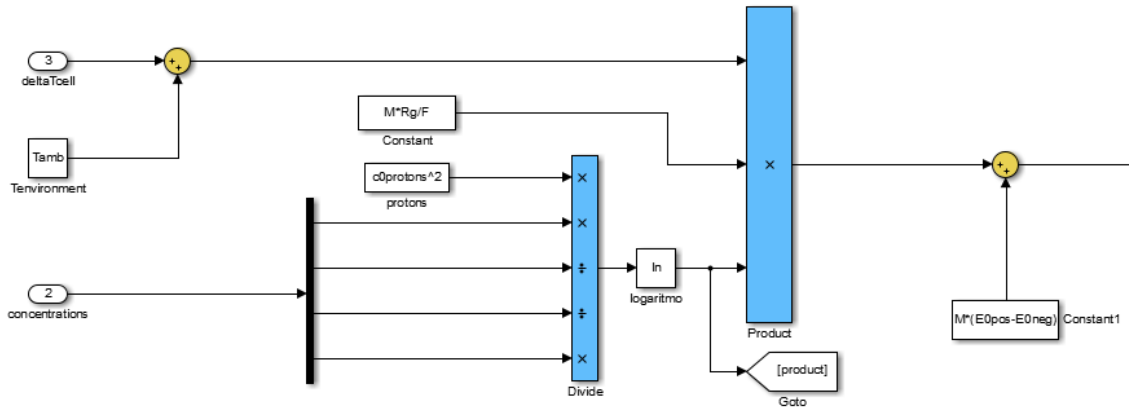


Figure 7: Nernst equation part in electrochemical reaction block

Equivalent circuit

All electrochemical power losses are considered as a resistance as in [12]. That R represents ohmic losses than Vanadium cell has and over voltages that could be produce by concentration or activation.

More complicated works as [5] and [14] considered that flow and vanadium concentration could affect the losses so they tried at finding an optimum point.

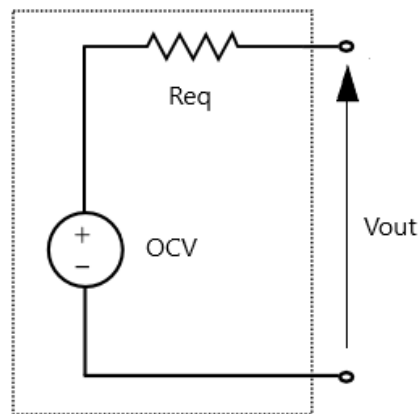


Figure 8: Equivalent circuit utilized in VRB model

Figure 8 represents the equivalent circuit model. It is an equivalent circuit made by open circuit voltage E_{OCV} , an equivalent resistance R_{eq} and a current I . Equation (8) represents it.

$$V_{out} = E_{OCV} - IR_{eq} \quad (8)$$

Figure 9 sums $-IR_{eq}$ and E_{OCV} to obtain V_{out} .

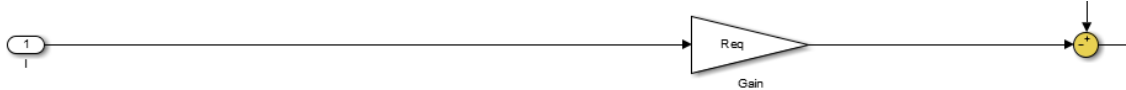


Figure 9: Block representation of equivalent circuit

3.3.3. Mass balance

There is a continuous flow that moves between tanks and the stack. The input is real time current value which affects cell concentrations. The outputs are real time concentrations of the different Vanadium species. It is considered that electrolyte flow that moves from tanks to battery is constant and it is not optimized. As it is explained above, some works like [14] and [5] try to find an optimal electrolyte flow that minimized loses. Figure 10 represents all the different elements that are inside mass balance block. **Orange square** marks a discrete system that computes mass balance. **Purple square** marks signals that let us calculate Nernst equation in electrochemical model. **Blue square** let us calculate SOC, knowing Vanadium concentrations of tanks and cells.

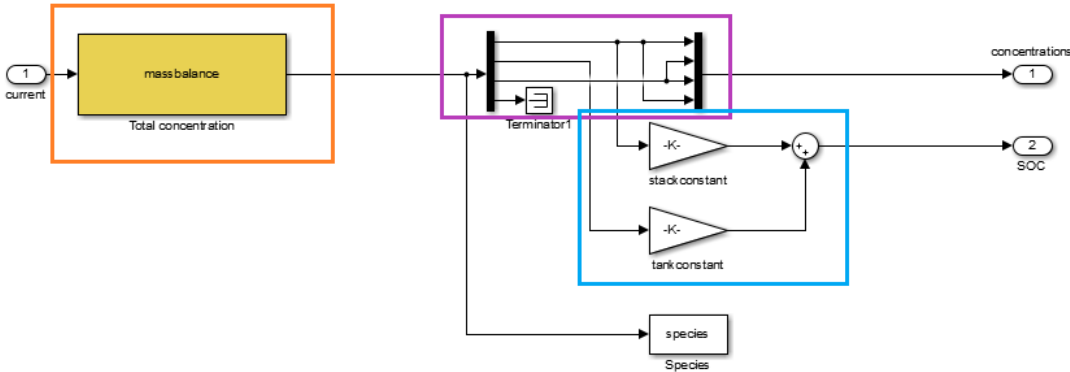


Figure 10: Mass balance subsystem block divided into parts

Total concentration

It is a discrete time invariant system that tries to represent flow equation and tank and stack concentrations in every time step. A linear time invariant block (LTI) is used and it is marked on Figure 11.

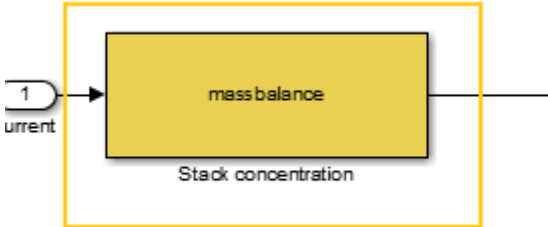


Figure 11: Mass balance LTI system block

There are two mass balances for each vanadium species. They are represented on that two equations where $c_{xcell}(t)$ is cell concentration of vanadium specie x , $c_{xtank}(t)$ is tank concentration of a vanadium specie, Q is the actual flow and it is considered constant in the case, M is the number of cell that compose the stack, V_{cell} is the volume of a battery cell, F is the Faraday constant and $I(t)$ is cell current.

i) Cells balance [5] that appears on equation (9)

$$\frac{dc_{xcell}(t)}{dt} = -\frac{Q}{M V_{cell}} c_{xcell}(t) + \frac{Q}{M V_{cell}} c_{xtank}(t) \pm \frac{I(t)}{F V_{cell}} \quad (9)$$

ii) Tanks balance [5] that appears on equation (10)

$$\frac{dc_{xtank}(t)}{dt} = \frac{Q}{V_{tank}} c_{xcell}(t) - \frac{Q}{V_{tank}} c_{xtank}(t) \quad (10)$$

It is assumed that Vn^{5+} concentration in one electrolyte is going to be the same Vn^{2+} concentration than in the other electrolyte. Vn^{4+} concentration in first electrolyte is going to be the same than Vn^{3+} concentration in second electrolyte. That means that 4 states which explain all battery concentrations are required:

- Cell concentrations of active species c_{acell}
- Tank concentration of active species c_{atank}
- Cell concentrations of reactive species c_{rcell}
- Tank concentration of reactive species c_{rtank}

All of these states have been grouped making a vector \mathbf{c} represented on equation (11).

$$\mathbf{c}(q) = \begin{pmatrix} c_{acell} \\ c_{atank} \\ c_{rcell} \\ c_{rtank} \end{pmatrix} (q) \quad (11)$$

Knowing that, it is possible to create a discrete steady state time invariant system like equation (12) where cell current is represented.

$$\mathbf{c}(q + 1) = \mathbf{A}\mathbf{c}(q) + \mathbf{B}I(q) \quad (12)$$

Where Q is flow, t_s is step time, M is the number of cells on the stack, V_{cell} is cell volume, V_{tank} is tank volume and F is Faraday constant.

Vanadium battery model

A is represented on equation (13):

$$\mathbf{A} = \begin{pmatrix} 1 - \frac{Qts}{MV_{cell}} & \frac{Qts}{MV_{cell}} & 0 & 0 \\ \frac{Qts}{V_{tank}} & 1 - \frac{Qts}{V_{tank}} & 0 & 0 \\ 0 & 0 & 1 - \frac{Qts}{MV_{cell}} & \frac{Qts}{MV_{cell}} \\ 0 & 0 & \frac{Qts}{V_{tank}} & 1 - \frac{Qts}{V_{tank}} \end{pmatrix} \quad (13)$$

And **B** is that 1x4 vector represented on equation (14).

$$\mathbf{B} = \begin{pmatrix} \frac{ts}{FV_{cell}} \\ 0 \\ -\frac{ts}{FV_{cell}} \\ 0 \end{pmatrix} \quad (14)$$

Nernst equation concentrations

Purple square signals that appears on Figure 12 represent a vector of concentrations that allows us to calculate OCV in electrochemical reaction block.

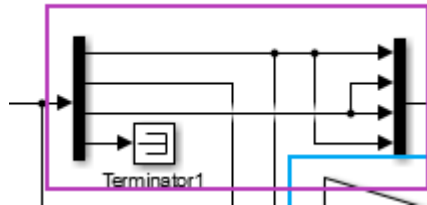


Figure 12: Concentration bus of stack Vanadium species

SOC calculation

It is a simple calculation based on stack concentrations and cell concentrations. Equation (15) calculated SOC as a coefficient between total quantities of active species divided by the maximum quantity that it is possible to have. V_{tank} is tank volume, M is the number of cells in the stack, V_{cell} is the cell volume of a battery cell, $c_{V(V)_{tank}}$ is the tank concentration of vanadium (5+), $c_{V(V)_{cell}}$ is the cell concentration of vanadium (5+), $c_{V(V)_{max}}$ is the maximum possible concentration of vanadium (5+) in the battery.

$$SOC = \frac{V_{tank}c_{V(V)_{tank}}}{c_{V(V)_{max}}(V_{tank} + MV_{cell})} + \frac{MV_{cell}c_{V(V)_{cell}}}{c_{V(V)_{max}}(V_{tank} + MV_{cell})} \quad (15)$$

Figure 13 shows blocks that can calculate SOC of Vanadium battery model with the knowledge of Vanadium concentrations in tanks and cells.

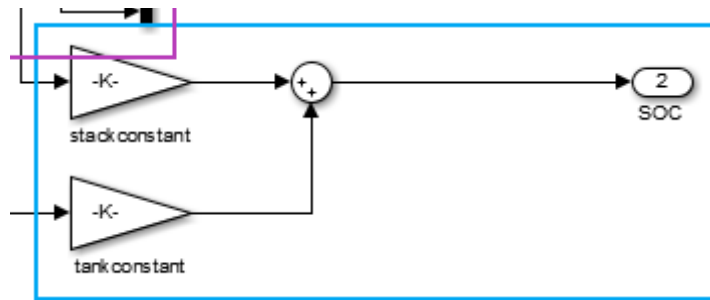


Figure 13: Blocks utilized to calculate SOC

3.3.4. Thermal model

It has two different blocks.

- i) Orange block, called heat generation, computes all the different heat sources that the battery has.
- ii) Yellow block, called temperature states, calculates energy exchanges between environment, tanks and stack.

Energy balance subsystem block is represented in Figure 14. Thermal balance subsystem block. Orange block calculates heat generation inside that battery, yellow block is a LTI system that computes temperature states.

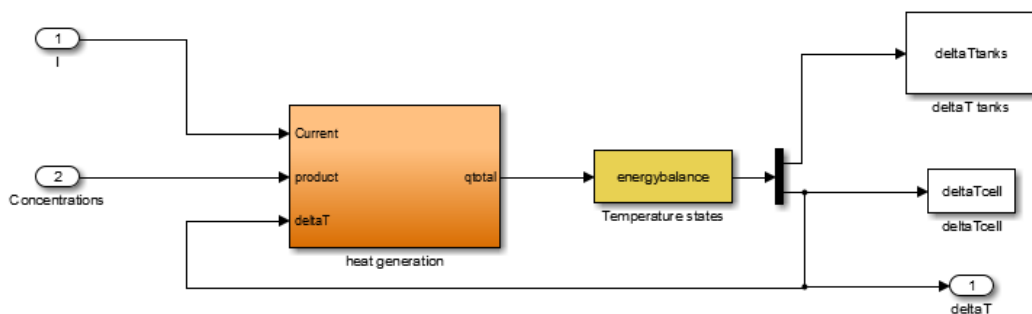


Figure 14: Energy balance subsystem blocks

Heat generation

Stack is considered as the only heat source because it is where reaction and drop pressure appears. Figure 15 shows what is inside the heat generation model. These are the 3 thermal sources that the battery has:

- i) Pump pressure drop
- ii) Electrochemical power dissipative losses
- iii) Reversible heat generation due entropy variation

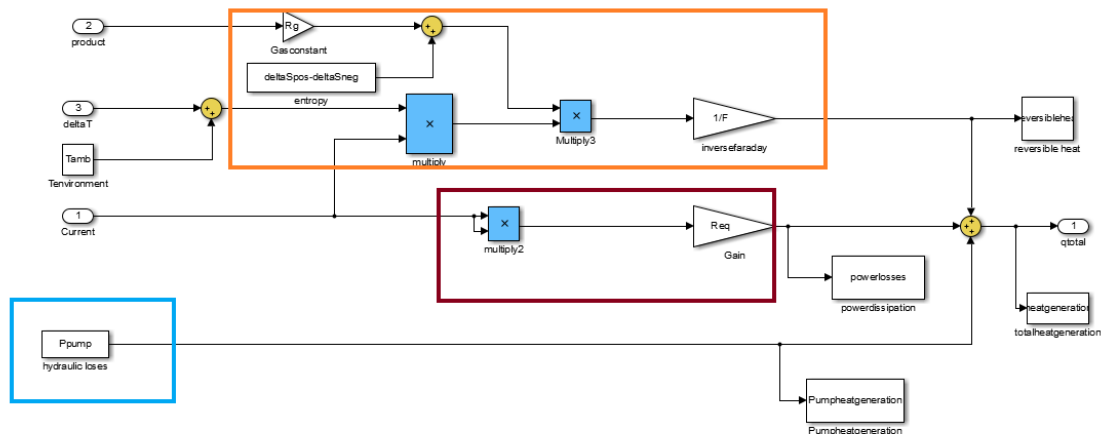


Figure 15: Heat generation subsystem block

Pump

It is considered that this battery is always working in the same point. That is 0.2L/s. Pump is considered to have an 85% efficiency power conversion. Pressure drop is calculated based on those articles [5] [14]. There are two causes of pressure drop:

- Pipelines friction: That could be considered negligible compared to electrode friction.
- Cell electrode friction: That is governed by Fick's law that explains how pressure drops in a porous material and it is calculated as it is shown in next formula.

Pressure dissipation losses have been considered as heat exchange

Figure 16 shows a constant value that is used as power pump losses.

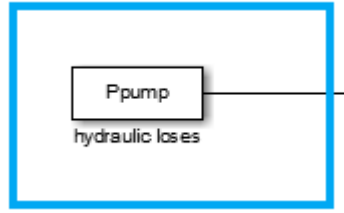


Figure 16: Block that represents pump power heat generation

Pressure drop calculation

These losses are due dissipation of the electrolyte flowing by the porous material. It is considered that it is not possible to regulate pump point of work. Most of scientific publications considered that an optimal work point is possible to obtain and try to work as near as possible. This value could be calculated based on equation (16) where μ is electrolyte viscosity, L is porous region length, Q is electrolyte flow, k is the permeability of the porous electrode

$$\Delta p_{drop} = \frac{\mu L Q}{k A} \quad (16)$$

The permeability of the porous electrode can be calculated as where d_f is the effective surface of electrode, ε is the porosity of electrode, K is Kozeny-Carman constant, a value that depends on electrode material. k is calculated on equation (17).

$$k = \frac{d_f^2 \varepsilon^2}{16 K (1 - \varepsilon)^2} \quad (17)$$

Total power dissipation \dot{q}_f is calculated on equation (18) where Q is electrolyte flow, Δp_{drop} is pressure drop inside electrode material:

$$\dot{q}_f = 2\Delta p_{drop} Q \quad (18)$$

This value has been contrasted with [12] and [14] values and it feels reasonable.

Electrical dissipative losses

Losses produced by overvoltage and ohmic losses. It is represented by resistive losses of equivalent circuit. \dot{q}_{losses} are the dissipative losses explained on equation (19) where I is cell current and R_{eq} are equivalent resistive losses. Its Simulink representation is Figure 17.

$$\dot{q}_{losses} = R_{eq}I^2 \quad (19)$$



Figure 17: Electrochemical dissipative losses

Reversible heat

Reversible heat \dot{q}_r is due entropy variation inside our cell. There are two main sources of heat in a battery, while irreversible heat transfer represents effects as ohmic losses or ion polarization, reversible heat represents heat exchange that is due entropy variations in reaction processes. Reversible means that the quantity of energy generated in reaction advance is equivalent to the absorb energy in a reaction advance with opposite sign. Explain by that equation (20) where T is cell temperature, z is 1 and represents how much the reaction advances, F is Faraday constant, $c_{V(V)}$, $c_{V(III)}$, $c_{V(IV)}$, $c_{V(III)}$ are the different vanadium species concentrations inside stack, R is inert gas constant, ΔS_r^0 is standard entropy reaction variation and c_{H^+} is protons concentrations:

$$\dot{q}_r = \frac{IT}{zF} \times \left[\Delta S_r^0 + R \times \ln \left(\frac{c_{V(V)}c_{V(III)}c_{H^+}^2}{c_{V(IV)}c_{V(III)}} \right) \right] \quad (20)$$

Thermal balance

It is considered similar to mass balance. There is a continuous flow from tanks to the stack. It is considered that tanks are refrigerated by natural convection and temperature is considered uniform inside of them. Stack heat transfer is by forced convection due electrolyte flow that is continuously pumped. Heat transfer that occurs in pipelines is considered negligible. Figure 18 shows a LTI system is build using as states tank temperature and stack temperature.

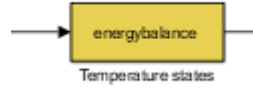


Figure 18: LTI system that represents energy balance

Thermal balance can be explained with two differential equations (21) and (22) that explain two thermal states [12] that are tank temperature and stack temperature. Q is electrolyte flow, H_{tank} is coefficient of heat transfer between environment and tank, V_{tank} is tank volume, ρ is electrolyte density Cp_{ed} is specific heat of electrolyte, M is the number of cells inside a stack, V_{cell} is the volume of each cell and ΔT_{tanks} and ΔT_{stack} are temperature differences between tanks and stack with the environment respectively.

$$\frac{dT_{tanks}(t)}{dt} = \left(-\frac{Q}{V_{tank}} - \frac{H_{tank}}{V_{tank}} \right) \Delta T_{tanks}(t) + \frac{Q}{V_{tank}} \Delta T_{stack}(t) \quad (21)$$

$$\frac{dT_{stack}(t)}{dt} = \frac{2Q}{V_{tank}} \Delta T_{tanks}(t) - \frac{2Q}{V_{tank}} \Delta T_{stack}(t) + \frac{q_{total}(t)}{M V_{cell} \rho C p_{ed}} \quad (22)$$

Equations (21) and (22) are discretized to obtain a linear time invariant system that allows computing temperature at each time step. That discrete equation is (23).

$$\begin{pmatrix} \Delta T_{tanks} \\ \Delta T_{stacks} \end{pmatrix} (t+1) = \begin{pmatrix} 1 - \frac{Q ts}{V_{tank}} - \frac{H_{tank} ts}{V_{tank} \rho C p_{ed}} & \frac{Q ts}{V_{tank}} \\ \frac{2 Q ts}{M V_{cell}} & 1 - \frac{2 Q ts}{M V_{cell}} \end{pmatrix} \begin{pmatrix} \Delta T_{tanks} \\ \Delta T_{stacks} \end{pmatrix} (t) + \begin{pmatrix} 0 \\ \frac{ts}{M V_{cell} \rho C p_{ed}} \end{pmatrix} q_{total}(t) \quad (23)$$

Equation (23) can be introduced inside a LTI system Simulink block, it is low cost computing and it can calculate temperature in each step.

3.3.5. Sizing Vanadium battery model

3.4.5.1. Rack dimensions

As it is explained, vanadium battery can decouple power and energy requirements. Knowing results of case study (chapter 5), it is assumed 1000 kWh capacity and 250 kW power requirements. Each cell, as it is explained in conclusions of article based [5] has a current of 160 A. and 1.25 V. as nominal voltage difference between electrodes. Two stack of 625 cells each allows having 250kW of nominal power as calculated on (24).

$$160A * 1.25V * 1250 = 250 kW \quad (24)$$

Total energy storage is possible to calculate knowing vanadium concentration on each electrolyte and total volume of each tank. The total amount of electrons that crosses from one tank to the other while battery is charging depends from those two parameters. It is calculated on equation (25). The energy storage inside 40 pair of vanadium tanks of 1000 l. with 1.5 mol/l. is:

$$\frac{40000 * (0.85 - 0.15) * 1.25 * F * 1.5}{3600 * 1000} = 1405.83 kWh \quad (25)$$

Battery requirements could be satisfied with the dimensions given in that chapter. Those are the sizes given to that:

- I) Two battery stacks that are divided in 625 cells each.
- II) 40 pair of Vanadium tanks of 1000 l. 1.5 mol/l. each.

Each one of the stack has a nominal voltage of 781.25 V, a nominal current of 160 A. and a nominal power of 250 kW. (24). Total energy storage inside that battery is 1405 kWh (25).

3.4.5.2. Power electronics

Inverter is explained in Lithium-ion chapter. Basically, what is necessary to know is power efficiency of a commercial inverter that calculates energy losses in that element. It is utilized the same ratio between battery nominal power and inverter power losses that in Lithium-ion battery case Figure 19.

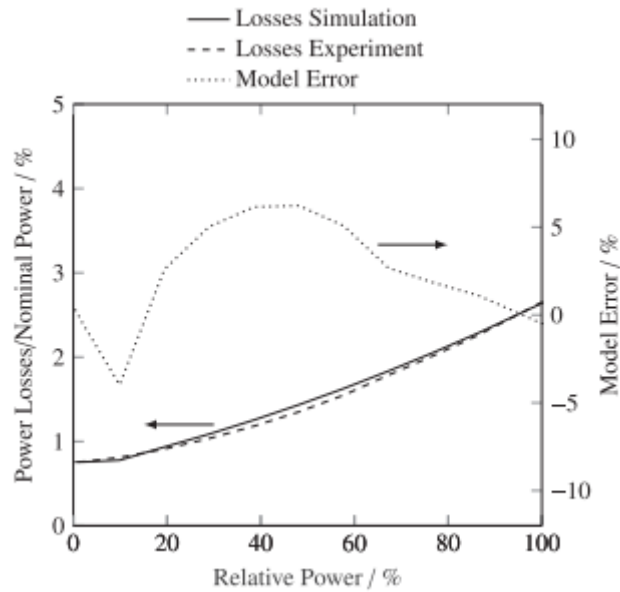


Figure 19: Ratio between inverter power losses and inverter nominal power

3.4.5.3. Vanadium battery power electronic and pump losses block

It is a subsystem that calculates battery equipment losses, divided into two points:

- i) It calculates power pump losses
- ii) It extracts inverter power losses

Power pump is extracted including its 0.85 typical efficiency. It is utilized the graph on Figure 19 that relates nominal power and inverter losses. Subsystem is represented in Figure 20.

Vanadium battery model

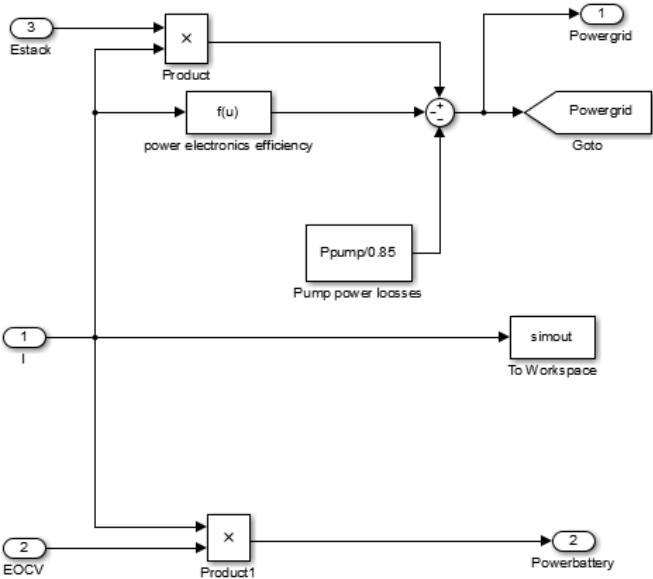


Figure 20: electronic converter and pump losses block

3.4. Results of the model

Experimental results of Vanadium are shown in two different scenarios:

i) Charge operation:

That stack is charging at a constant power rate of 250 kW. From a 0.15 SOC initial condition to 0.85 SOC condition in which that battery stop charging. Variables like temperature, heat generation, OCV and stack concentrations are represented.

ii) Discharge operation:

That stack is discharging at a constant power rate of 250 kW. From a 0.85 SOC initial condition to 0.15 SOC condition in which that battery stop charging. Variables like temperature, heat generation, OCV and stack concentrations are represented.

3.4.1. Charge operation

That simulation shows a 250 kW battery charge. It takes around 25000 seconds that means a period of time around 7 hours. Most significant variables have graphical representations.

Figure 21 represents heat generation decoupled into its different sources that are reversible heat, electrical losses and pressure losses in porous material.

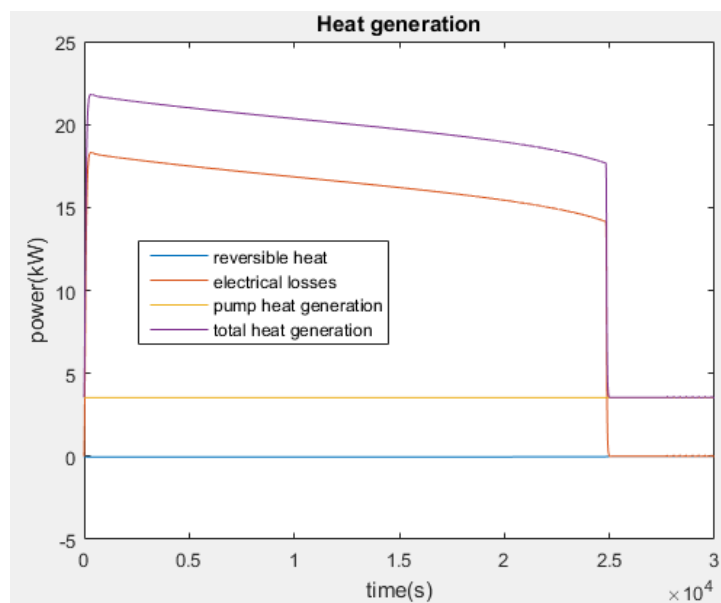


Figure 21: Heat generation of Vanadium stack while it is charging

Figure 22 represents state of charge variation that has a ramp shape and grows continuously from an initial state of 0.15 to a final state of 0.85.

Vanadium battery model

Figure 23 compares power that is extracted from the battery and power that goes to the grid from the battery. Differences between these values are losses that could be due electrical efficiency, pump power requirements or inverter efficiency.

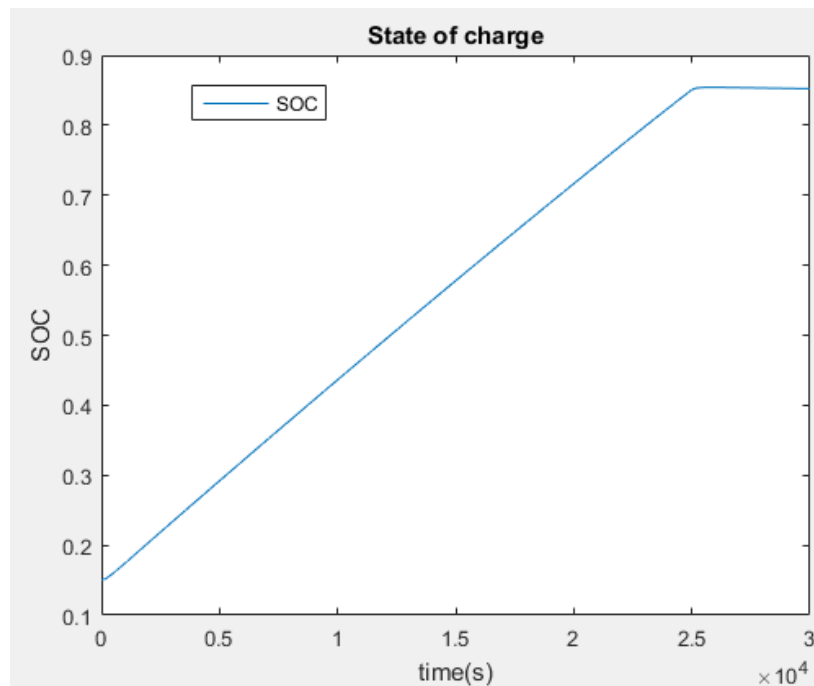


Figure 22: State of charge variation while Vanadium stack is charging

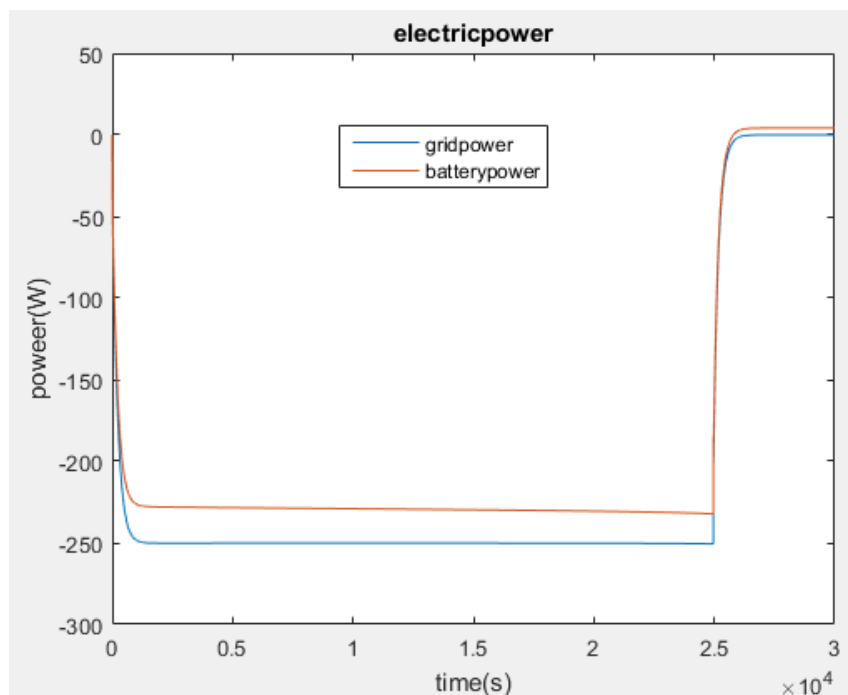


Figure 23: Grid power and stack power while Vanadium battery is charging

Figure 24 represents temperature increment in tank and in stack while battery is charging. It is possible to see that entire electrolyte has a lot of thermal capacitance because temperature doesn't stabilize while it was charging.

Figure 25 represents concentration species of different vanadium valences that are present in tank and stack. As that battery is charging, it is possible to see that active species concentration keeps growing.

Figure 26 compares OCV and output voltage. As that battery is charging, OCV value is less than output voltage. Difference between them represents voltage losses and inefficiency inside battery.

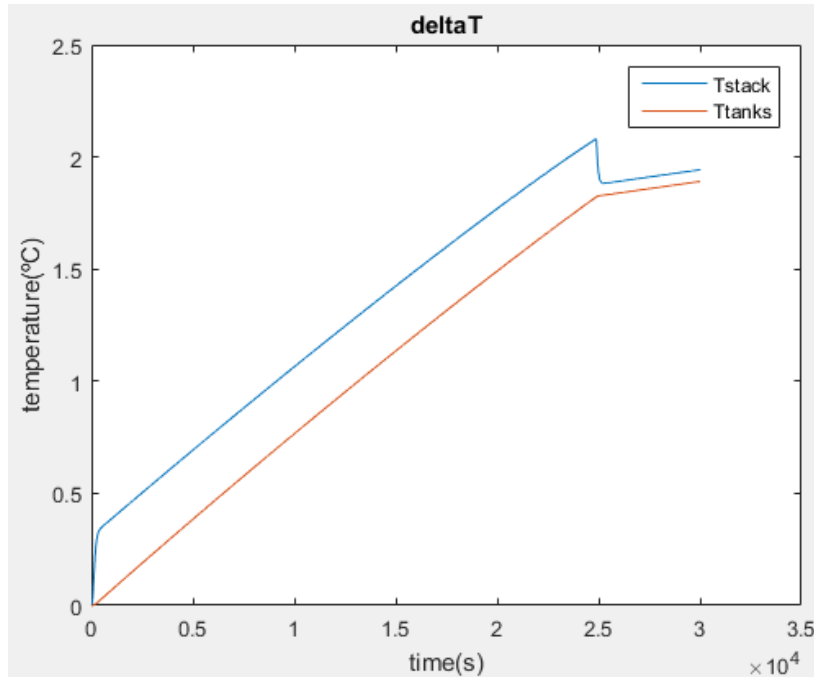


Figure 24: Vanadium temperature variation during a charge

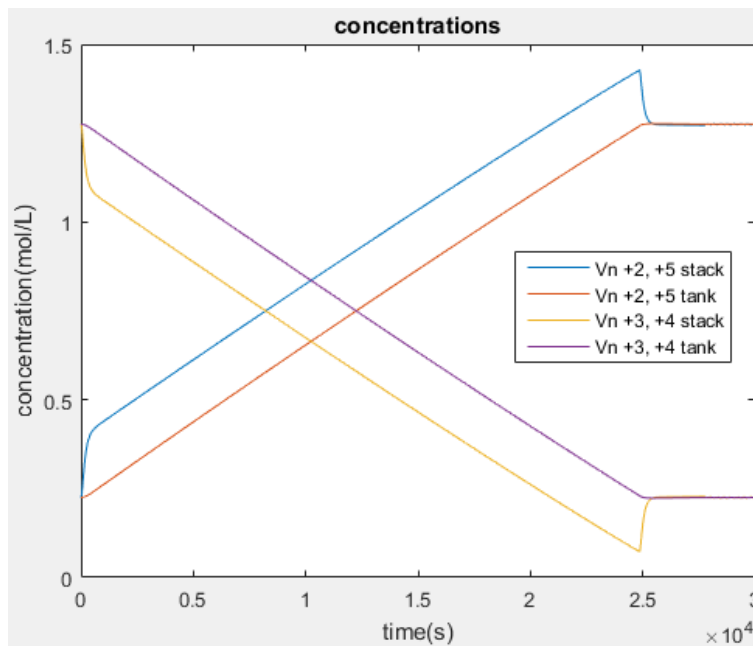


Figure 25: Vanadium stack concentrations during a charge operation

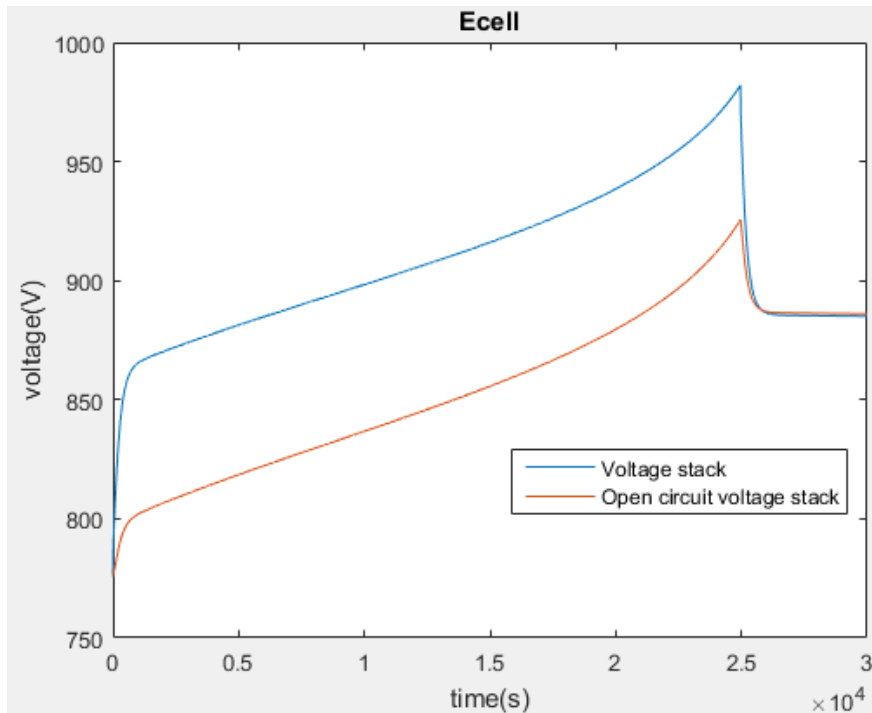


Figure 26: OCV and voltage stack compared during charge operation

3.4.2. Discharge operation

Following graphs represent an inverse process that previous chapter simulation, a discharge of Vanadium flow battery from a 0.85 SOC to an 0.15 SOC. The most significant variables are represented in next figures.

Figure 27 represents SOC evolution and it is an inverse ramp as expected. It moves from 0.85 SOC to 0.15 SOC in a period of time of 21000 seconds (around 6 hours).

Figure 28 represents power that is extracted from the battery and power that is injected in the microgrid by the battery in that discharge process.

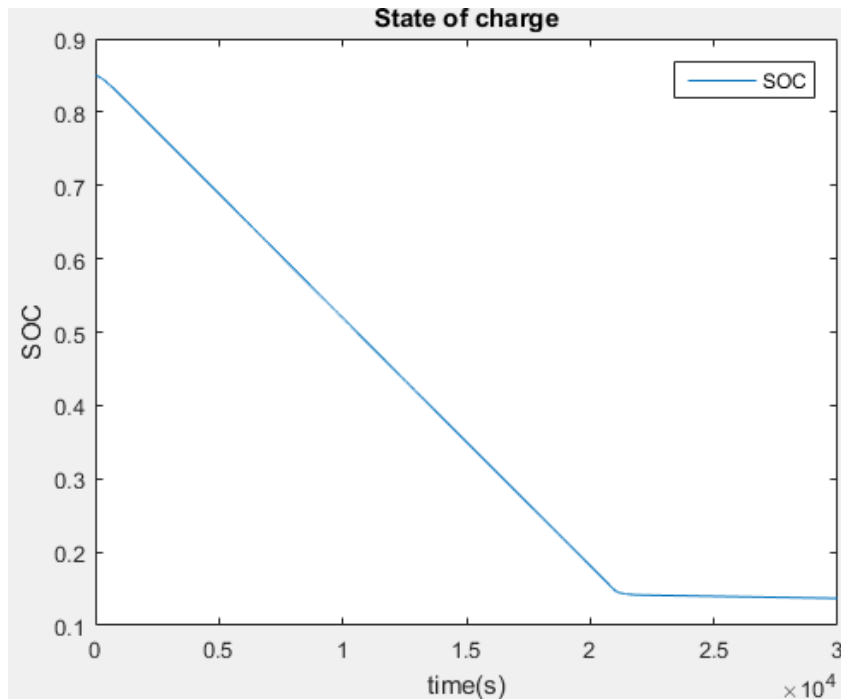


Figure 27: SOC of Vanadium battery under discharge operation

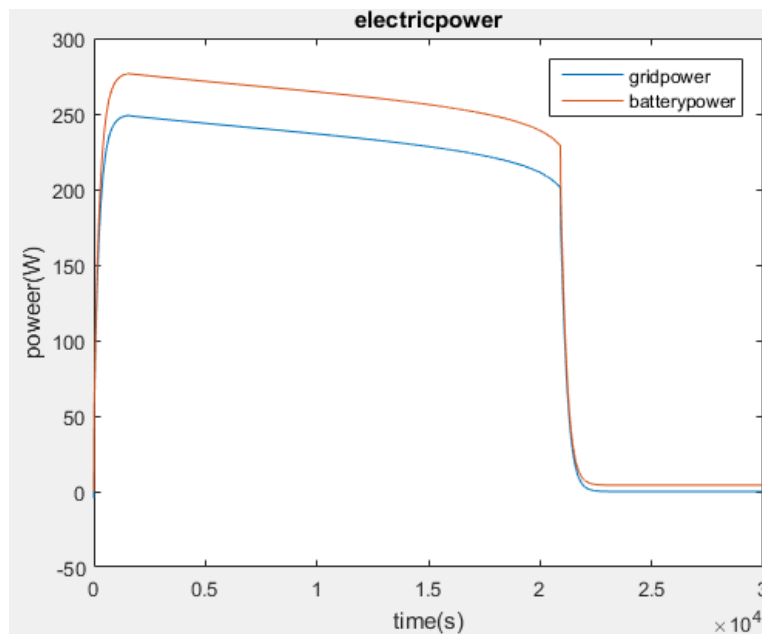


Figure 28: Battery power and grid power under a discharge condition.

Figure 29 compares OCV and output voltage of the stack. It is a discharge process so OCV should have a bigger value than output voltage.

Figure 30 represents Vanadium species concentration in stack and tank. It is a discharge process so active species concentration decrease and reactive increase.

Vanadium battery model

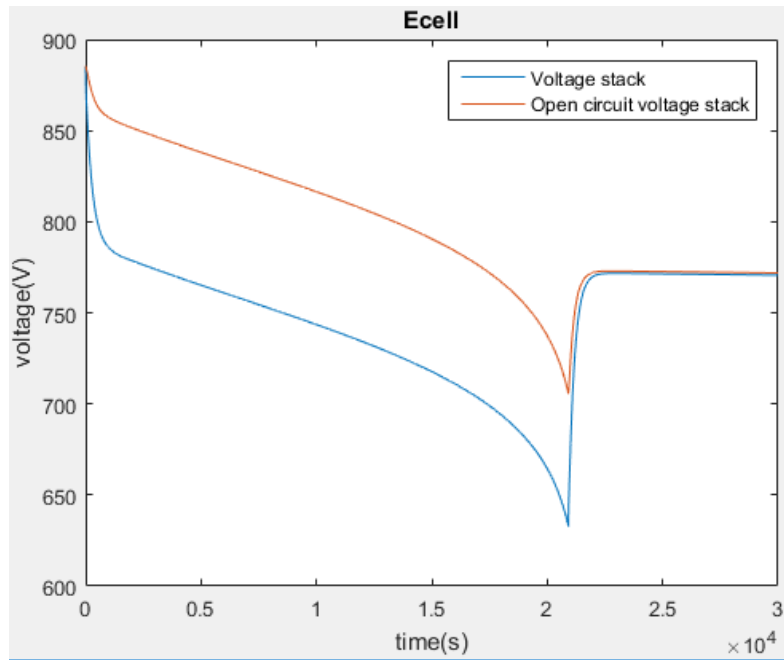


Figure 29: OCV and stack voltage comparative under a discharge condition in Vanadium battery

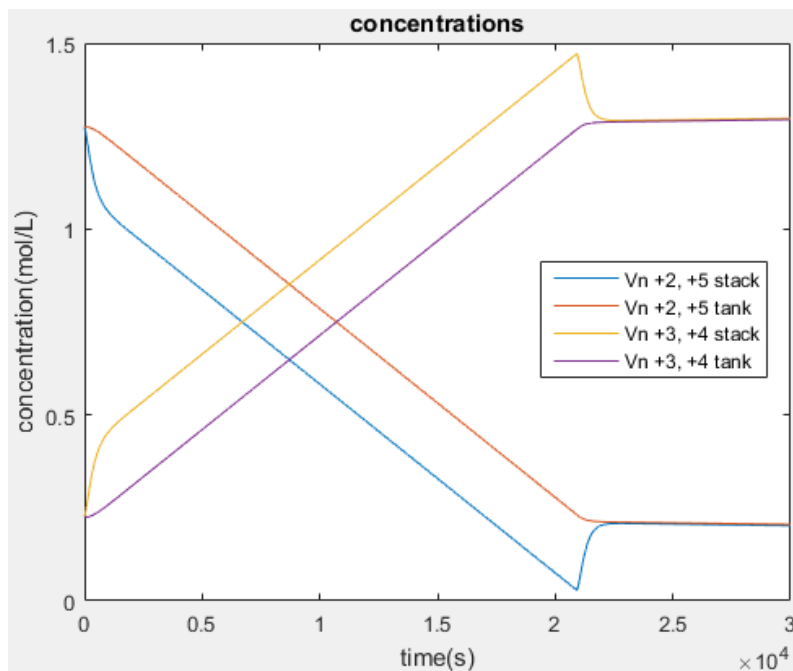


Figure 30: Vanadium battery model species concentration under a discharge situation

Figure 31 represents temperature variation of that process that changes 2 °C. It is possible to see as in charge operation that tanks heat capacitance is high and temperature keeps growing in that simulation.

Figure 32 represents heat generation in that process decoupled in sources. Electrical dissipation, reversible heat and pump pressure losses are the heat sources that changes battery temperature.

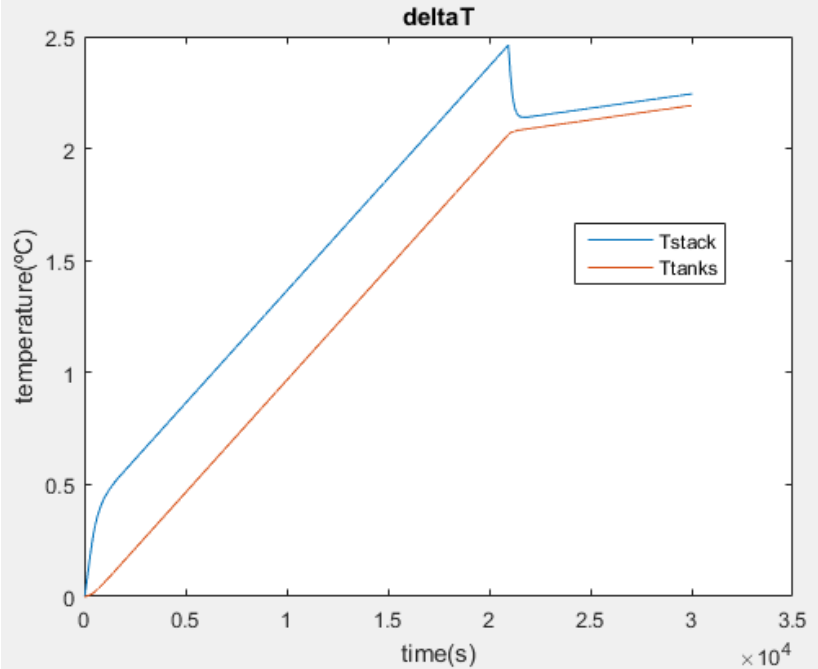


Figure 31: Stack and tanks temperature variations under a discharge operation conditions

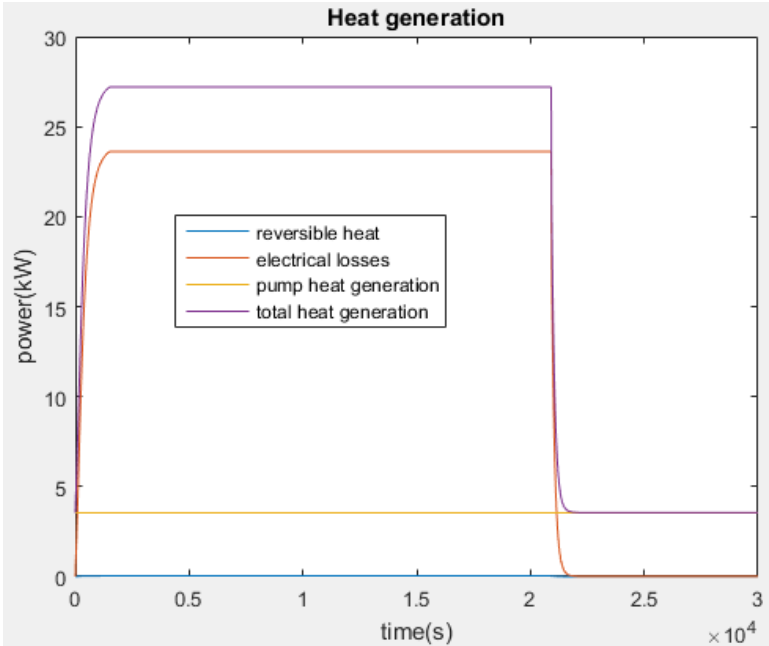


Figure 32: Heat generation of the Vanadium stack under discharge conditions

3.5. Vanadium battery model validation

Different Vanadium battery models have been compared to know if values obtained are appropriated or not.

Table 3: VRF battery model validation

models	Main characteristics	Concentration	Output voltage	Power losses	Pump losses and flow	Stack Temperature variation
The model	625 cells in each of the 2 stacks	1.5 M	800/625 =1.28 V	30 kW->12% Including pump losses	4 kW 10 l/s	10°C Environment fluctuations are not included
[5]	25 cells 5 kW/30 kWh	1.5 M	Around 1.25V. each cell.	12% – 15% Including pump losses	0.2l/s 150 W	8°C
[14]	40 cells 5 kW/15kWh	2 M	1.4V 1.0V	20% - 30% including pump losses	90W 0.5l/s	No data
[12]	2.5/15Kwh 19 cells stacks. 200 L. tank is used	1.6 M 200L. tanks	An average of 1.4 V.	400W as maximum	No data	15 °C Temperature must be around 10-35°C. 1.2°C with 30A currents.
[1]	19 cells in each stack 2.5 KW nominal power 100 A nominal power	2 M	1.70V 1.1V	83% efficiency 390 W	0l/s 2l/s 25 W	15 °C maximum
[15]	UNSW 10 cells stack with currents of 120 A. Meaning 1.33 kW.	2M	1.1V 1.78V	It moves around 85% of efficiency	3% less than 40 W	20°C in the worst scenario possible (during switch of pumps)
[13]	1kW/2.5kWh Vanadium system	1.6 M	1.1V 1.7V	No data	No data	No data

4. Lithium-ion battery models

4.1. Lithium-ion battery description

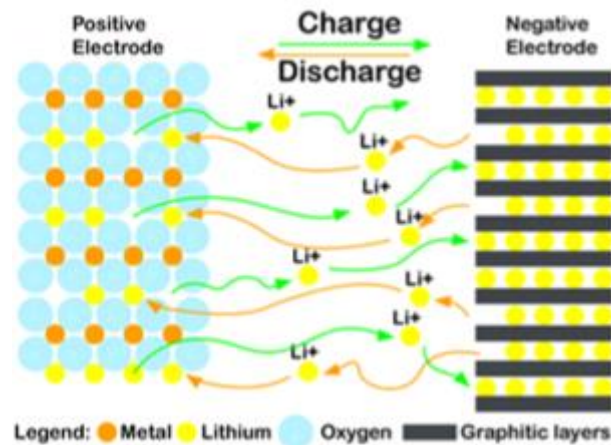


Figure 33: Lithium-ion schematic representation [16]

Lithium is the most promising metal in energy storage applications. Its use is well known in laptops, tablets and smartphones. It also has been considered reference in electric vehicles development. Some works consider that material also important in integration of renewable energy sources in power supply [17].

Its main characteristics are due nature of this element. It is very light and electropositive that lends high specific energy and power [17].

Lithium-ion has 4 different parts in which are divided:

Anode: It is usually made of graphite. It accepts Li^+ ions that cathode donates when battery is charging.

Cathode: Instead of pure metal lithium that is very electropositive and difficult to isolate, it is made by compounds that can donate Li^+ lithium-ions. Cathode is the most expensive component of each cell and it gives the different properties that every type of Lithium-ion battery can have. There are five main types of cathode: lithium cobalt oxide (LCO), lithium manganese oxide (LMO), lithium iron phosphate (LFP), lithium nickel cobalt aluminum oxide (NCA) and lithium nickel manganese cobalt oxide (NMC). Every one of these cathode has their own properties that makes it different to the others.

Separator: Safety element that prevents direct contact between electrodes but allows lithium-ion flow. It is equivalent to membrane element in vanadium-redox flow batteries.

Electrolyte: It is a mixture between an organic solution and a lithium salt that is solved on it. It transports Li^+ ions between electrodes.

Lithium-ion battery model

[17] represents Li-ion battery industry from raw materials to final product. It shows a long chain divided into mining industry, the inorganic chemical industry to obtain cathode active materials, the organic chemical industry for electrolyte, the polymer chemical industry for the binder and separator, the metal industry for the can and electrode foils and the electronics industry for the BMS. A variety of industry players take part on this industry from companies such as Tesla that have a big role in the entire supply chain to other companies more specialized in specific parts of it. It is possible to notice that with the exception of Tesla the main industry players of these devices are East Asian companies (Japan, China and South Korea) such as Panasonic, Sony, GS Yuasa, LG Chem, Samsung, Kokam, BYD Company or ATL.



Figure 34: Lithium-ion industry [17]

Lithium-ion batteries are available in a numerous range of applications and some of them are emerging in last years. Their main market is portable electronic devices such as laptops or smartphones. Road transport is starting to be one of the main uses that this type of battery has. It has a niche in aerospace applications, including in satellites and aviation. It is possible to use it in power supply systems that work grid-connected and off-grid. Lithium-ion batteries could work in miniaturized, reliable, high density and hermetically sealed rechargeable power sources that makes that technology useful in some medical advices such as hearing ads, drug-delivery, glucose sensing and neuro stimulation.

Their use in power supply systems is limited by energy storage cost. It is considered that any cost that is higher than 0.15 €/kWh is not competitive for a grid connected use. When it works in a range of applications smaller than 0.10 €/kWh its use start to be competitive in on-grid connected use that has a strong prize variation during the day, replacing diesel generation that has lower efficient than energy storage.

In any case, their energy storage cost is far from the cost competitive range for grid-connected use, as it is explained in [17]. Compared to other types of energy storage systems such as lead-acid, NaS or Vanadium redox, it is possible to see that lithium-ion high specific energy and lower operation and maintenance requirement are not worth due high specific energy costs that type of battery has. Energy storage market promises to be fragmented due all that aspects.

Advantages

As conclusion, these are the reasons why this type of battery is so developed [17].

- Outstanding specific energy and power.

Modelling of Lithium and flow batteries for micro-grid energy management

- Long calendar and cycle lives.
- High roundtrip efficient.
- Low operation and maintenance costs.
- Satisfactory operating temperature ranges.
- High reliability.
- Technological diversity; several chemistries.
- Intensive global research efforts.
- Chemistries with eco-friendly materials available.
- Reasonable self-discharge rate relatively fast recharge.

Disadvantages

On the other side, these are the reasons that limit their use [17].

- High initial cost.
- Advanced Battery Management System required.
- Safety concerns; thermal runaway incidents.
- Material bottleneck concerns; lithium and cobalt.
- Currently weak recovery and recycling schemes.

4.2. Different Lithium-ion comparative models

Name	Model type	Advantages	Disadvantages	Description
[18]	Electrochemical model	It gives a complex approach to the battery showing all effects that happens inside it.	Very cost-computing	Pseudo two dimensional model
[2]	Electrochemical model	Detailed approach to that battery.	Very cost-computing Complexity	It explains some simplifications to pseudo-2-dimensional model as single particle model.
[10]	Equivalent circuit	Accuracy Easy to compute for real-time applications.	It needs time to adjust variables	It uses an adaptive control to estimate SOC and capacity loss.
[7]	Equivalent circuit with variables temperature dependant	Accuracy Fast computations It has been utilized in a microgrid control strategy	Requires a thermal model. It does not include capacity losses.	A complicated numerical model utilized to researched an equivalent circuit one
[19]	Equivalent circuit	Accuracy Includes a thermal model Fast computations It includes a thermal model	It does not include capacity losses.	An equivalent circuit model obtained by an ARX system identification method

4.3. Lithium-ion model

4.3.1. Cell description

A rechargeable stack of LiFePO₄ and graphite is modeled here based on equivalent circuit models [20] [19]. A commercial spirally wound cylindrical cells of 26 mm. diameter and 65 mm. length weighed 0.074Kg is represented.

It has a nominal voltage of 3.3 V. and it's able to produce 75 W. It has a charge capacity of 2.3 Ah (0.0069 kWh).

A Simulink model is created to represent a cell Lithium-ion battery model. There are two parts that are clearly differenced:

- i) Its electrochemical model that is basically an equivalent circuit model and a SOC current integrator.
- ii) Its thermal model.

Cell Lithium-ion battery is represented on Figure 35. There are some inputs and outputs from that block cells. The main input is current that flows from each cell. The most important outputs are SOC in the electrochemical reaction and temperature in the thermal model. That figure shows the division of battery cell. Blue block represents electrochemical part of the cell and orange block represents thermal model block. Both blocks are correlated and variables from one block affect variables of the other and vice versa.

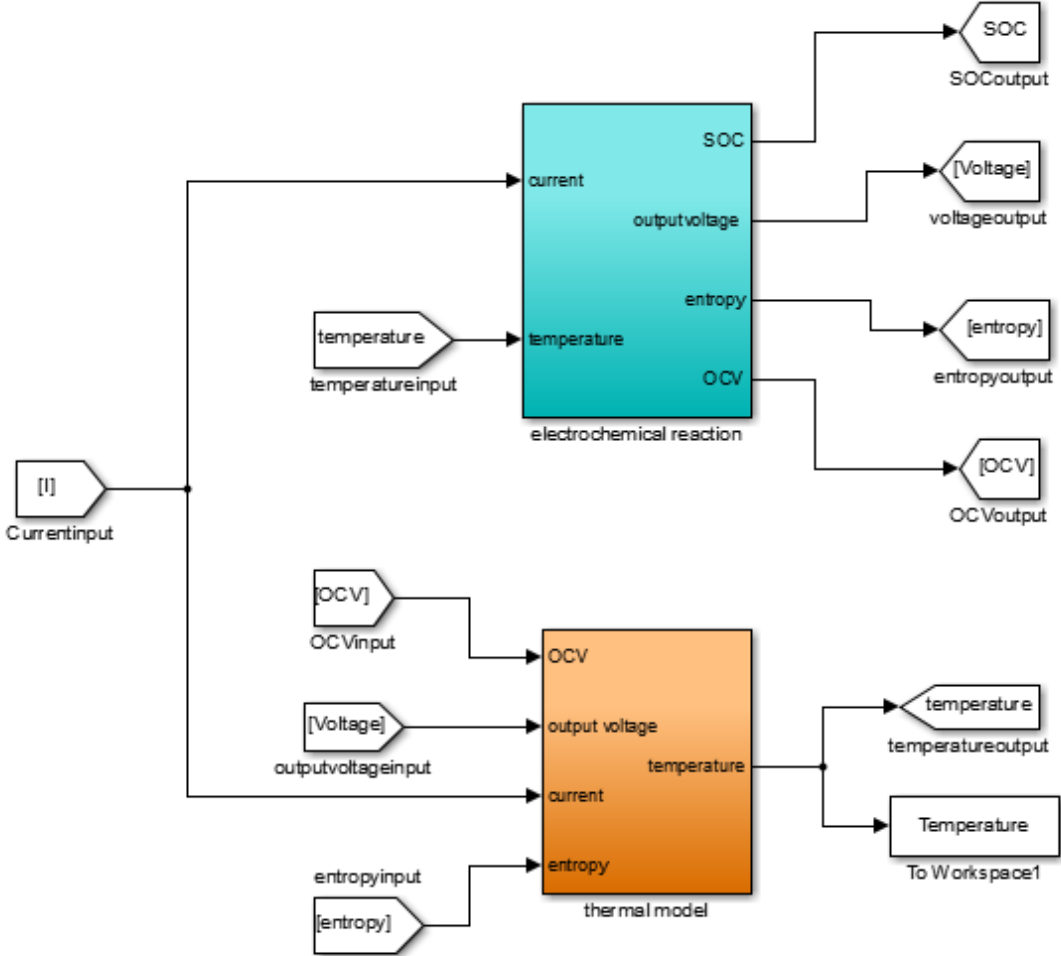


Figure 35: Lithium-ion cell subsystem representation

4.3.2. Electrochemical reaction

The Lithium-ion cell model is explained as an equivalent circuit. It has two parts clearly differenced.

- i) An equivalent circuit.
- ii) A current integrator that computes SOC.

It is necessary to find all the equations that account for this model. Then all that expressions must be represented as Simulink blocks. Figure 36 shows the different blocks that are inside the electrochemical subsystem block. These are explained below.

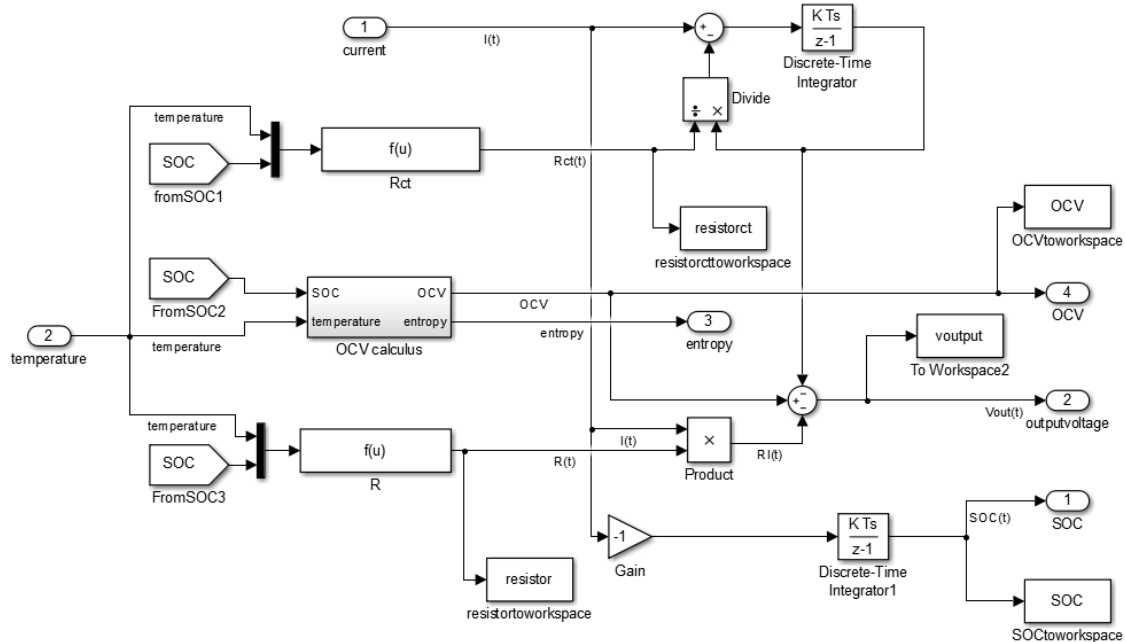


Figure 36: electrochemical reaction subsystem block

Equivalent circuit

There are three parameters in that electric circuit representation R , C and R_{ct} , an input E_{OCV} and an output value V_{out} . Figure 37 shows a representation of an electrochemical equivalent circuit with the three parameters, the input that is E_{OCV} and the output that is V_{out} .

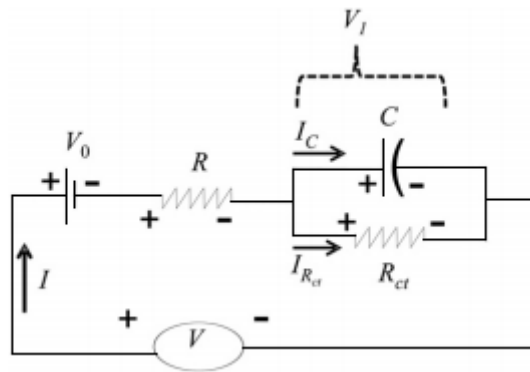


Figure 37: Equivalent circuit schematic representation [19]

It is necessary to know how all of these parameters interact between each other in order to express this circuit schematic as equations. There are two equations in that equivalent circuit:

- i) V_{out} in equation (26) where V_1 is equivalent circuit capacitor voltage, R is a resistor value and I is cell current [19] .

$$V_{out}(k) = E_{OCV}(k) - V_1(k) - R(k)I(k) \quad (26)$$

Where V_1 could be explained as that second differential equation (27) [19] where C is equivalent circuit capacitor capacitance and R_{ct} is parallel resistor resistance. It could be discretized and it would be as equation (28).

$$I = \frac{d}{dt} [CV_1] + \frac{V_1}{R_{ct}} \quad (27)$$

$$V_1(k+1) - V_1(k) = \frac{t_s}{C} \left(\frac{V_1(k)}{R_{ct}(k)} - I(k) \right) \quad (28)$$

Figure 38 marks all the different elements that the electrochemical model has. **Red circles** represent R , R_{ct} and C values (inside an integrator block). **Green square** show the subsystem block where OCV is calculated and the **blue squares** represents V_{out} from (26) and V_1 is integrated based on (28).

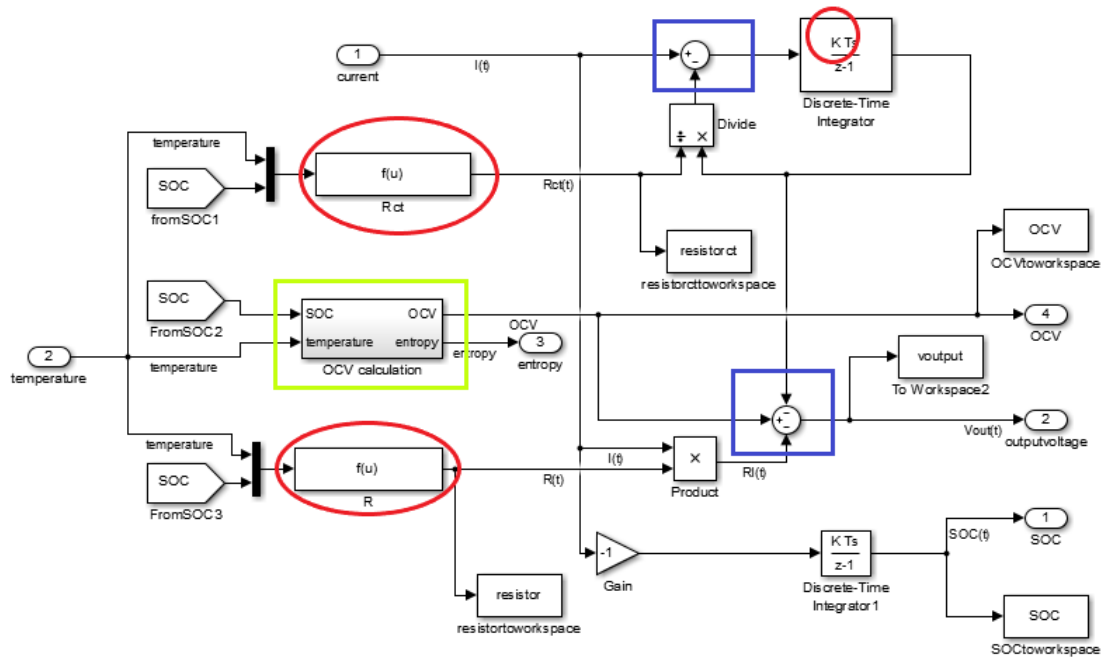


Figure 38: Different parts of equivalent circuit model of Lithium-ion battery

OCV calculation

There is an expression that relates SOC and temperature with OCV that could be seen on equation (29). It is inside block marked on Figure 39 and it is divided in Figure 40 block components.

$$E_{OCV}(x, T) = E_{OCV}(x, T_0 = 25^{\circ}C) + \frac{dV}{dt}(T - T_0) \quad (29)$$

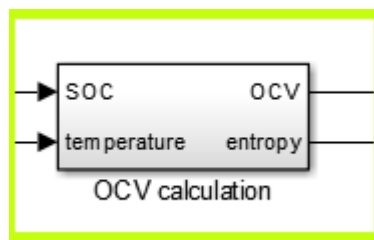


Figure 39: Subsystem block that computes OCV values in Lithium-ion model

Lithium-ion battery model

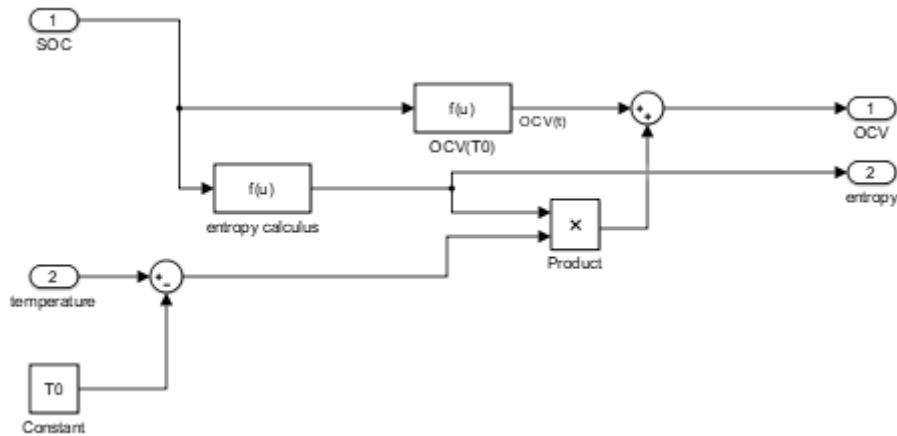


Figure 40: Internal structure of Figure 39 block

It only needs an OCV at constant temperature (in that case 25°C) and an entropy function.

OCV at constant temperature

Instead of using Nernst equation, a SOC dependent function was built that relates SOC and OCV. For a LiFePO₄ Lithium-ion battery, there is a polynomial function (30) [20] that relates SOC at 25°C with OCV where x represents SOC. Error between that expression and real value is less than 10 mV [19]. Figure 41 shows a graphic representation of function (30).

$$E_{OCV}(T_0, x) = 0.0582x^6 - 0.1939x^5 - 0.5444x^4 + 2.1870x^3 - 2.3821x^2 + 1.1627x + 3.0896 \quad (30)$$

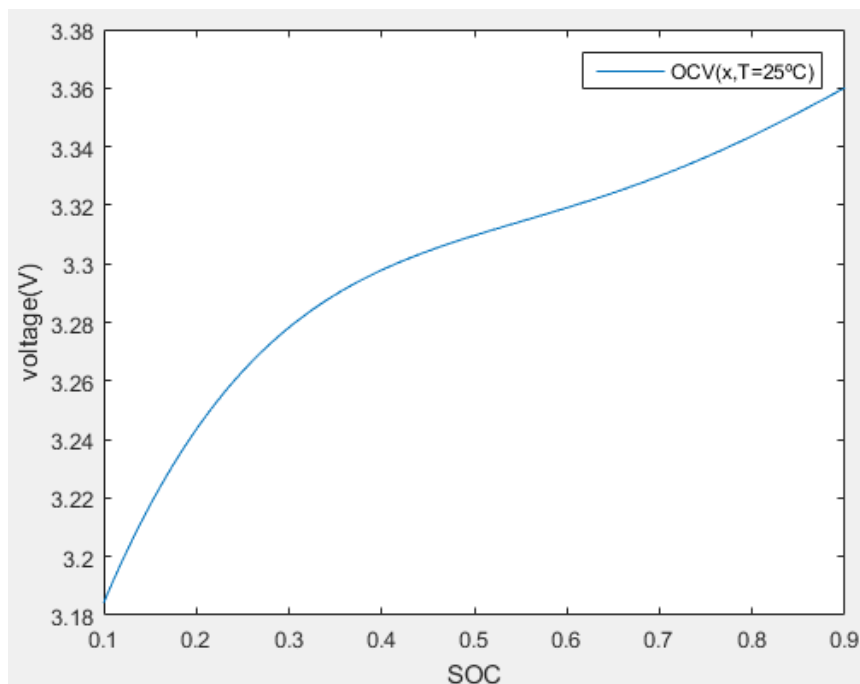


Figure 41: Graphic representation of OCV as a variable SOC dependant as in (30)

Entropy is defined as a voltage / temperature variation. An OCV function SOC dependent has been located. A polynomic function that relates SOC and entropy (31) is used where x represents SOC value. There is a graphical representation of function (31) on Figure 42.

$$\Delta S(x) = \frac{dV}{dT}(x) = 0.0044x^4 - 0.0100x^3 + 0.0064x^2 - 0.0006x - 0.002 \quad (31)$$

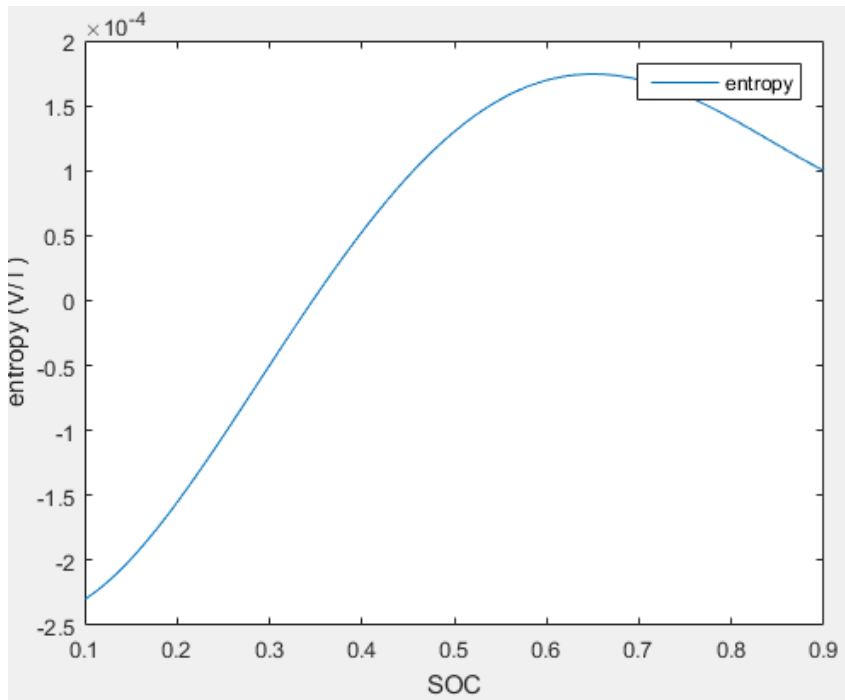


Figure 42: Lithium-ion LiFePO4 entropy as a function SOC dependant (31)

Parameters

As it is said in previous chapters, there are three parameters that represent different electrical components:

R and R_{ct} are resistances value that are temperature and SOC dependent.

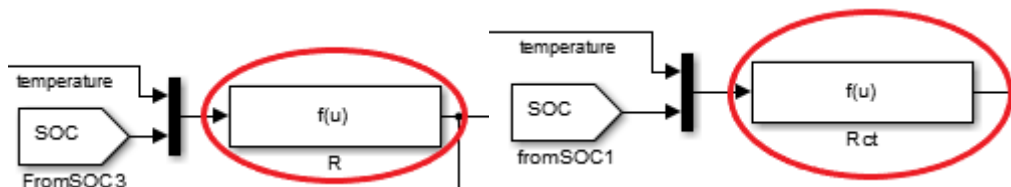


Figure 43: Function Block of $R(T, x)$.

Figure 44: Function Block of $R_{ct}(T, x)$.

Their equations (32) and (33) have an exponential representation where E is an activation energy for resistor R and E_{ct} is the activation energy of R_{ct} .

$$R(T, x) = R_0(x)e^{-\frac{E}{RT}} \quad (32)$$

$$R_{ct}(T, x) = R_{ct0}(x)e^{-\frac{E_{ct}}{RT}} \quad (33)$$

Their SOC dependence can be considered linear in both cases.

C has no temperature or SOC dependence so its value is directly include as a constant in the integrator block where it appears.

Equations representation

V_{out} (26) and V_1 (27) equations are computed from two different equations previously explained. Equation (27) is discretized in equation (34). (34) It is possible to see that equation on Figure 45.

$$V_1(k + 1) - V_1(k) = \frac{t_s}{C} \left(-\frac{V_1(k)}{R_{ct}(k)} + I(k) \right) \quad (34)$$

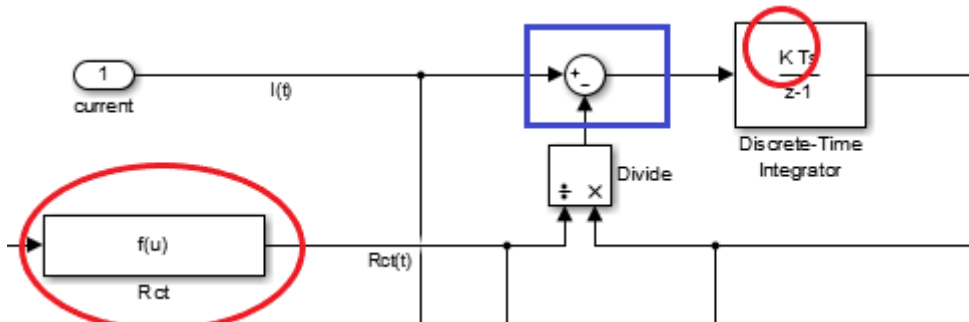


Figure 45: V1 block representation in Lithium-ion battery model

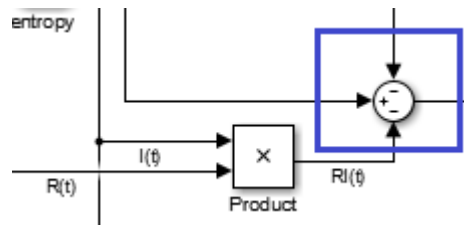


Figure 46: Vout sum block in Lithium-ion battery model

SOC calculation

At the bottom of the electrochemical reaction subsystem block. It is included an integrator that calculates SOC at every step where I is current that crosses each lithium cell and Q_{max} is the total capacity of each cell. It is shown in Figure 47. These blocks represent equation (35).

$$SOC(k + 1) - SOC(k) = -\frac{t_s}{Q_{max}}I(k) \tag{35}$$

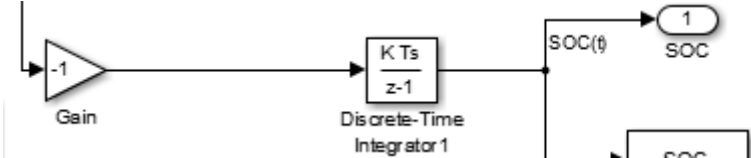


Figure 47: SOC block integrator in Lithium-ion battery model.

4.3.3. Thermal model

It is similar to Vanadium one, but there is only a temperature state instead of two of them (tanks and cells) for Vanadium redox battery.

There are three energy exchanges:

- i) Heat generation due to dissipative losses
- ii) heat generation due reversible
- iii) Heat and due convection with the environment.

Equation (36) is a Differential equation that represents thermal variation inside the battery model, where T represents battery surface temperature and T_A represents environment temperature; MC_p is thermal capacitance of each cell of the system. dV/dT is entropy that reaction has and hA is a heat transfer coefficient between environment and each cell that is dependent of refrigeration method and surface area.

$$MC_p \frac{dT}{dt}(t) = I(t)(V_{out}(t) - E_{ocv}(t)) + I(t)T(t) \frac{dV}{dT}(t) + hA(T_A(t) - T(t)) \tag{36}$$

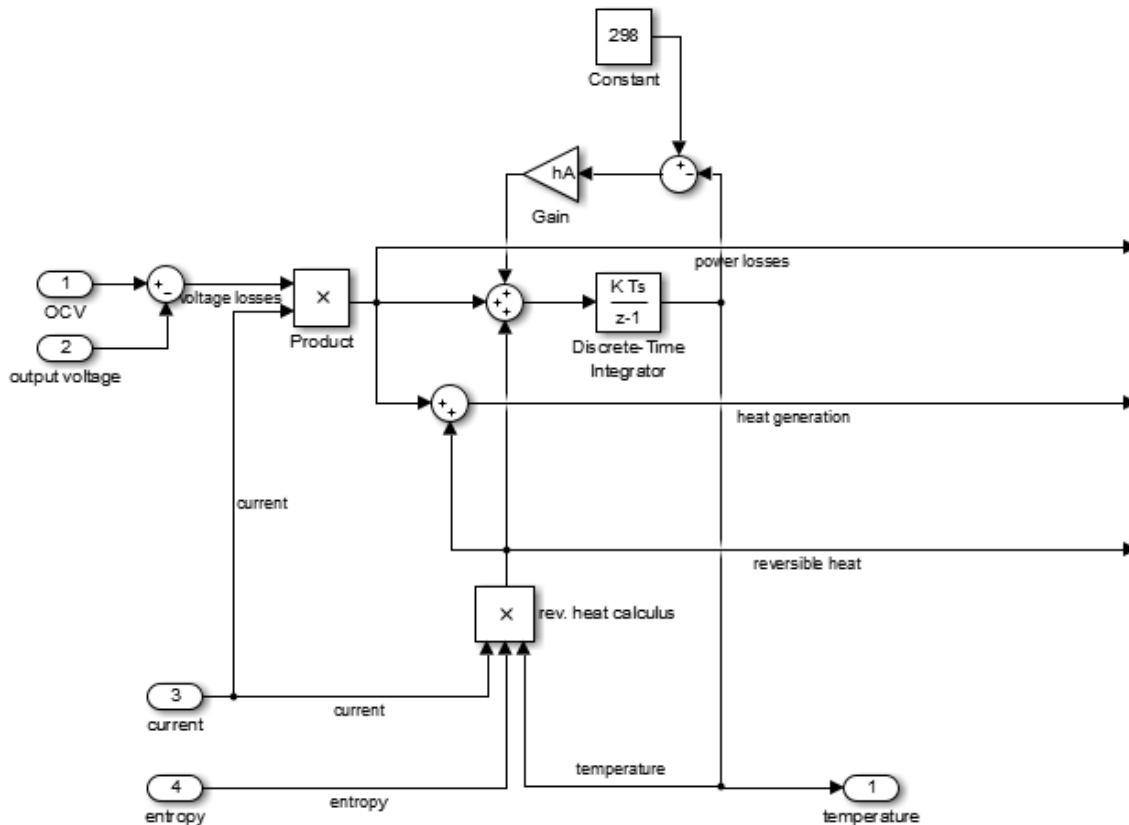


Figure 48: Thermal balance block representation in Lithium-ion battery model

Its discrete form will be equation (37). It appears represented in Figure 48 and it is detailed explained in Figure 49.

$$T(k + 1) - T(k) = \left(\frac{I(k)\Delta s(k)t_s}{MC_p} - \frac{hAT(k)t_s}{MC_p} \right) T(k) + \frac{hAT_A(k)t_s}{MC_p} + \frac{I(k)(V_{out}(k) - OCV(k))t_s}{MC_p} \quad (37)$$

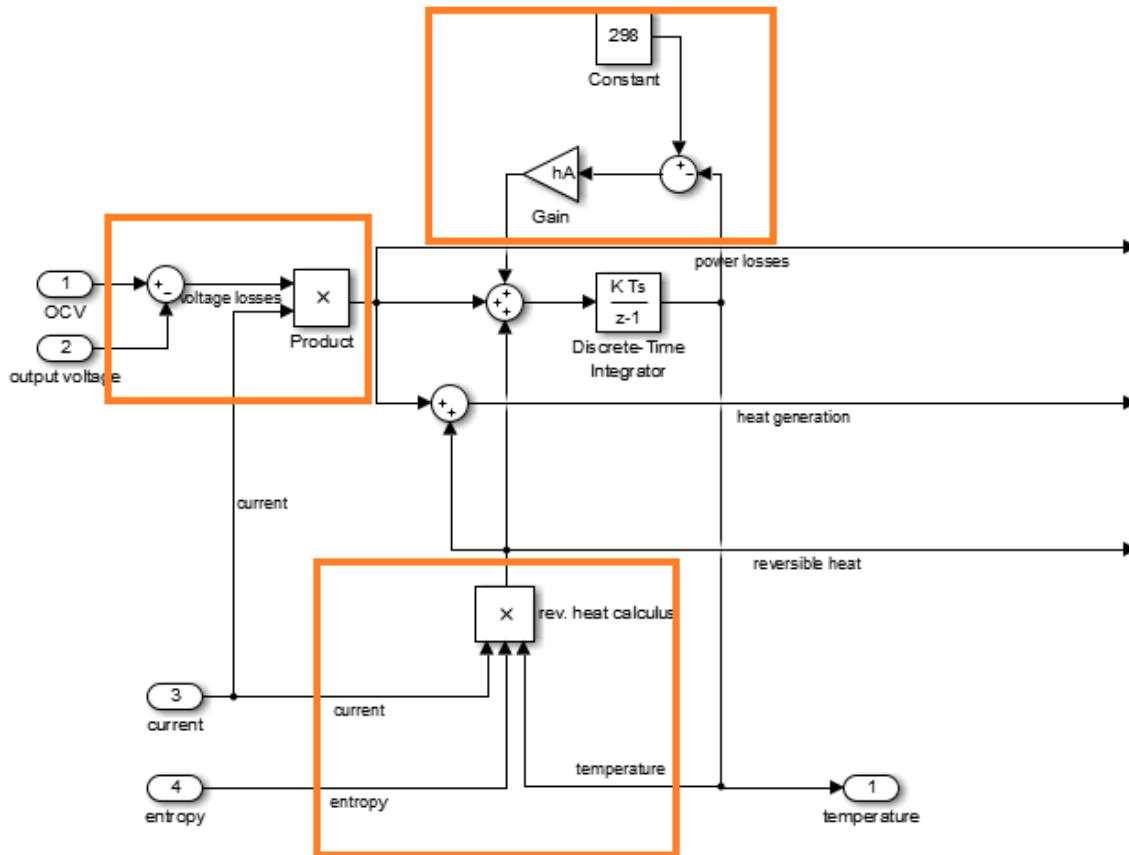


Figure 49: Thermal balance subsystem of Lithium-ion. Energy balances are marked.

Convection heat exchange

Figure 49 is divided into three heat exchanges. Figure 50 represents heat exchange and it is explained on equation where $\dot{q}_{exchange}$ is heat exchanged, h is a heat transference coefficient that is proportional to cells surface and depends on convection source (air forced convection in that case)

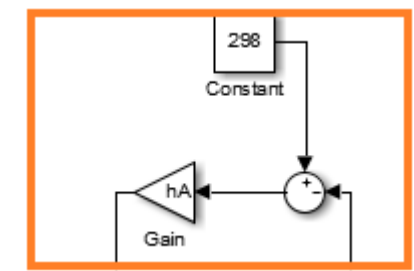


Figure 50: Convection exchange with the environment in Lithium-ion.

$$\dot{q}_{exchange} = hA(T_A(t) - T(t)) \tag{38}$$

Dissipative losses

Figure 51 represents power losses that are due voltage overpotential inside battery. Values that are part of that losses are ohmic losses, activation overpotential and concentration overpotential. It is calculated applying equation (39) where I is cell current, V_{out} is output voltage and OCV is opencircuit voltage.

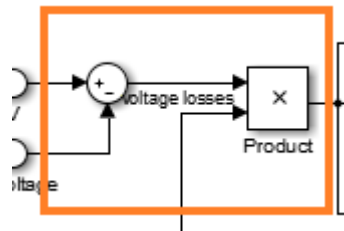


Figure 51: Electrochemical dissipative losses in Lithium-ion equation (39) (39).

$$\dot{q}_{losses} = I(t)(V_{out}(t) - E_{OCV}(t)) \tag{39}$$

Reversible heat

Figure 52 represents energy exchange due entropy variations. \dot{q}_r is calculated applying equation (40) where T is temperature, I is cells current and $\frac{dV}{dT}$ is entropy. There are two main sources of heat in a battery, while irreversible heat transfer represents effects as ohmic losses or ion polarization, reversible heat represents heat exchange that is due entropy variations in reaction processes. Reversible means that the quantity of energy generated in reaction advance is equivalent to the absorb energy in reaction advance with opposite sign.

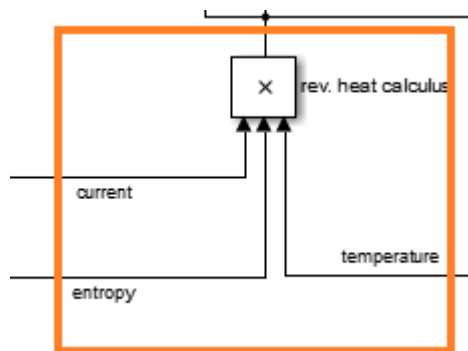


Figure 52: Reversible heat equation (40).

$$q_r = I(t)T(t) \frac{dV}{dT}(t) \tag{40}$$

Heat integrator

All of that energy exchanges signals are add and connected to an integrator. It computes temperature changes that occur in every time step. Its constant value is $\frac{1}{MC_p}$ that is a thermal capacitance that relates heat and temperature variation. It appears represented on Figure 53.

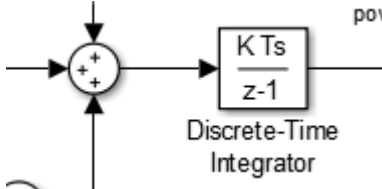


Figure 53: Heat sum and temperature integrator in Lithium-ion (37)

4.3.4. Integration of all the cell stacks

4.3.4.1. Rack dimensions

It is not possible to decoupled power and capacity of that battery as it has been done in Vanadium one. Knowing results of case study chapter, it is assumed a 1200 kWh capacity and 250 kW power requirements. Each cell, as it is explained at the beginning of that chapter, has 0.0069 kWh and 25 W power. It is important to note that this type of battery has a high quantity of specific power. That means that nominal power is going to be much larger than required.

17500 cells are a good number for that energy storage. It brings a total energy storage capacity of 1200 kWh and 437.5 kW power supply, that is optimal for the micro-grid requirements. As it is explained in validation part of that model.

Division of that cell is considered as in an article [20] but adjusting energy storage requirements to the necessities:

- i) A battery rack that is divided in 25 modules.
- ii) Each of those modules is divided into 7 blocks
- iii) Each block is made of 1000 cells.

So that battery stack has a nominal voltage of 570 V and approximately 25 kWh capacity. If conservative values of 5 A of nominal current is given to each cell, it is possible to conclude that this battery has a specific nominal power of 437.5 kW that is more than power required for that microgrid.

Table 4: Lithium-ion stack distribution explained

	Unom	Cnom	Enom
Cell	3.25V	2.1 Ah	0.0069 kWh
Block	3.25V	2100 Ah	6.9 kWh
Module	22.75V	2100 Ah	48.3 kWh
Rack	568.75V	2100 Ah	1207.5 kWh

4.3.4.2. Power electronics conversion

Based on that article [20], power electronics part is made by a commercial power electronics inverter/rectifier Siemens unit in a three phase connection 400V AC/600V DC [20] (see on Figure 54).

Power rack explained In Table 4 has 570 V as nominal voltage output. It has the advantage that it directly converts rack DC voltage into AC voltage without the necessity of include a DC-DC power converter as it was required for Vanadium battery model case. That inverter will work as it appears in Figure 54 between battery DC current bus and the micro-grid node.

The only information that is necessary for the model is inverter power efficiency conversion. Figure 55 represents it. It is similar to Vanadium battery model inverter, a linear power dependent

has been made between the nominal power, in that case 250kW and power losses in the inverter. It is accurate for calculating inverter power losses.

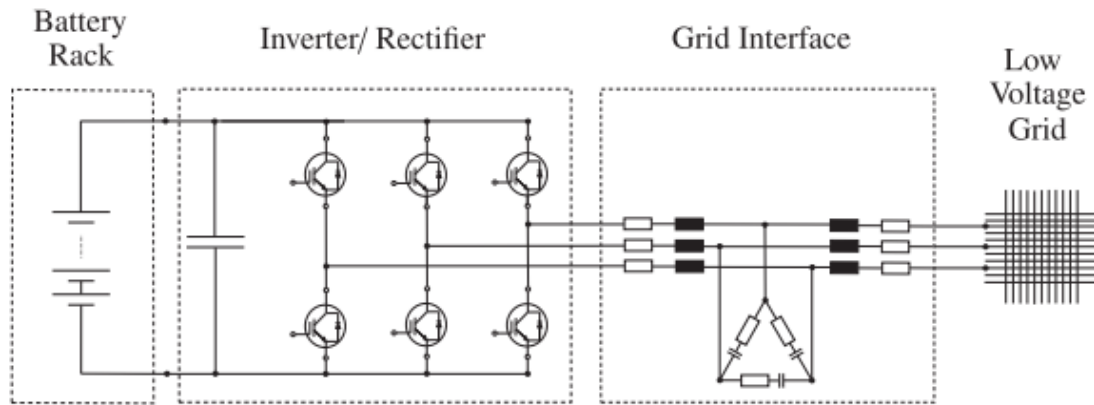


Figure 54: Battery, inverter and microgrid distribution [20]

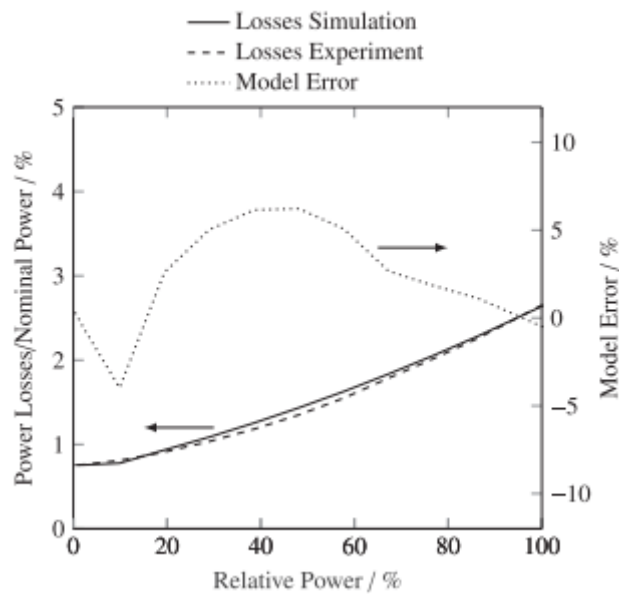


Figure 55: Ratio between power dissipation inside the inverter and power movement between the battery and the microgrid [20]

4.3.4.3. Integration of rack dimensions into that model

Figure 56 shows an auxiliary model block subsystem included in Lithium-ion battery model. It makes three basic operations:

- i) It multiplies cell current by the number of cells that are in each block to obtain the current flow from the battery to the inverter.

Lithium-ion battery model

- ii) It multiplies total voltage cell by the modules and blocks that have a series connection to calculate the output voltage and the open circuit voltage.
- iii) It multiplies total output power by a coefficient current dependent based on Figure 55 that takes out of power calculation all the dissipative values lost on inverter conversion.

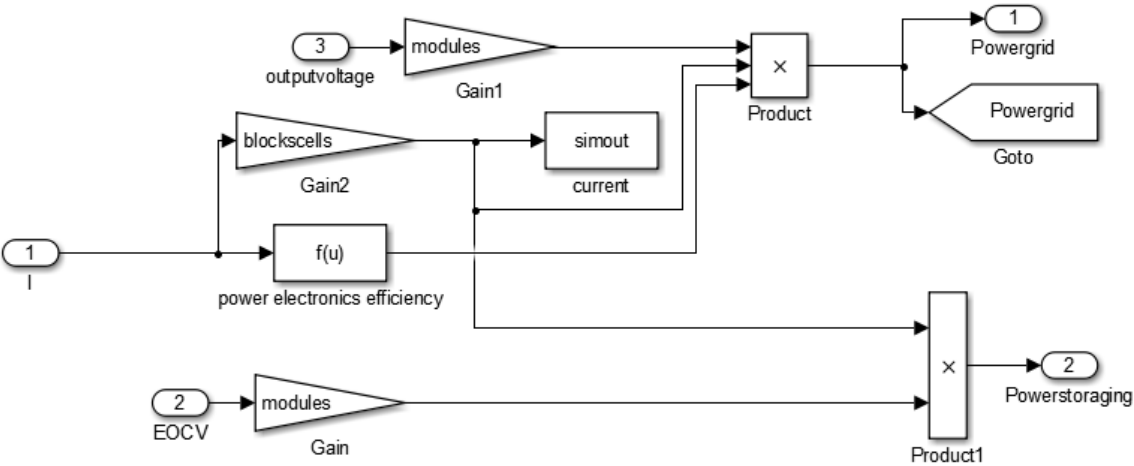


Figure 56: A subsystem block that gives dimensions to the rack and include inverter dissipation losses

4.4. Results of Lithium-ion model

A Simulink simulation in discrete mode 1 second time step is made to show Lithium-ion performance. It is considered battery as a generator which means that positive power and current flows from the battery to the microgrid and negative power flows from the microgrid to the battery.

Experimental results of Lithium-ion are shown in two different scenarios that are considered as the most important:

i) Charge operation:

Rack is charging at a constant power rate of 250 kW. From a 0.10 SOC initial condition to 0.90 SOC condition in which that battery stop charging. Variables like temperature, heat generation, OCV and stack concentrations are represented.

ii) Discharge operation:

That stack is discharging at a constant power rate of 250 kW. From a 0.85 SOC initial condition to 0.15 SOC conditions in which that battery stop charging. Variables like temperature, heat generation, OCV and stack concentrations are represented.

4.4.1. Discharge of a Lithium-ion cell

That simulation has been a 250 kW power discharge from a 0.9 state of charge to a 0.1 SOC energy level and it is represented in next graphics. Discharge takes around 4 hours.

All variables are expressed in next figures.

Figure 57 represents OCV and output voltage in a full discharge from 0.9 to 0.1 SOC.

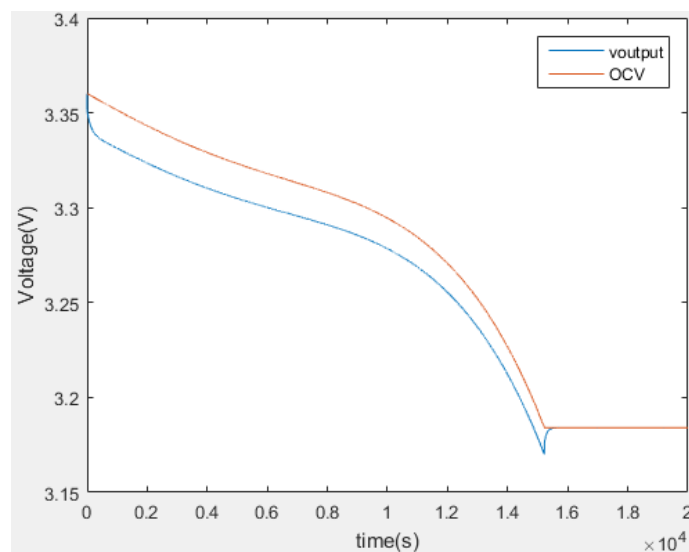


Figure 57: OCV and voltage output of each cell of Lithium-ion model while it is discharging

Lithium-ion battery model

Figure 58 shows SOC. That discharged is power constant during that entire period of time. As a result it can be seen that SOC graphic representation is an inverse ramp.

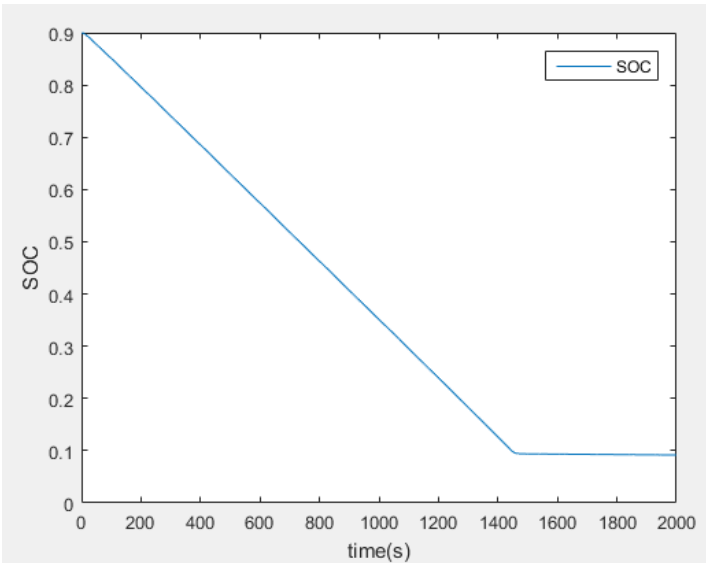


Figure 58: SOC variation in lithium-ion battery while it is charging

Figure 59 represents surface temperature. It is around 1°C higher than external temperature.

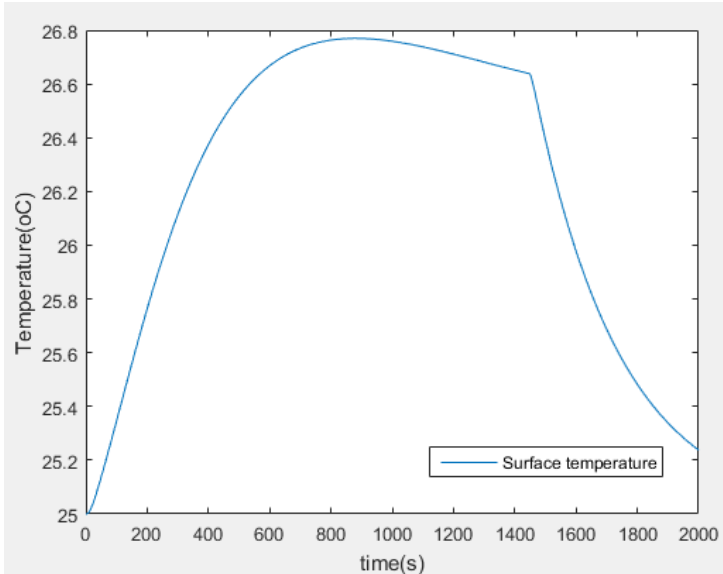


Figure 59: Surface temperature variation while Lithium-ion battery is discharging

Figure 60 shows heat generation inside the stack. It can be seen that entropy heat generation is negligible compared on dissipative losses that are inside the cells.

Figure 61 show equivalent resistance of equivalent circuit. It is possible to see that resistive values are SOC and temperature dependent.

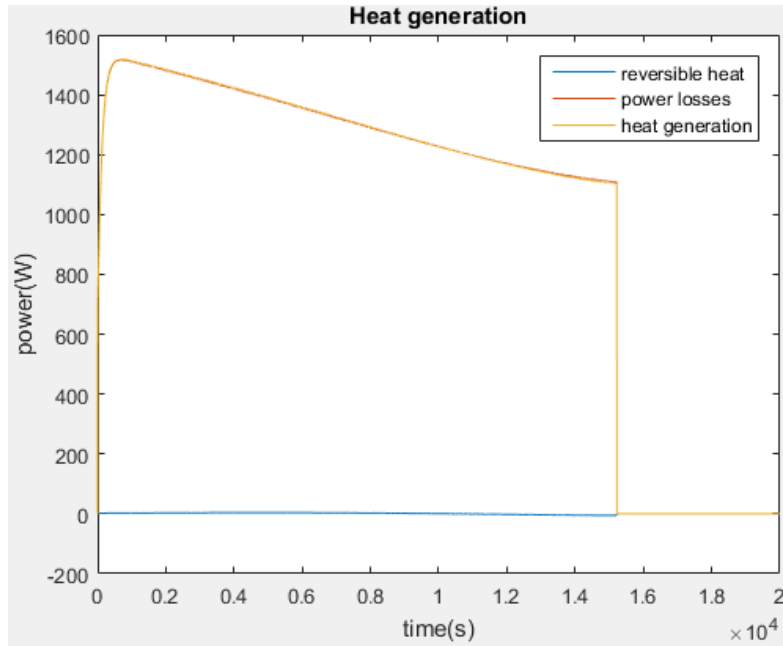


Figure 60: Heat generation by the battery while it is discharging

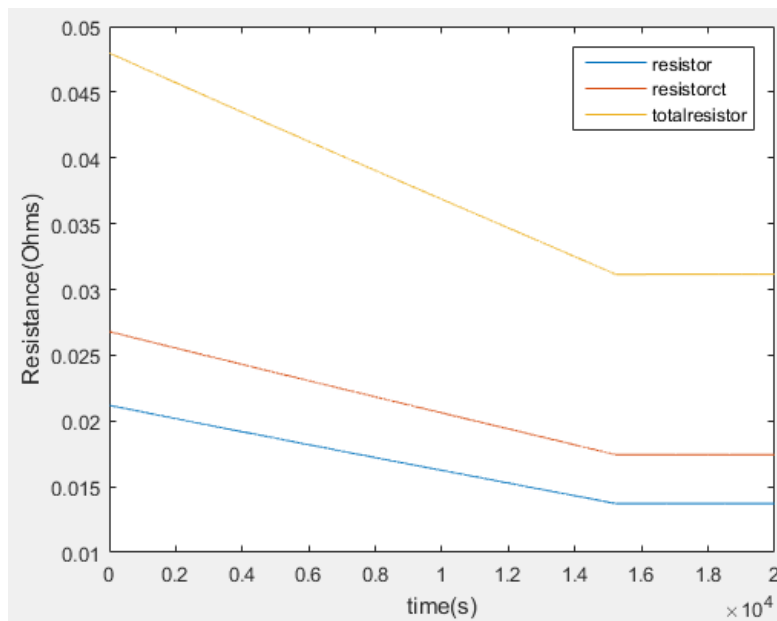


Figure 61: Resistance value variance while Lithium-ion battery is discharging

Figure 62: This image shows all the stack power that is generated. Grid power is energy that grid is able to absorb where dissipated losses are taken out of it. It is compared with energy that is generated.

Figure 63 shows how current cell has to adapt to different voltage outputs to keep power output constant.

Lithium-ion battery model

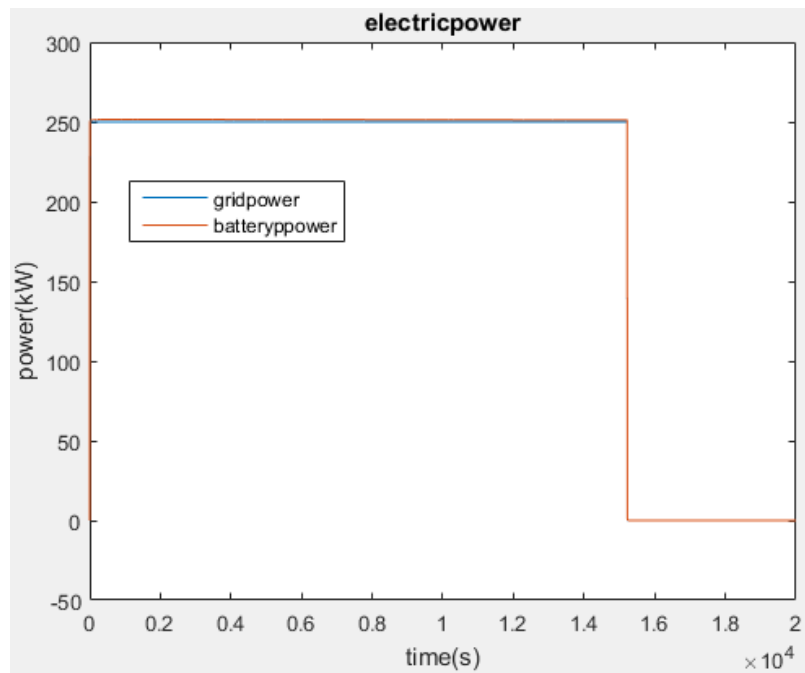


Figure 62: Power generated by the battery and power absorb by the microgrid while it is discharging

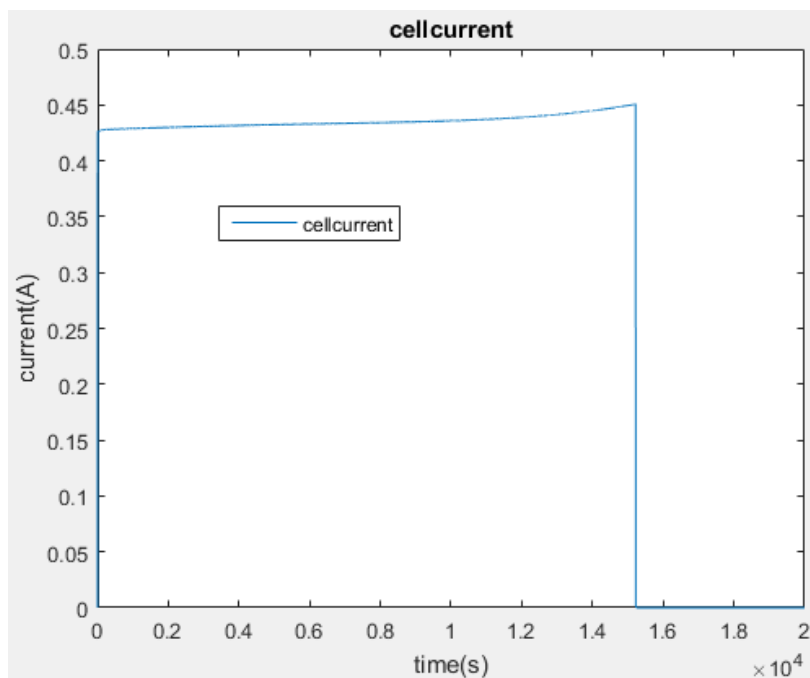


Figure 63: Cell current of Lithium-ion while it is discharging

4.4.2. Charge of a Lithium-ion cell

That simulation has been a 250 kW power charge from a 0.1 state of charge to a 0.9 SOC energy level and it is represented in next graphics. Discharge takes around 20 minutes.

All variables are expressed in next figures.

Figure 64 compares OCV and output voltage of a single lithium-ion cell. It is possible to notice that in charge operation output voltage value is bigger than OCV.

Figure 65 represents SOC values while charge simulation occurs. It is possible to see that looks similar to a ramp.

Figure 66 compares heat generation sources while battery was charging. Reverse heat generation looks negligible when it is compared to heat losses.

Figure 67 compares ohmic value of equivalent circuit resistances. It is possible to see that are temperature and SOC dependent.

Figure 68 compares power absorb by the battery and power injected to the battery by the microgrid. That simulation is a good visual view of energy efficiency.

Figure 69 represents cell current in lithium-ion battery.

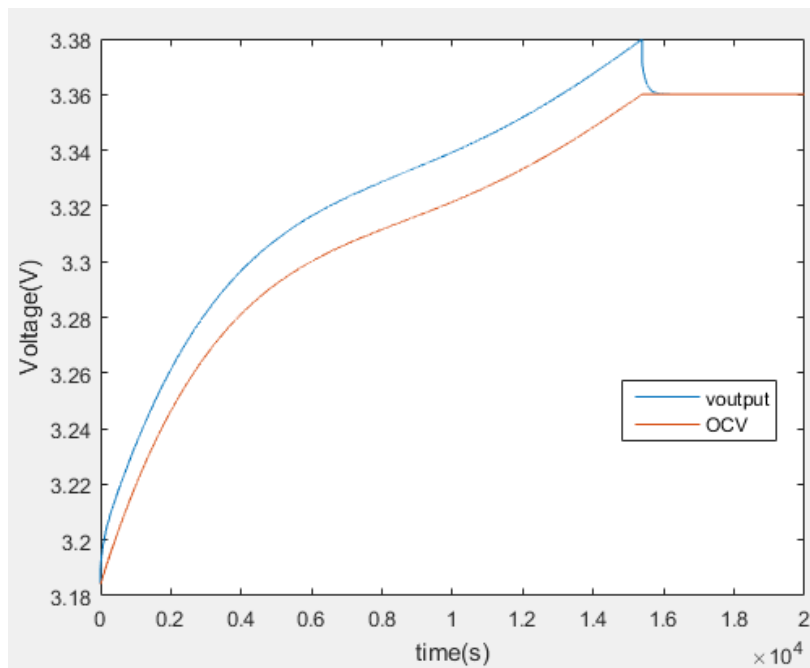


Figure 64: Cell OCV and output voltage while Lithium-ion is charging

Lithium-ion battery model

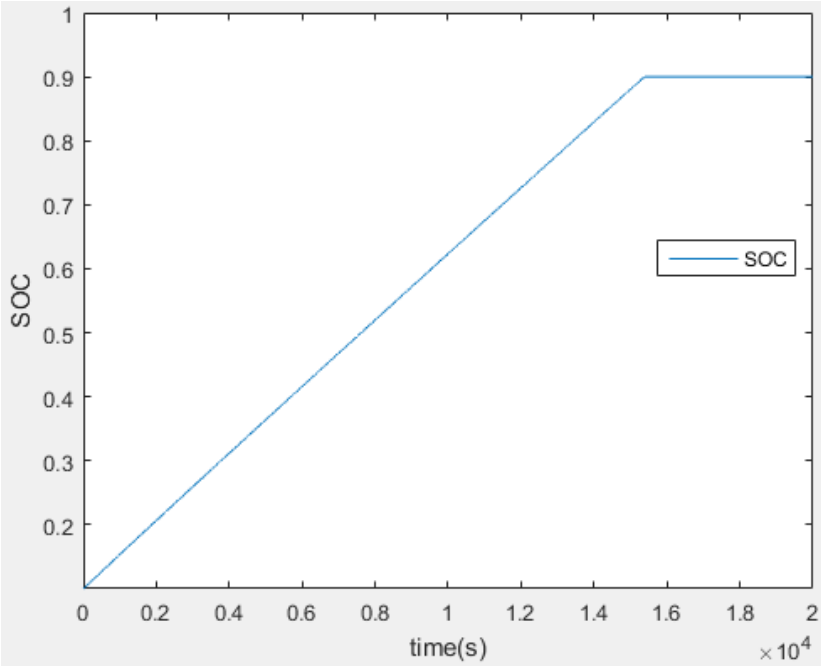


Figure 65: SOC variation while Lithium-ion rack is charging

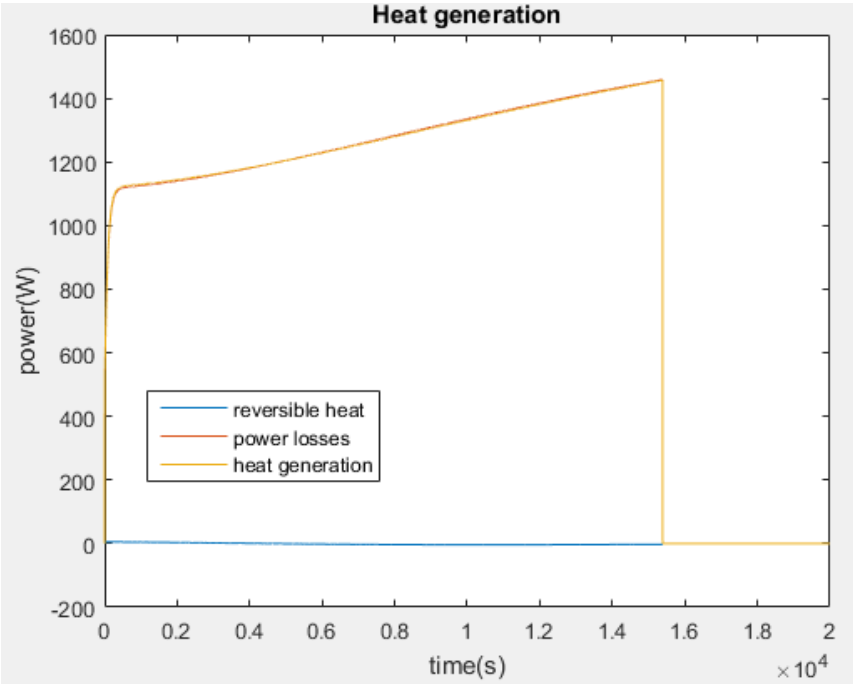


Figure 66: Heat generation while charging Lithium-ion battery

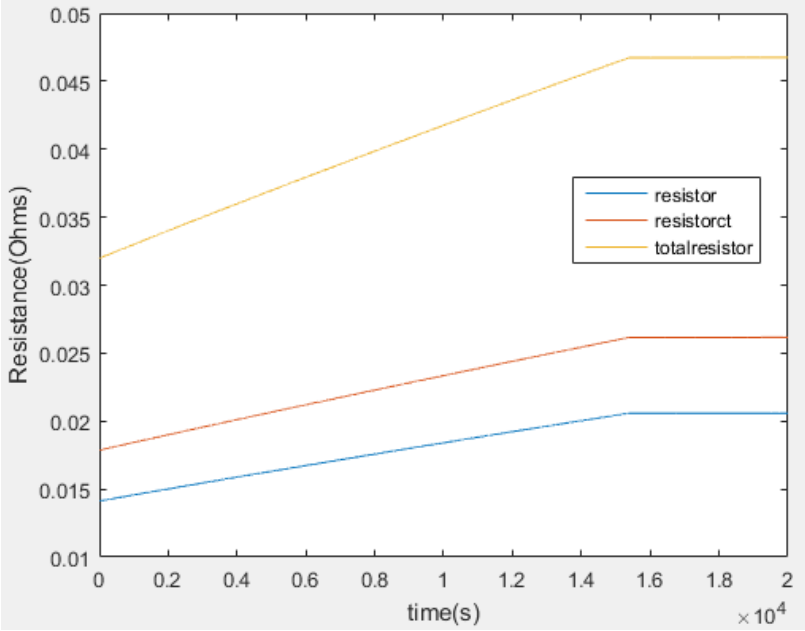


Figure 67: Resistance values variation during charging process

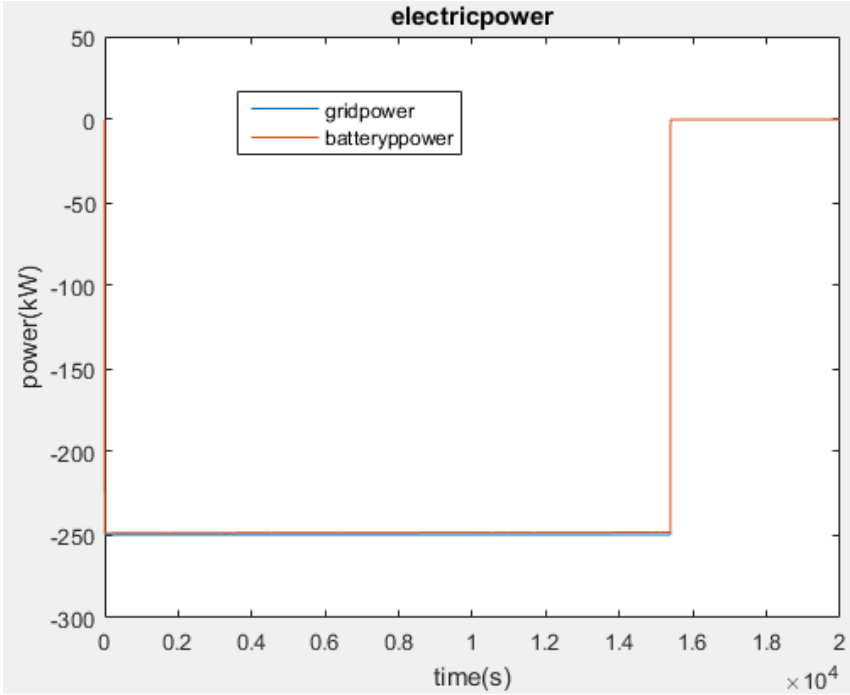


Figure 68: battery power generated by the battery and power absorb by the grid

Lithium-ion battery model

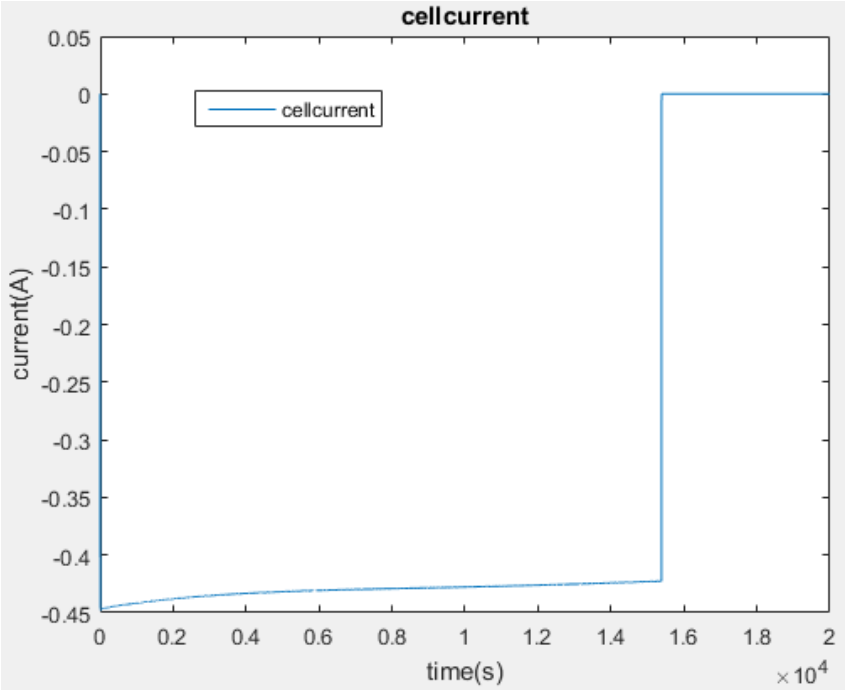


Figure 69: Cell current during Lithium-ion charge

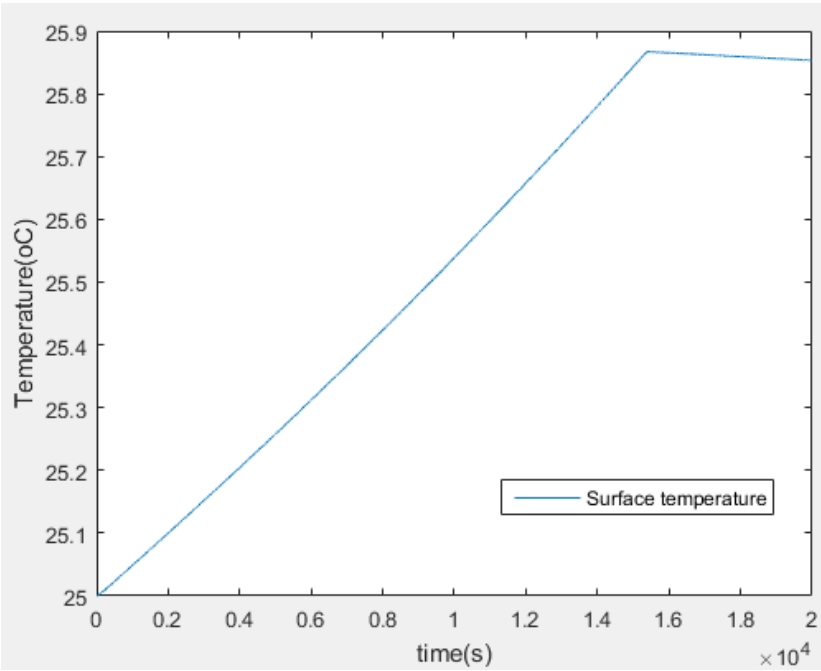


Figure 70: Temperature variation on Lithium-ion cell

4.5. Validation of the model

Here different cell models of Lithium-ion battery that appears on academic articles are discussed and compared in order to know if values of simulation are reasonable.

Table 5: Validation of Lithium-ion cell

Models	Main characteristics	Total Resistance value (ohms)	Cell output voltage	Power losses	Temperature variation	Energy capacity	Output power
The model	LiFePO4	0.032-0.048	3.25 V	5 W	2 °C	6.9 Wh 93 Wh/Kg	75 W 202kW/Kg
[20]	LiFePO4	0.050	3.25 V	9%	15°C	9.6 Wh	12.4 W
[10]	LiFePO4 (num. method)	No data	3.25 V	No data	No data	75-100 Wh/Kg	200-300 kW/kg
[7]	LiFePO4	0.032	3.25 V				
[8]*	LiFePO4	0.020	3.25 V	1.51 W 3%	5-10°C	10 Ah 30 Wh	31 W 500 kW/kg
[19]*	LiFePO4	0.032	3.25		20°C		75 W 1000kW/kg

*It should be noticed that some of that articles work in overcharge conditions. According to an article [20] specific power where LiFePO4 is around 200-300 kW/kg.

5. Case study

This chapter includes a case study of a microgrid that is going to serve for simulation purpose. It is described in the following sections.

5.1. Description

The case study is a grid-tied node of a residential area. It is connected to some photovoltaic power generators that are able to provide 200 kW power supply.

All the elements that are part of the microgrid are represented in Figure 71. They are explained below:

- i) There is a three phase transformer that works between two nodes:
 - Point of Common Coupling (PCC) that operates in medium voltage (21 kV line to line). It is considered as a reference node (Its voltage is considered time invariant in angle and magnitude).
 - Microgrid node that is connected to all microgrid elements. Its voltage value could change slightly depending on power fluctuations between microgrid and the distribution grid around 400 V (line to line).
- ii) There is a dynamic load that represents power consumption by the residential area. Data is analysed together with photo voltaic power generation.
- iii) There are some photovoltaic generators that inject energy in the microgrid. It is a renewable resource that is impossible to regulate. Some graphics are included in this section that analysed data from PV generation and data from the residential area.
- iv) There is a battery (that could be Vanadium or Lithium-ion type) that tries to minimize reverse power flow. They have been studied in previous chapters.

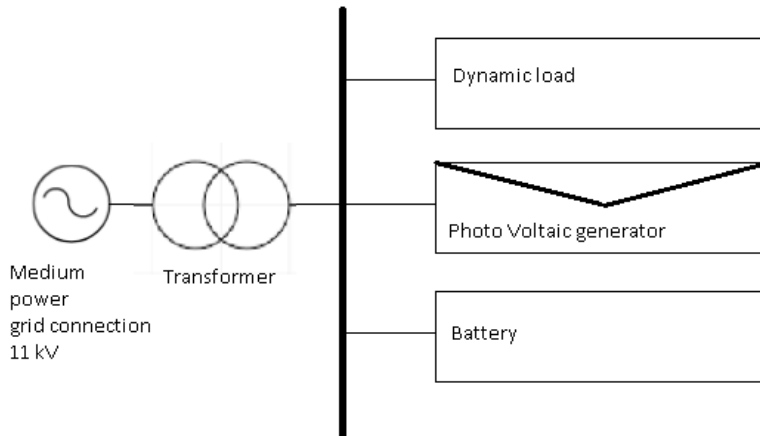


Figure 71: Single line diagram with microgrid elements (designed with AutoCad)

5.2. Distribution transformer

Distribution transformer connects secondary nominal voltage of 400 V (line to line) and Point of Common Coupling (PCC). It is chosen by looking at small distribution catalogue of ABB [21]. It is a 250 kVA transformer that has the characteristics explained below.

Oil Type/Small Distribution Transformers															
kVA	HV1 (V)	HV2 (V)	LV1 (V)	Vector Group	Impedance (%)	No-Load Loss (W)	Load Loss (W)	Noise level (dB)	Total weight (kg)	Oil weight (kg)	Length (mm)	Width (mm)	Height (mm)	Wheel base (mm)	Tank description
250	21000	0	400	Dyn5	4.5	460	3260	51	945	175	990	720	1340	520	▲

Figure 72: Catalogue of small distribution transformers of ABB [21]

It will be considered only series impedance for modelling transformer characteristics.

Series impedance is 4.5% in pu units which represents 0.0288 Ω. It is calculated using equations (41) and (42).

$$Z_{base} = \frac{V_N^2}{S_N} = 0,64 \Omega \quad (41)$$

$$Z_{cc} = Z_{pucc} Z_{base} = 0.0288 \Omega \quad (42)$$

Its resistive value is obtained knowing its series losses.

3260W-460W=2800W → Power losses

$$R_n = \frac{P_{losses}}{3I_n^2} = 0.0070 \Omega \quad (43)$$

Where, I_n represents transformer nominal current.

Finally, an inductive value X_N is calculated using R_N and Z_N .

$$X_N = \sqrt{Z_N^2 - R_N^2} = 0.0280 j\Omega \quad (44)$$

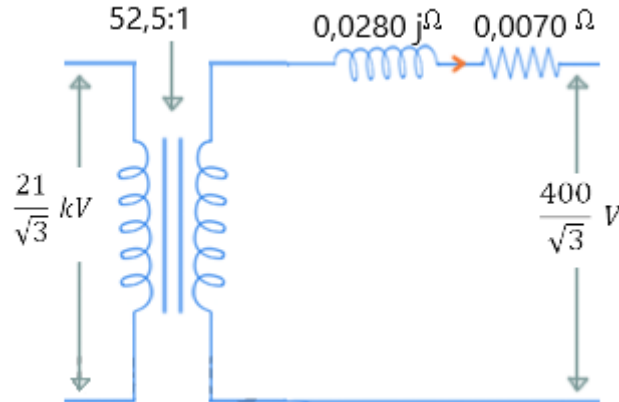


Figure 73: Distribution transformer equivalent circuit (designed with AutoCad).

5.3. Dynamic load and PV generator

Data from dynamic load and PV generator are shown together because it is easier to compare both of them together.

Figure 74 represents power demand of only one day. It is possible to see:

- Residential load that is continually changing. It is represented as a blue graphic.

- Photovoltaic generation. It changes around the day. It has a maximum level in middle day hours. There is no power generation at night as expected. It is represented as a red graphic.

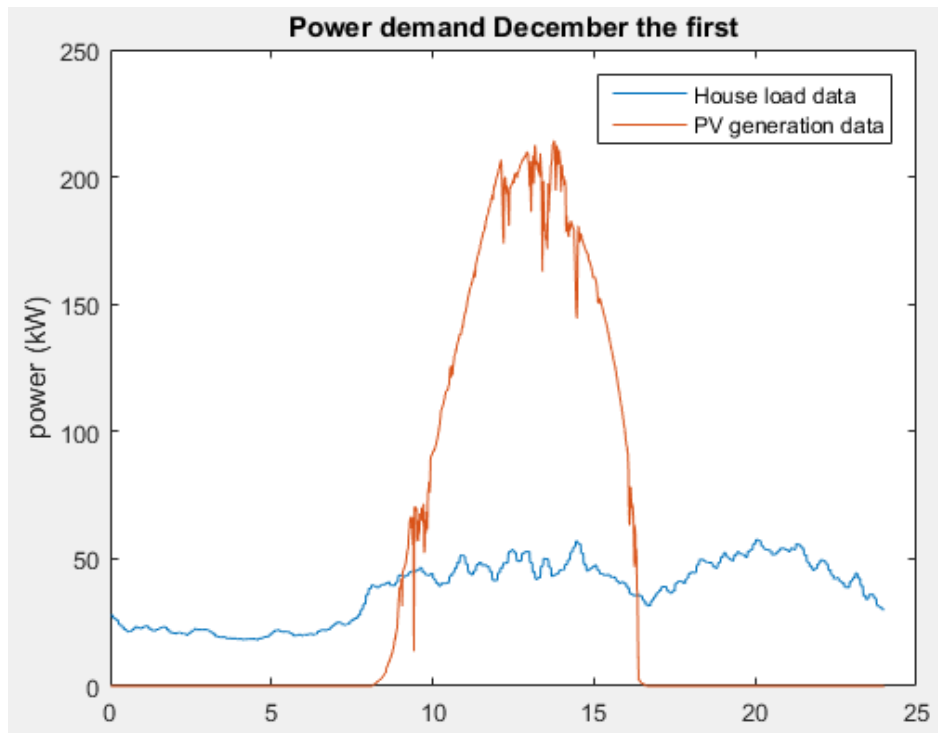


Figure 74: Example of one day power demand.

Figure 75 shows two month power consumed. It shows a noisy graph so another figure is created that divides the total amount of power demand in different levels of energy so it makes easy to observe power demand. So Figure 76 presents power consumed these two months as bar graphs. Power requirements are divided into different levels from -250kW to 100kW. It shows the total amount of hours that every level of power is required. The main goal of the batteries is to compensate the maximum quantity of reverse power flow with some of the positive levels that this batteries have.

A good way to reduce inverse power flow is trying to maintain power demand as constant as possible. The case study has an average demand that is closed to zero, so that would allow to save energy when it is produced and to utilize it when it is necessary. It is also a good way to reduce resistive losses inside distribution grids and inside transformer.

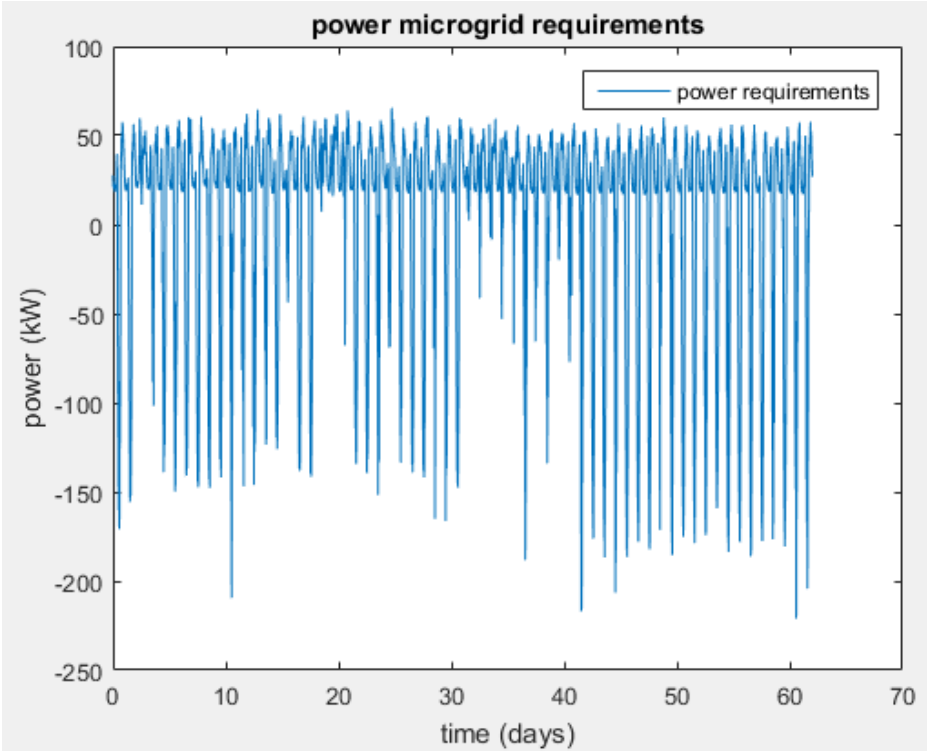


Figure 75: Power microgrid requirements on these two months.

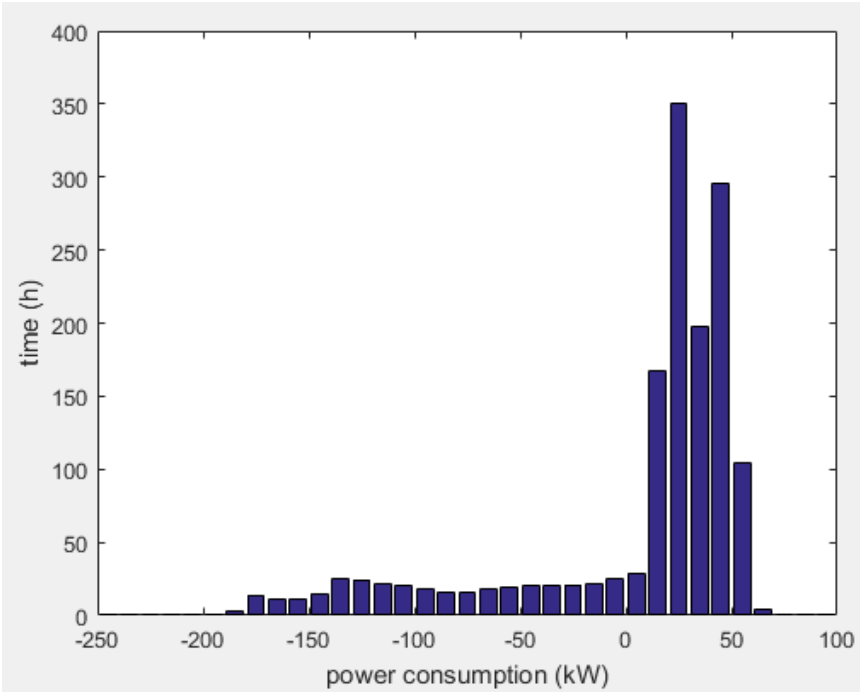


Figure 76: Power consumption of these two months divided in levels of power demand.

5.5. PCC voltage and power flow

Data consumption of this microgrid covers two months from December the 1st to January the 31st.

Voltage in microgrid node is represented as a module and an angle by phasor diagrams (Figure 77) where V_N is voltage referred to the secondary of the transformer high voltage side, Z_N is the transformer impedance, I is current that crosses the transformer in microgrid direction and $V_{microgrid}$ is voltage of transformer low voltage side. Power flow that crosses the transformer could be explained using three equations that appear below. It is consider that there is no reactive power flow from the distribution grid and all that compensation is made by the battery power inverter (that is the reason why V_N and I have no angle difference).

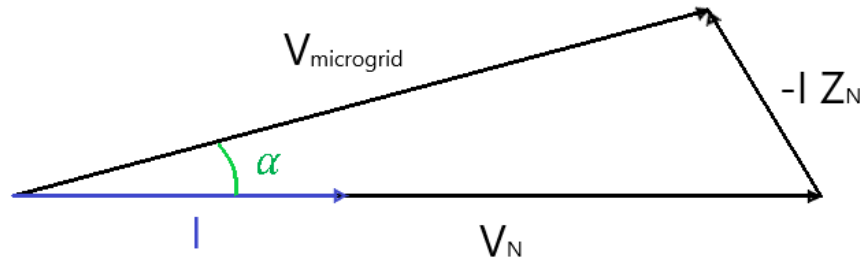


Figure 77: Phasor diagram of current and voltages in CCP

Newton-Raphson is not utilized to calculate voltage value as it is usual in power systems problems. As there are only two nodes and a transformer that connects them, it is solved as an analytic problem. Equations are (45), (46) and (47). Solutions are represented in (48) and (49). Where V_N is nominal voltage of distribution grid referred to the secondary, I is current that crosses transformer in microgrid direction, $V_{cosmicr}$ is projection of microgrid voltage over distribution grid voltage, $V_{sinmicr}$ is the perpendicular part of microgrid voltage with the distribution voltage.

$$P_{req} = \sqrt{3} * V_N * I - 3 * R_N * I^2 \quad (45)$$

$$P_{req} = \sqrt{3} V_{cosmicr} * I \quad (46)$$

$$3 * X_N * I^2 = \sqrt{3} V_{sinmicr} * I \quad (47)$$

Simulation and results

Current is calculated solving a second order equation (48). There are two possible solutions to that equation. Smallest current value solution is selected as correct in (49).

$$3 * R_n * I^2 - \sqrt{3} * V_n * I + P_{req} = 0 \quad (48)$$

$$I = \frac{V_N}{2\sqrt{3}R_N} - \sqrt{\frac{V_N^2}{12R_N^2} - \frac{P_{req}}{3R_N}} \quad (49)$$

The microgrid voltage is calculated knowing current flow. First, voltage projections should be calculated with the current value of equation (49). The different microgrid voltage projections could be calculated using (50) and (51).

$$V_{sinmicr} = \sqrt{3}X_N I \quad (50)$$

$$V_{cosmicr} = \frac{P_{req}}{\sqrt{3}I} \quad (51)$$

All that equations have been represented as Simulink blocks represented in Figure 78. Fcn is a block where second order equation is solved (48). The other blocks represent equations (49) and (50).

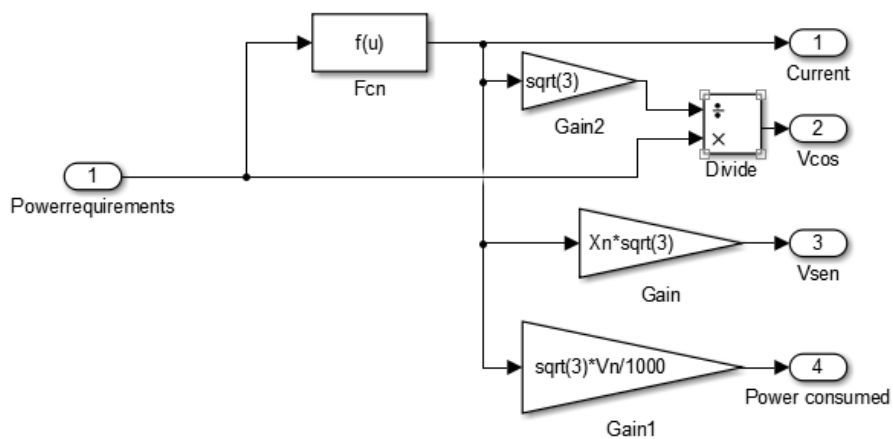


Figure 78: Current, microgrid voltage components and power consumed calculated from power that is demand from the microgrid side.

Figure 79 represents a subsystem that computes microgrid voltage (module and angle) and current. It uses as input the power that flows in PCC and it obtains reactive power required by transformer, angle difference between microgrid node and distribution grid node, microgrid node module and current that crosses the CCP. The equations are represented below:

- i) Reactive power injection by the microgrid to compensate transformer inductive power. It is calculated in equation (52).

$$Q = \sqrt{3}V_{sinmicr}I \tag{52}$$

- ii) Angle difference between microgrid node and distribution grid $\alpha_{microgrid}$. It is calculated using equation (53).

$$\alpha_{microgrid} = \tan^{-1} \left(\frac{V_{sinmicr}}{V_{cosmicr}} \right) \tag{53}$$

- iii) Microgrid voltage calculation. It is calculated with equation (54).

$$V_{microgrid} = \sqrt{V_{sinmicr}^2 + V_{cosmicr}^2} \tag{54}$$

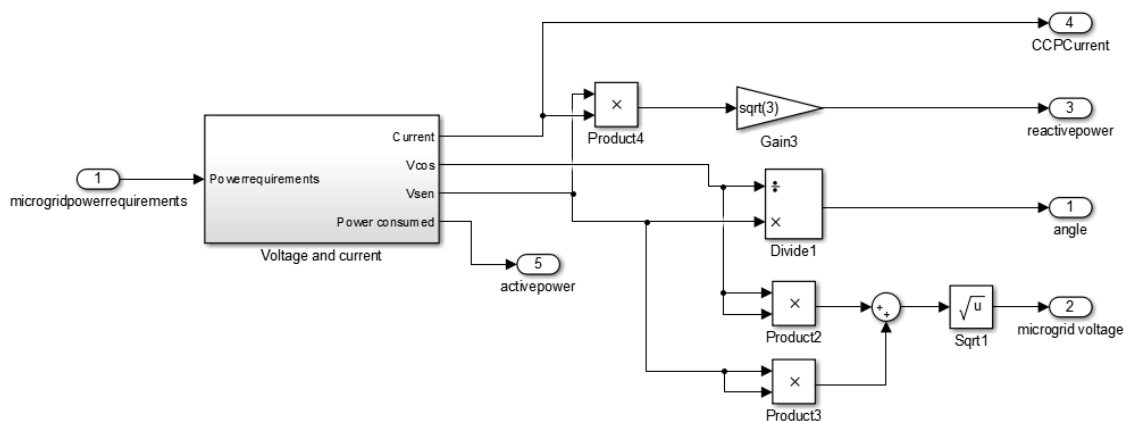


Figure 79: Subsystem that computes power flow across distribution transformer.

6. Control strategy

This chapter will explain the control strategy. It could be divided into two parts:

- i) Power reference calculation
- ii) Current regulator

6.1. Power control strategy

This part tries to minimize reverse power flow in CCP. The power strategy is based on a work [22] that could be seen on Figure 80. Basically, it calculates an average power required that is close to zero if PV generators are well scaled and let battery reduce any kind of variation that could exist. That includes most of the reverse power flow.

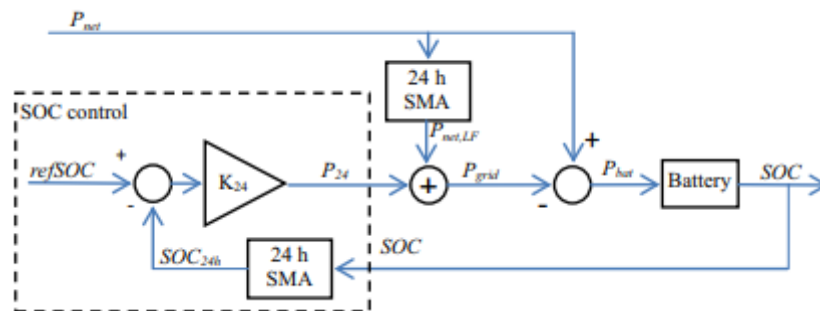


Figure 80: Power management strategy of UpNa [22].

Main objective of control strategy is to calculate a power reference value that battery must follow. Figure 82 is a subsystem block that calculates it. It uses SOC and mean average value of the last 24 hours to calculate it and to use it as reference. As it is possible to see in results chapter, power demand from the distribution grid keeps always close to 0 kW power requirements avoiding inverse power flow.

Another way to analyse all that data of these two months is doing a simple mean average with the power generated. With that on mind, it is possible to find tendency without any possible hour-dependant variation. Figure 81 is the Simple Mean Average that is improved in the control strategy. It is possible to see that average power requirements are bounded between -10 kW (sunny days) and 34 kW (some cloudy winter days that have no PV generation).

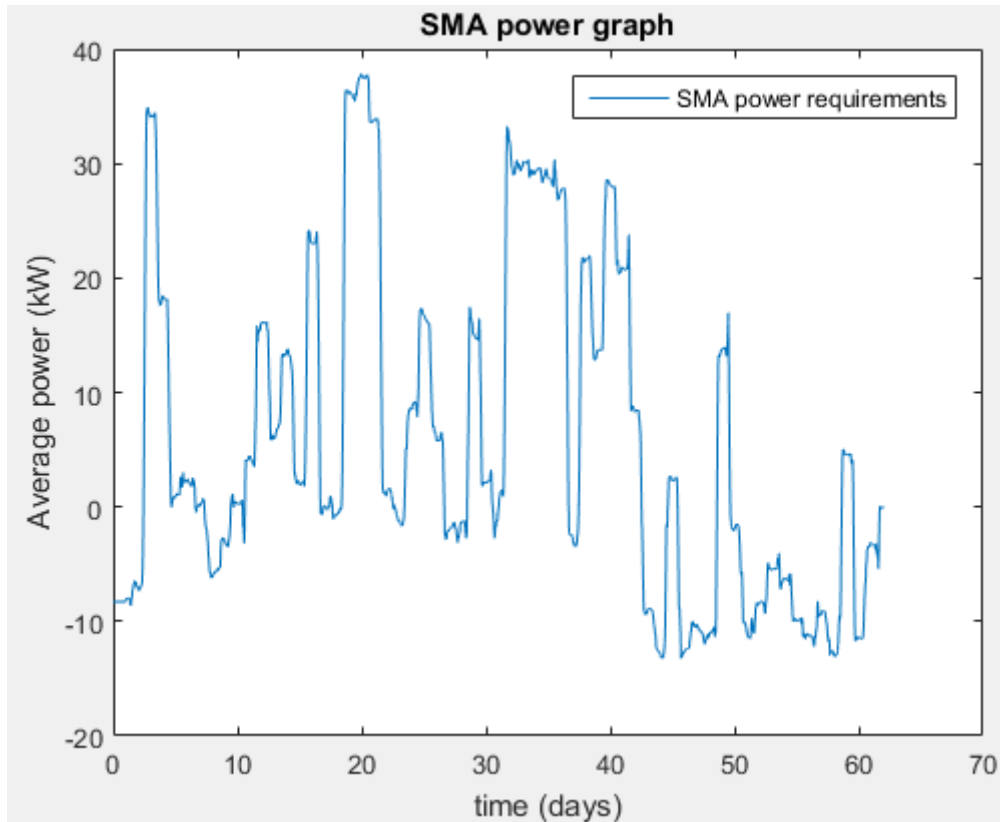


Figure 81: Simple Average Power requirements that is used as power reference by the control strategy

Figure 82 represents that control part that calculates battery power reference. It represents an average value of last 24 hours that is used as reference for power consumption of the microgrid. Main objective of battery is provided power or save it to maintain as close as possible to SMA value power required by the battery. It also tries to maintain SOC far away from 0 and 1 values. Scenarios in where capacity to regulate batteries is lost.

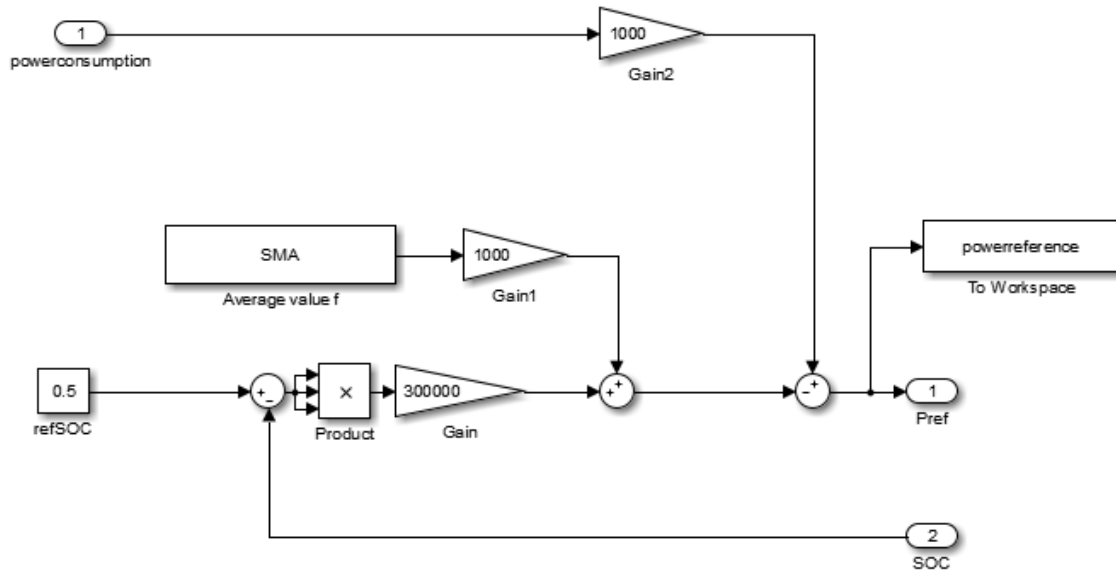


Figure 82: Power reference subsystem control block

6.2. Current regulator

That second part of the battery control is a close loop control strategy that has as input the power reference and it has as output the current that enters into the battery. Figure 83 is the Simulink subsystem current regulator that is divided into two parts:

- i) Yellow part tries to maintain SOC battery values inside a safety region. It is based on SOC safety values to not produce secondary reactions.
- ii) Blue part is a PI anti wind-up current controller that tries to maintain battery power output as closed as possible to power reference calculated in yellow part.

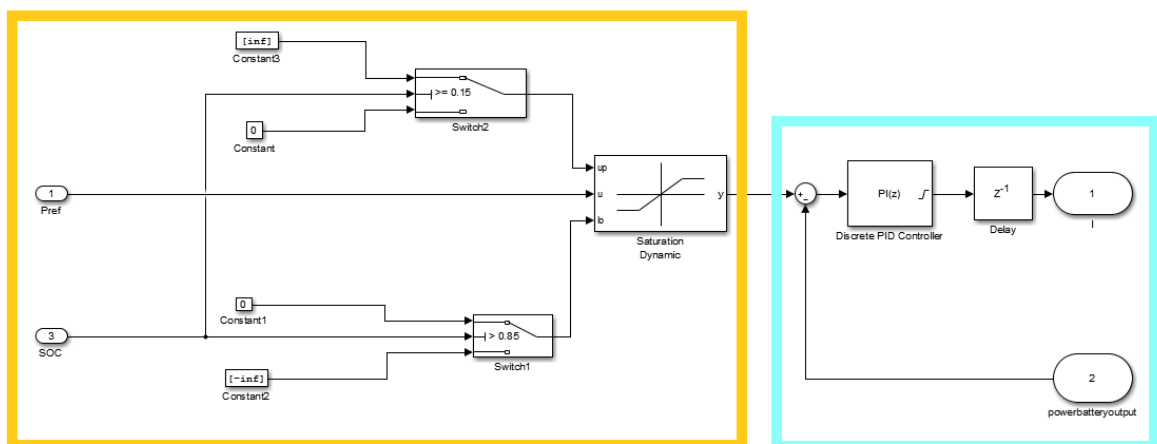


Figure 83: Current regulator

Figure 84 is explained with Table 6. Basically it considers that under certain value of SOC, power reference should not be positive to not over discharge battery. It also considers that over certain value of SOC, power reference should not be negative, to not overcharge battery.

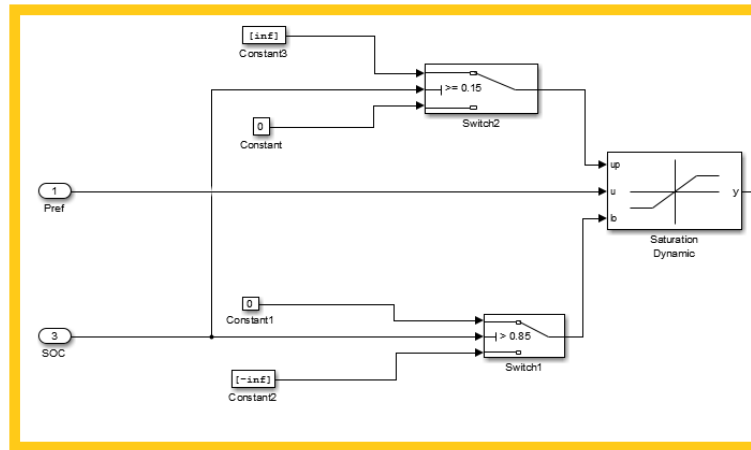


Figure 84: Security margins in current regulator

Table 6: Power reference limits calculated in Figure 84.

Power limits	SOC < 0.15	0.15 >= SOC <= 0.85	SOC > 0.85
Upper limit	0	[Inf]	[Inf]
Down limit	[-Inf]	[-Inf]	0

Figure 85 is a closed loop that compares power required and battery power output. A Proportional-integrator controller computes current input of the battery. There is a safety saturation margin and an anti-wind up system that doesn't allow higher currents than battery limits.

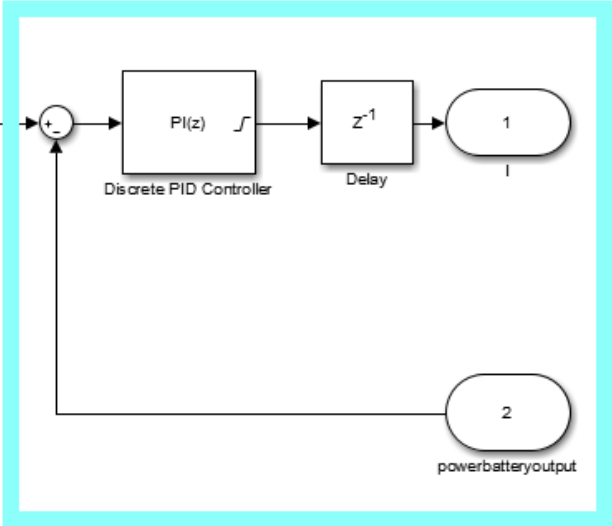


Figure 85: Current regulator closed loop

7. Simulation and results

7.1. Simulation description

Figure 86 show all the subsystems that completely divide the model. Blue block is control strategy that is discussed in chapter 6. Yellow block is battery that could be Vanadium flow (chapter 3) or Lithium-ion one (chapter 4). Green block represent rack aggregation and inverter and pump losses (discussed in last part of chapters 3 and 4). Orange block represents microgrid variables and it is explained in chapter 5.

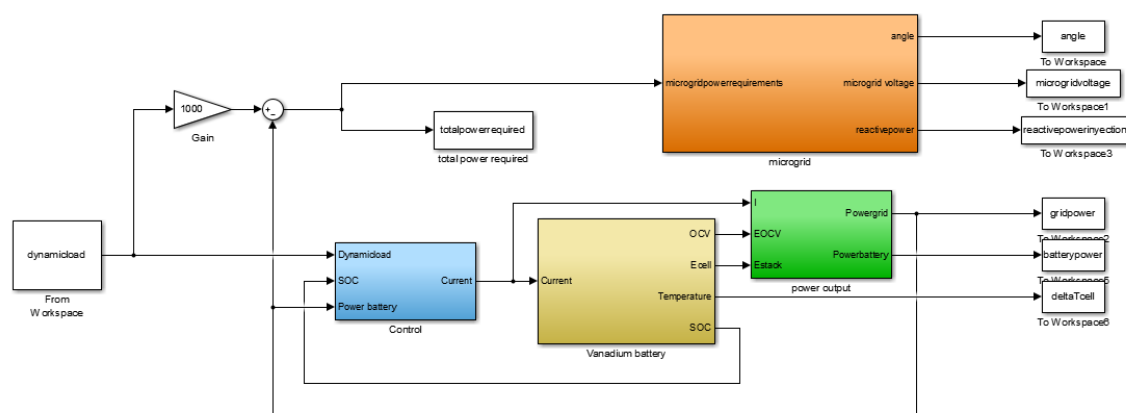


Figure 86: Control + battery model validation

Simulations (Vanadium and Lithium-ion) are made in discrete mode (1 second time step). A period of time of 2 months has been simulated to provide enough data. It provides information from December the 1st to January the 31st. A comparative between different simulations is represented in next figure.

Figure 87 groups distribution power grid demand in three different scenarios.

- i) First scenario is power demand without any battery. Data is taken from Figure 76 (from chapter 5. Case study) and represents different levels of power requirement and the number of hours that this quantity of power is required these two months.
- ii) Second scenario represents Vanadium flow battery and it is possible to see that grid power requirements start to be close to 0 kW, avoiding reverse power flow.
- iii) Third scenario is power required by microgrid when lithium-ion battery is helping to reduce reverse power flow. It is a more efficient battery than Vanadium one, so power flow is moved to the left.

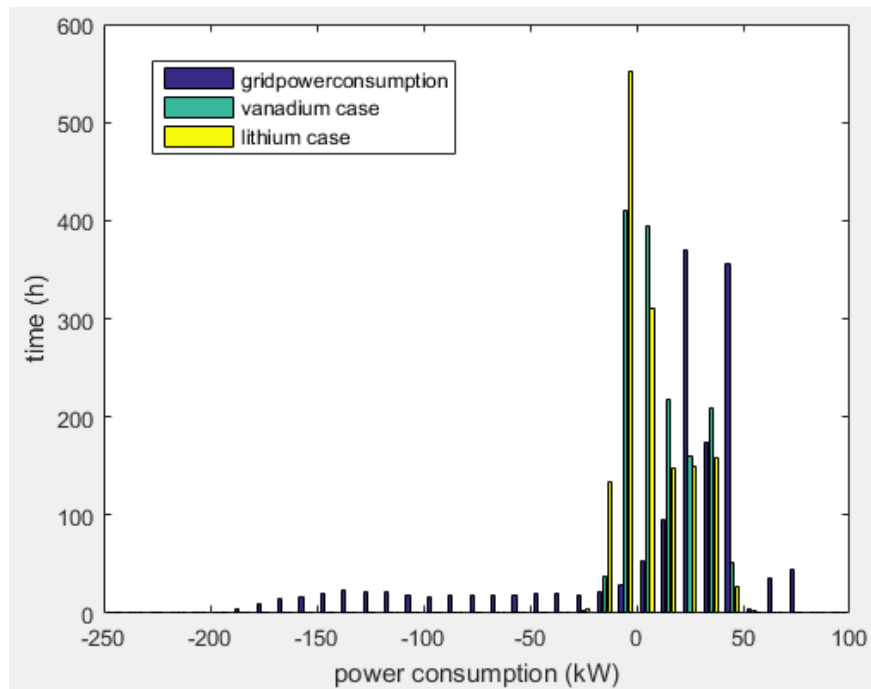


Figure 87: Power levels required in three different scenarios. Without battery, with vanadium one and with lithium-ion.

7.2. Results in Vanadium-flow battery simulation

These are the values of different vanadium flow battery variables in that simulation. Variables as temperature, heat generation, OCV, output voltage, SOC and power flow are simulated and represented in the following pages.

Figure 89 represents power flow from the transformer to the microgrid node on January the 9th. Red graph represents active power and it is close to 30 kW of continuous power injection that is the average power required that day (it is a cloudy day). Blue line represents reactive power injected in the transformer and that is necessary to compensate reactive power requirements. It is around 0.15 kVAR.

Figure 90 and Figure 91 represent microgrid line voltage and angle gap. Line voltage variation allows to the microgrid the ability to compensate reactive power requirements by the microgrid in order to maintain a power factor of 1. Angle gap is the angle difference between the microgrid voltage and CCP voltage and is what allows active power movements between those two nodes.

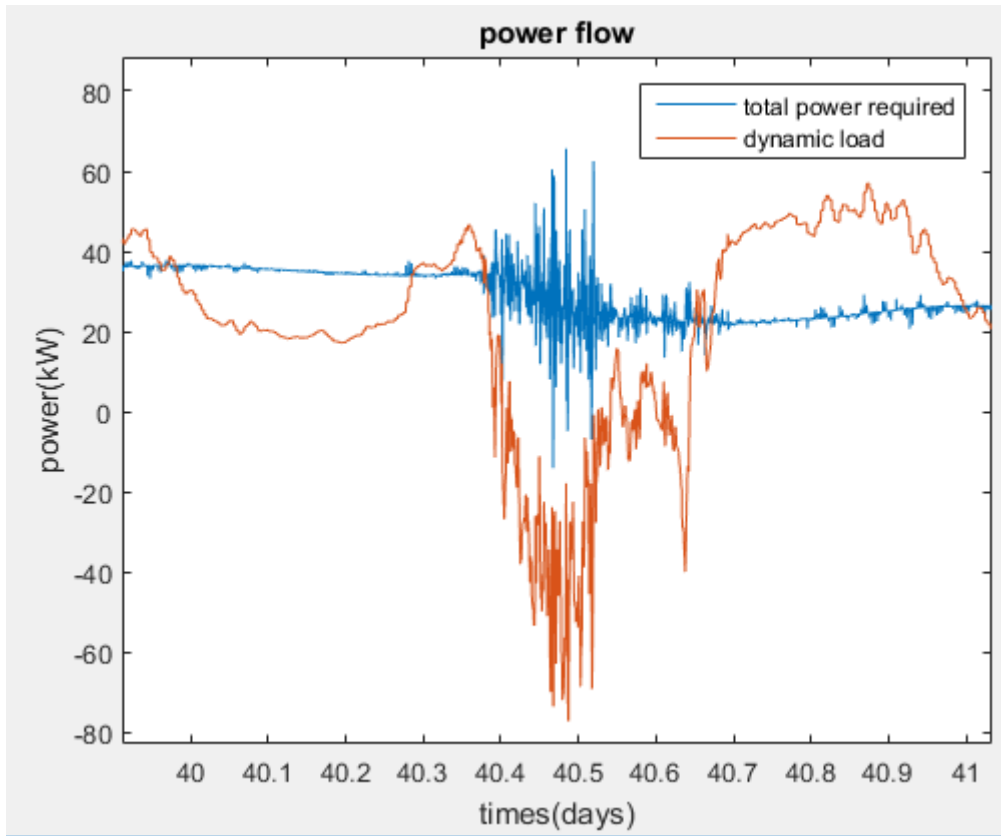


Figure 88: Power required using the control strategy selected and power required by the residential load and PV generators

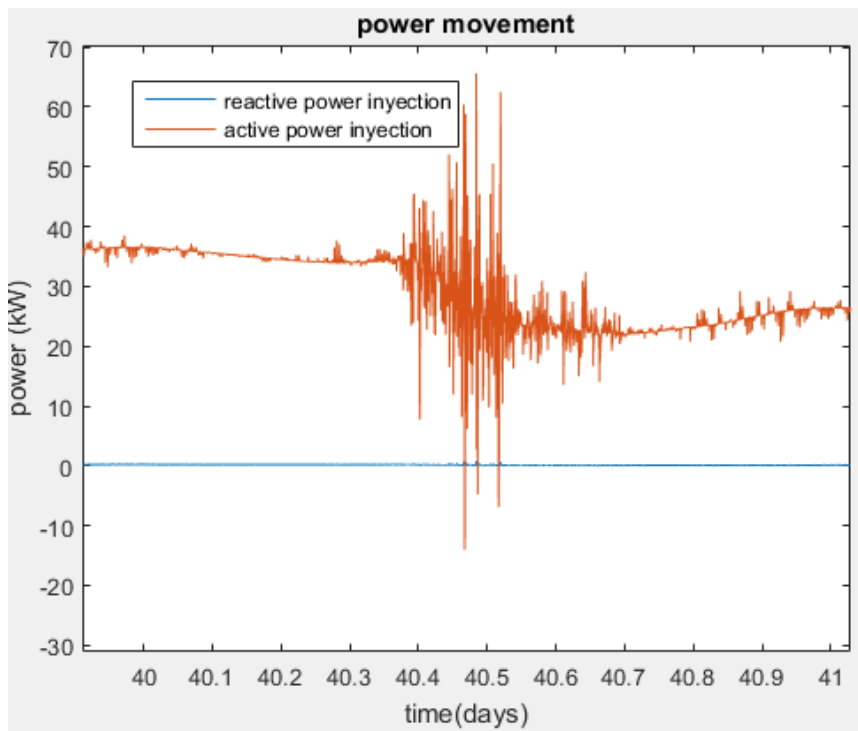


Figure 89: Power flow between microgrid and distribution grid in Vanadium battery case in January the first.

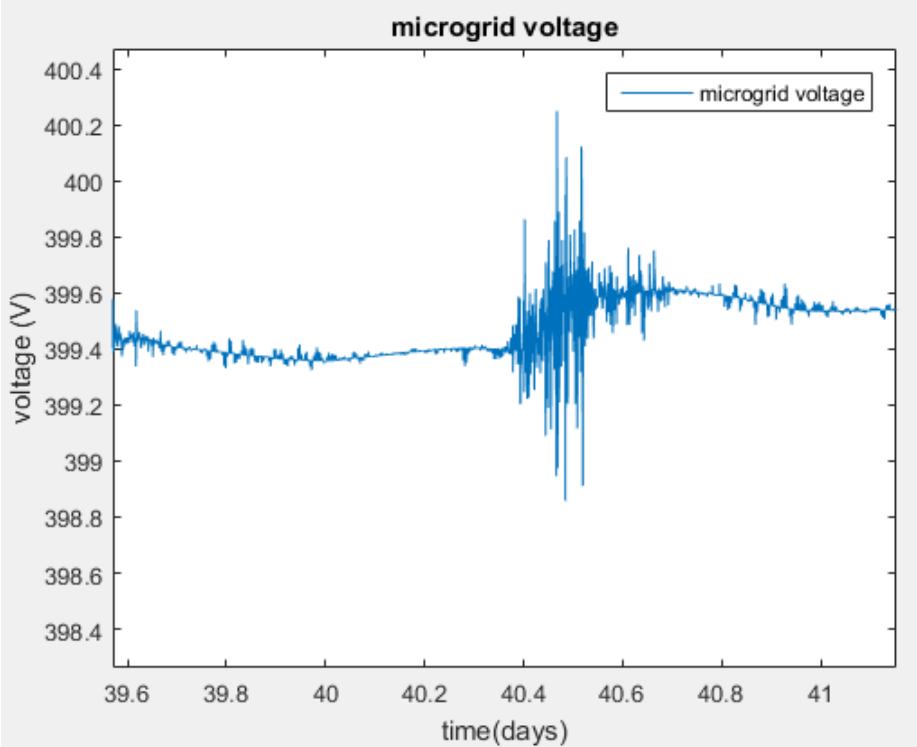


Figure 90: Voltage value of microgrid node in Vanadium flow case on January the 9th.

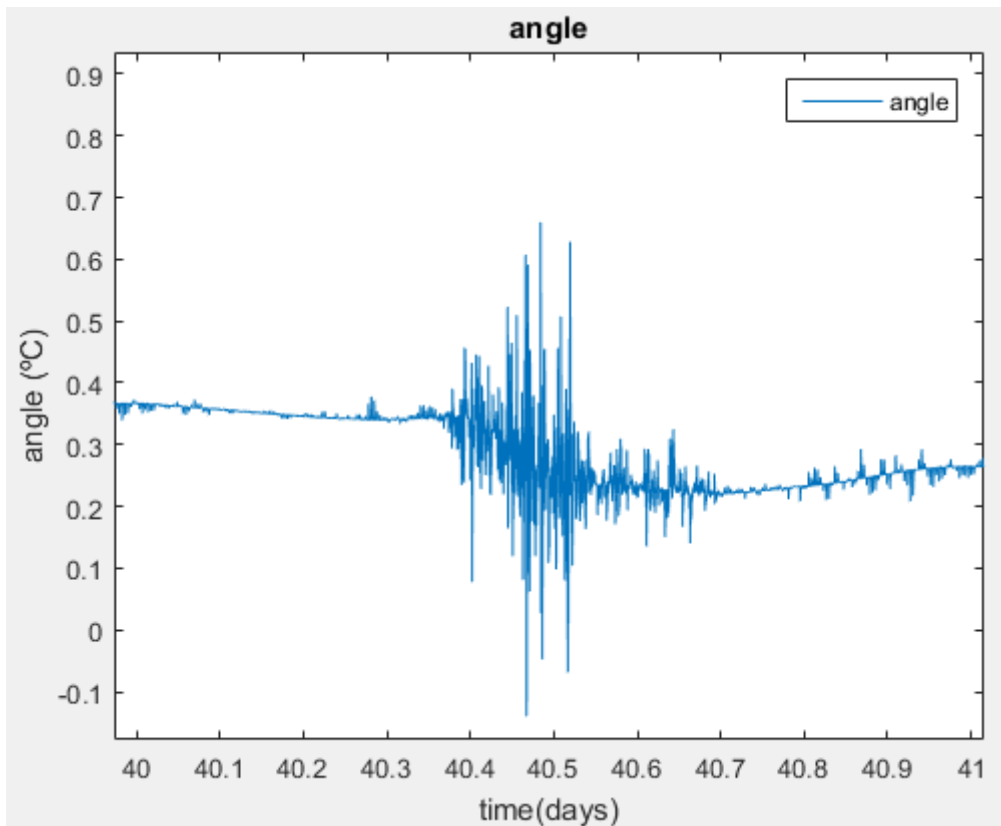


Figure 91: Angle difference between microgrid node and distribution node in rad in Vanadium case in January the 9th.

Figure 92 represents power injection by the battery following the control strategy discussed in the previous section. Battery is able to take from the grid power fluctuations in order to reduce power fluctuations and some large power requirements maintaining microgrid power requirements as smooth as possible.

Figure 93 represents heat generation at each moment of time by the battery modelled. It is possible to see that heat generated increases with power demand from the battery. When power flow between battery and microgrid is high, heat generation is greater. It is also noticeable that power pump losses are one of the main power losses and to reduce that is something that could be improved from that model.

Figure 94 represents temperature inside tanks and inside cells. External temperature keeps constant at 25°C so due to heat generation temperature increases around 10 °C inside the battery.

Figure 95 shows SOC values on January the 9th. It is possible to see how these values keep changes during the day. SOC increases at night while the battery is charging and dynamic low demand is low and discharges during the day that is when power consumption increases.

Figure 96 represents species concentrations that are in stack and in tanks. It is possible to see that stack concentration species change faster than tank ones.

Figure 97 compares OCV that is obtained by Nernst equation and output voltage that is going to be smaller when battery is discharging and bigger when battery is charging.

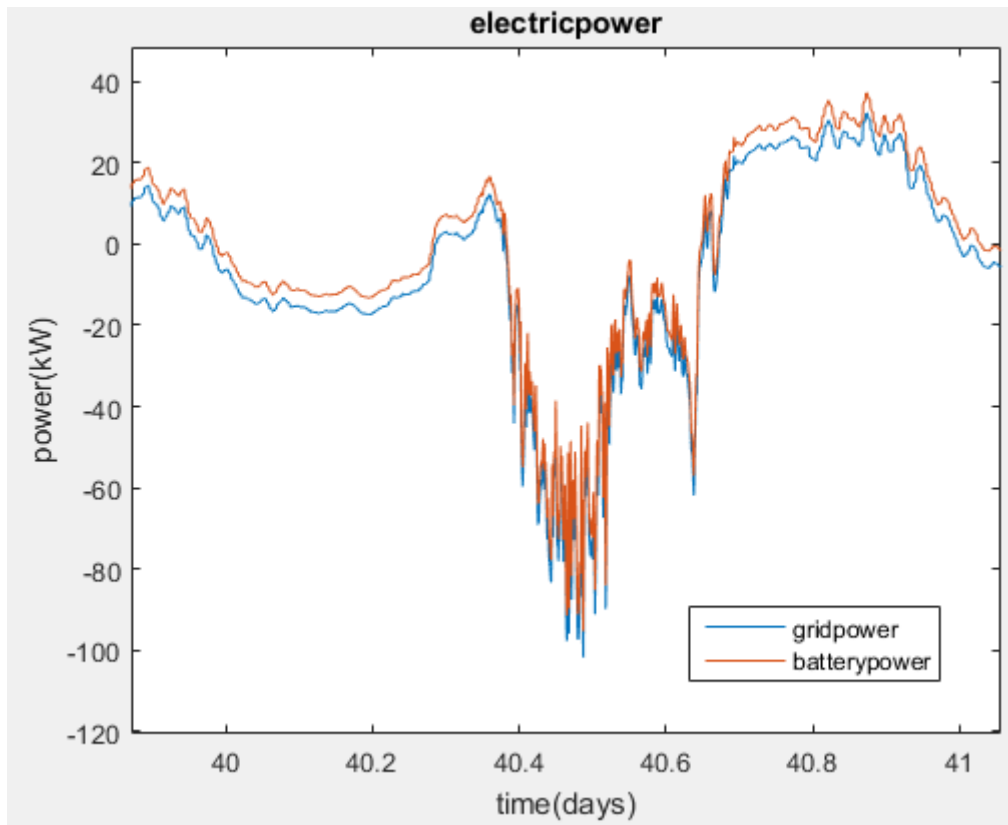


Figure 92: Battery power injection in Vanadium case on January the 9th.

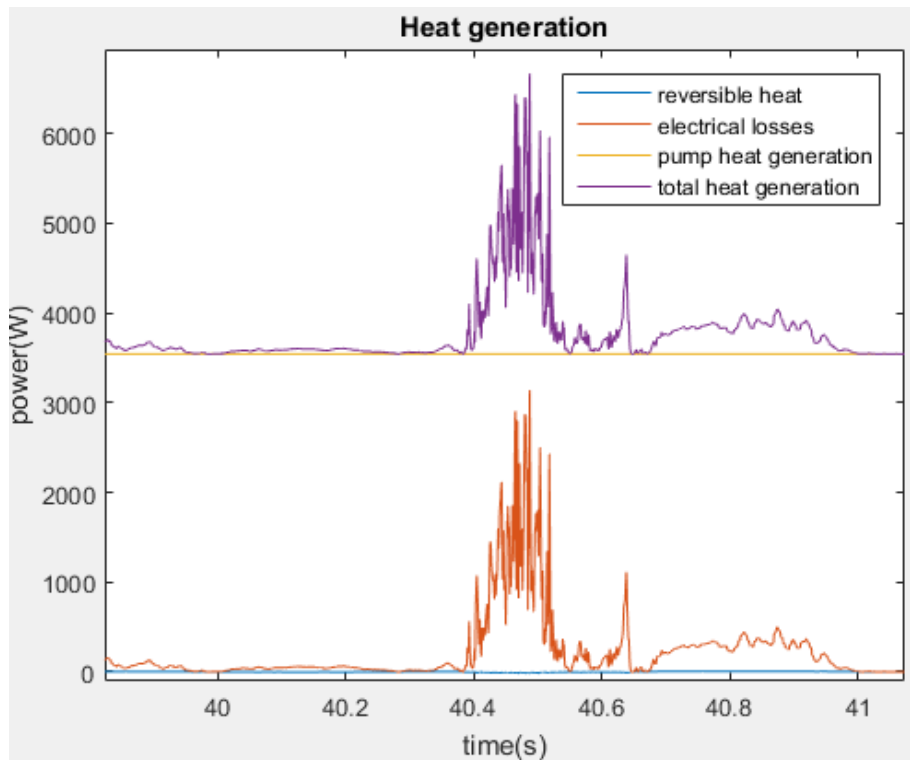


Figure 93: Heat generation in Vanadium case on January the 9th.

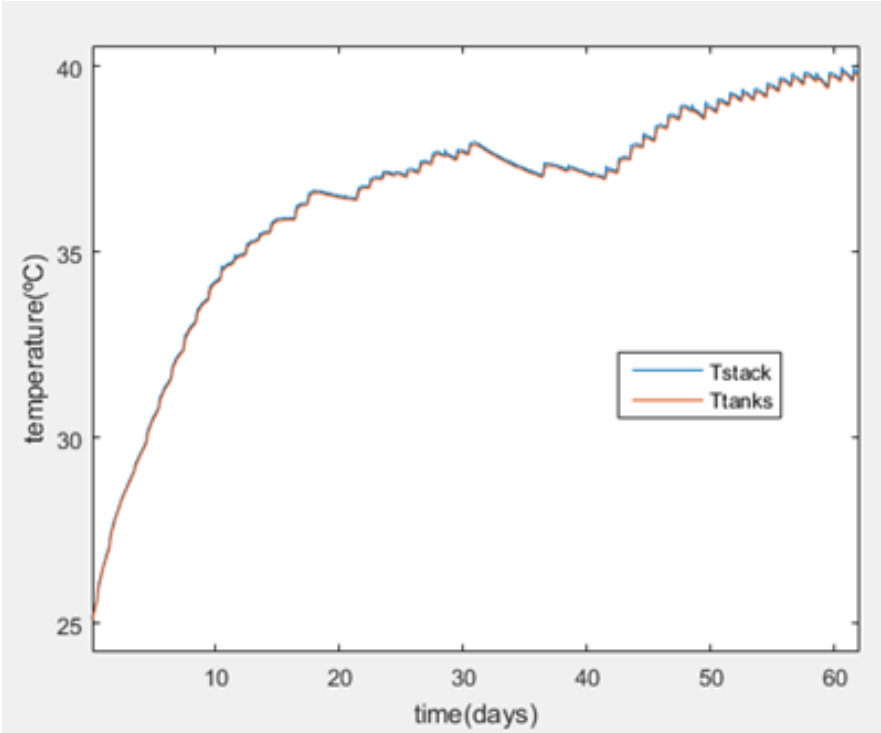


Figure 94: Temperature variation in Vanadium case on these two months

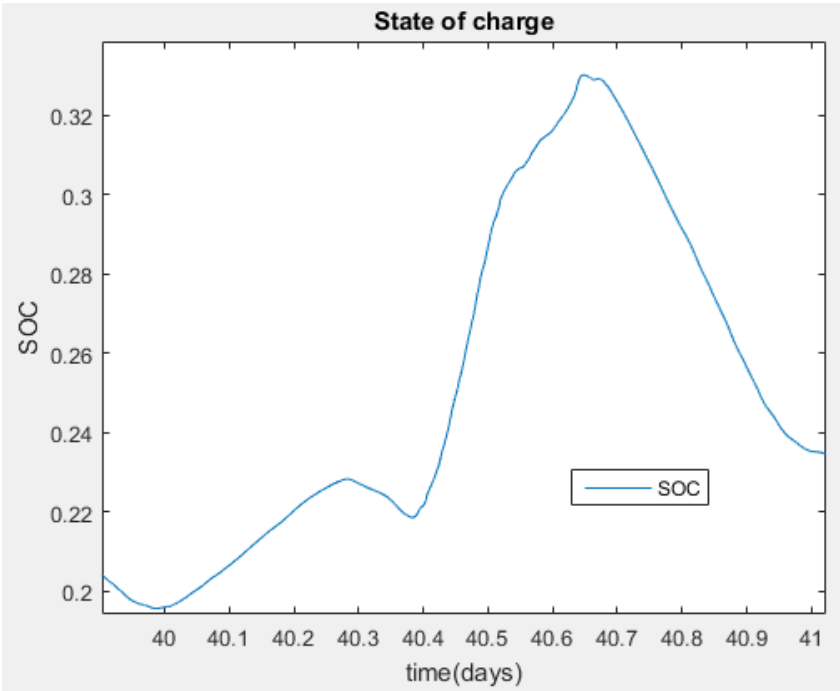


Figure 95: SOC variation on Vanadium case on January the 9th.

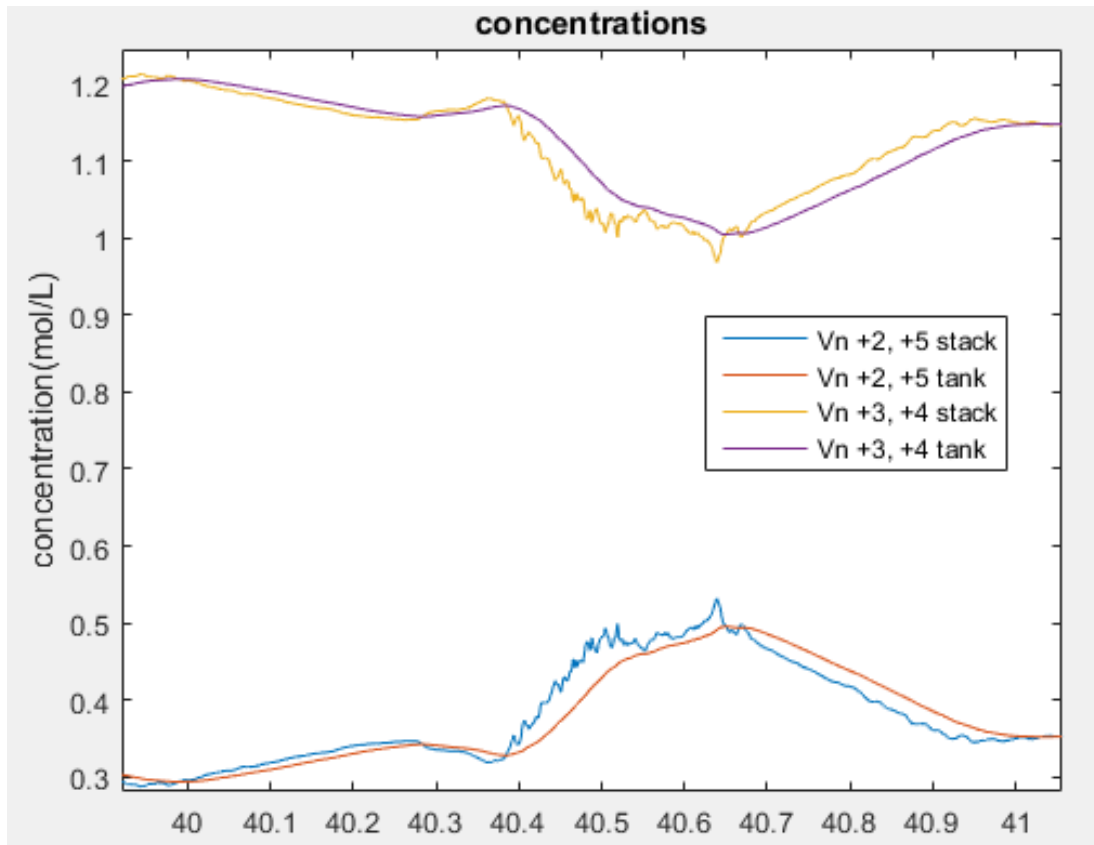


Figure 96: Stack and tank concentrations in Vanadium case on January the 9th.

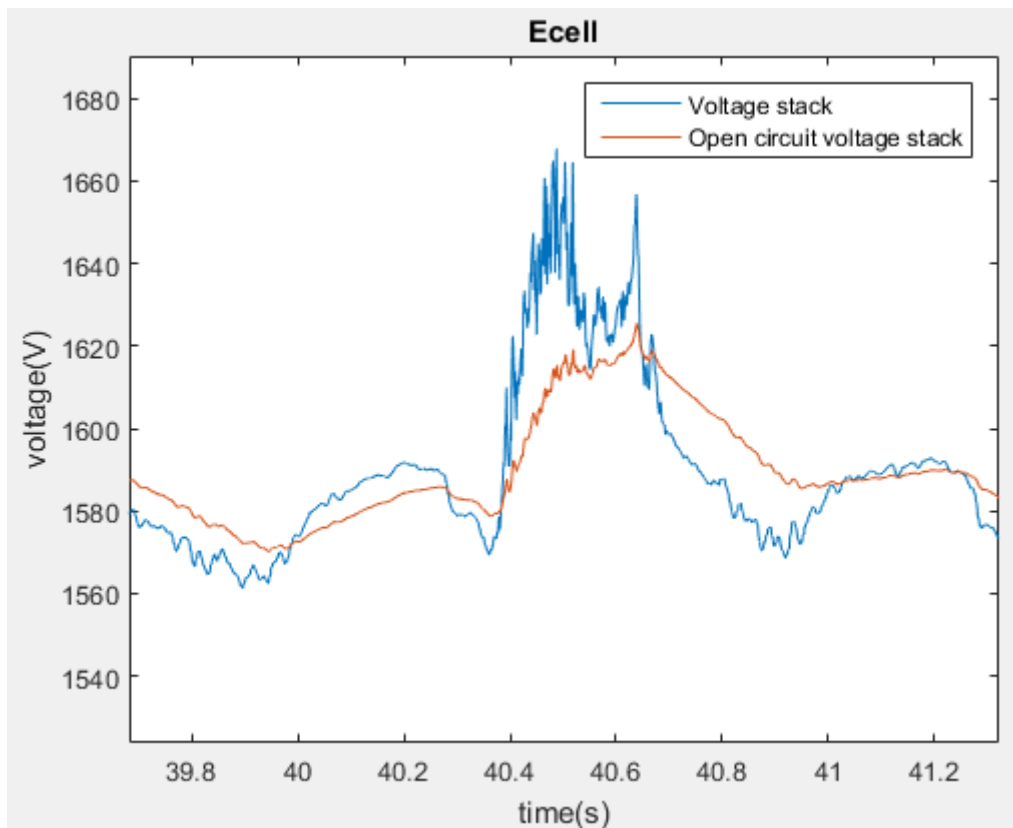


Figure 97: OCV and output voltage comparative in Vanadium case on January the 9th.

7.3. Results in Lithium-ion battery simulation

These are the values of different lithium-ion variables in that simulation. As in Vanadium case, some of the physical variables are represented. That is the case of SOC, OCV, output voltage, power flow, heat generation or surface temperature.

Figure 98 represents OCV and output voltage. As it happens in Vanadium case output voltage used to be bigger in discharging processes and it used to be smaller while battery is charging.

Figure 99 represents SOC in Lithium-ion case and it is possible to see that values are similar to those obtained in Lithium-ion case. SOC is increasing its value at night in valley hours and it decreases during peak hours.

Figure 100 represents power flow between microgrid and distribution node. It is similar to Vanadium case. Control strategy tries to minimize active power flow movements in CCP and there is a reactive power injection around 0.15 kVAR that compensates transformer inductive effects to the distribution grid and it could be considered despicable.

Figure 101 compares different heat generation values that are inside that battery. It is important to notice that this battery is moving less specific power than nominal power so losses are less than planned and efficiency is higher than expected.

Figure 102 shows surface temperature of each cell. Temperature variations are smaller than 1°C.

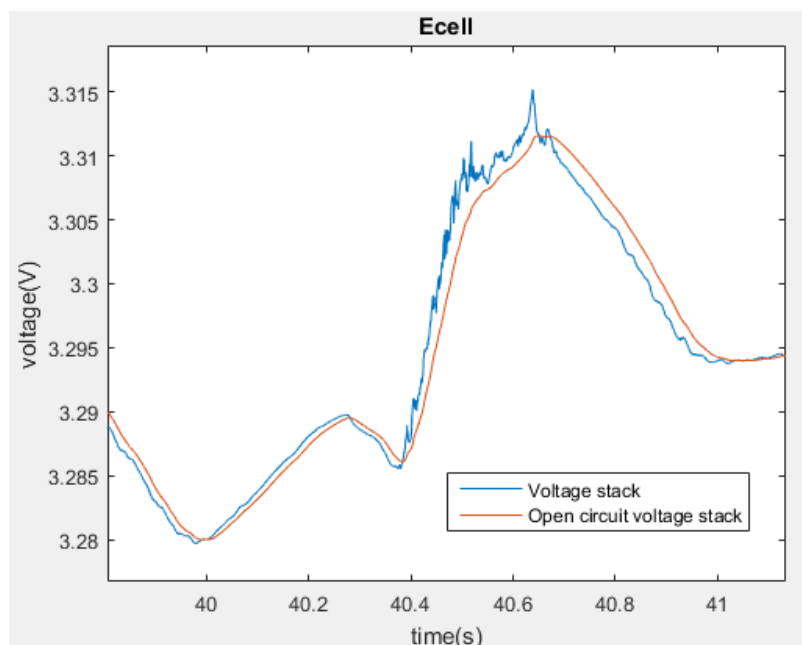


Figure 98: Cell voltage in Lithium-ion on January the 9th.

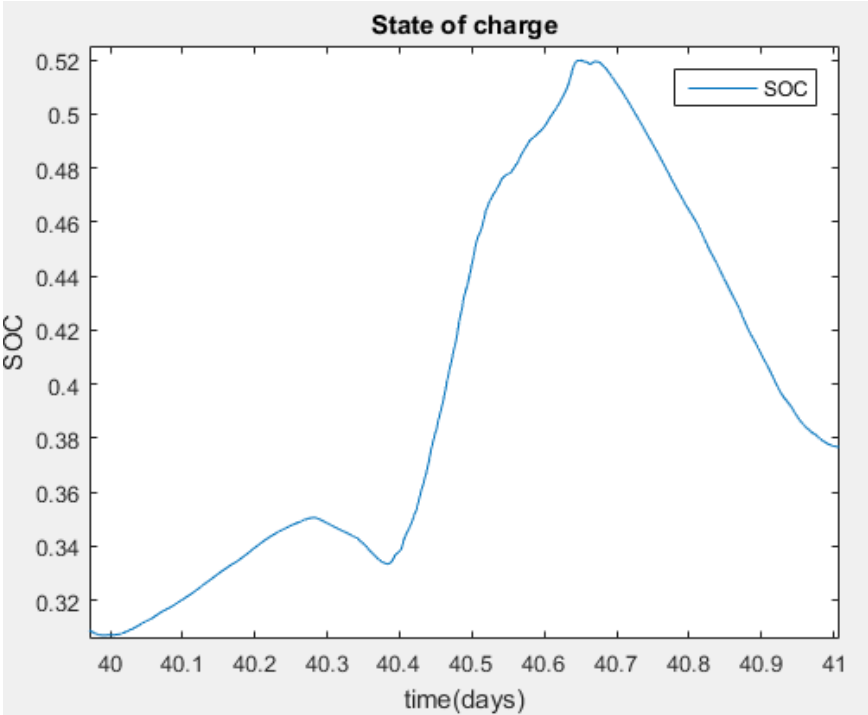


Figure 99: SOC for Lithium-ion on January the 9th.

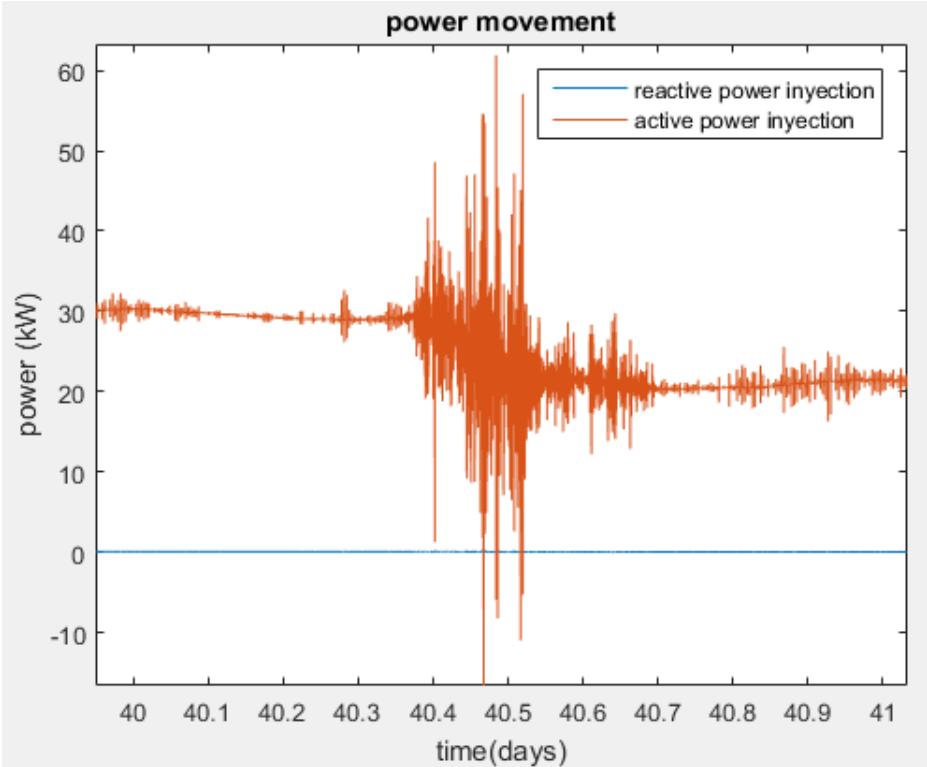


Figure 100: Power flow in Lithium-ion on January the 9th.

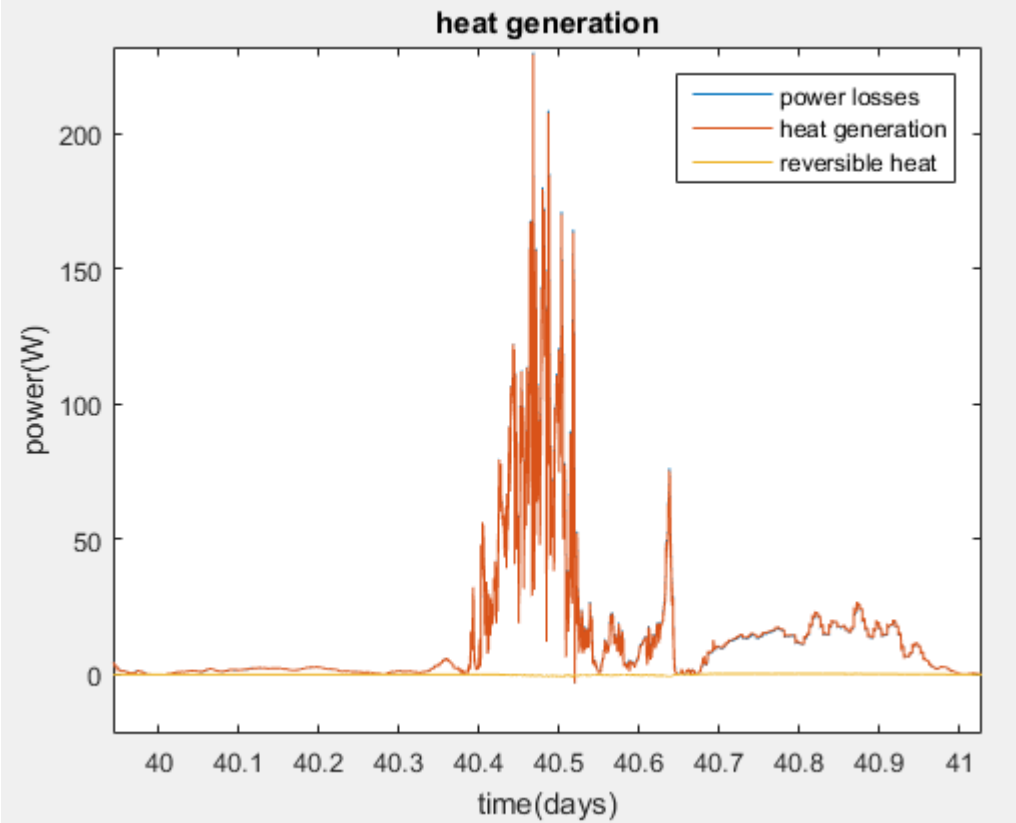


Figure 101: Heat generation in Lithium-ion on January the 9th.

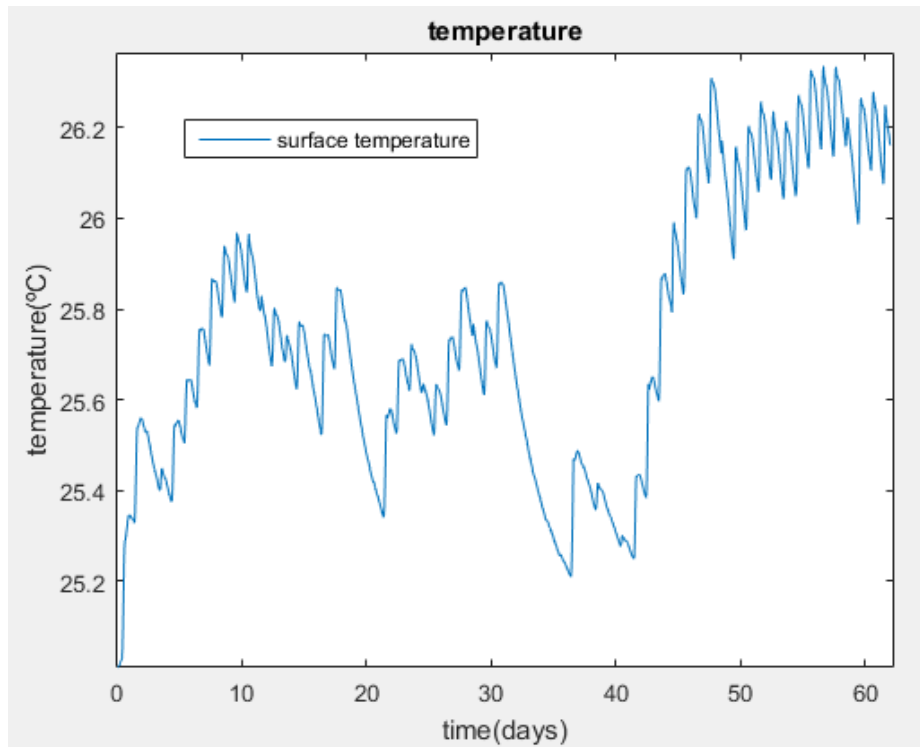


Figure 102: Temperature variation in Lithium-ion on these two months.

Figure 103 represents active power injection that is made by the battery. It tries to reduce power flow between these two nodes.

Figure 104 and Figure 105 represents microgrid line voltage and angle gap that exists between the two nodes.

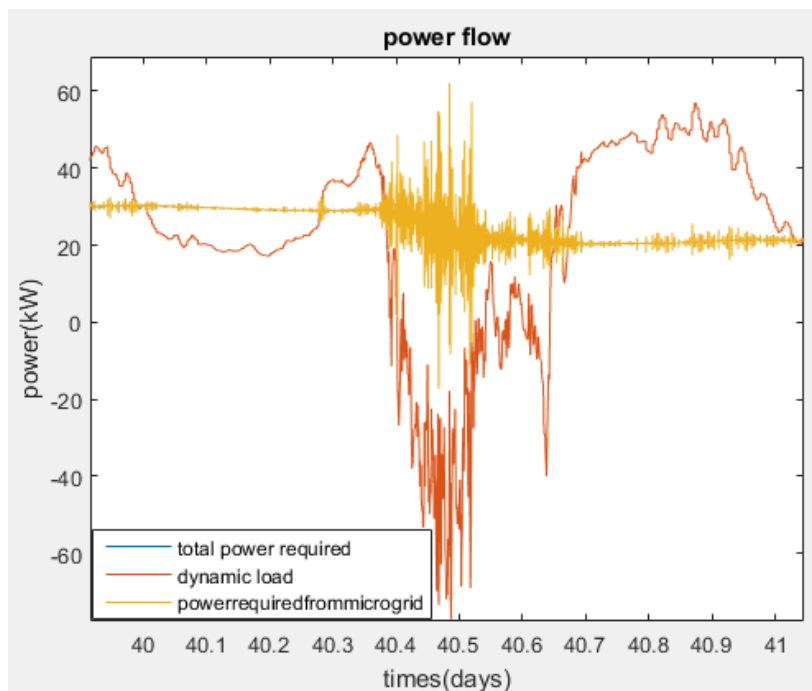


Figure 103: Battery power generation in Lithium-ion on January the 9th.

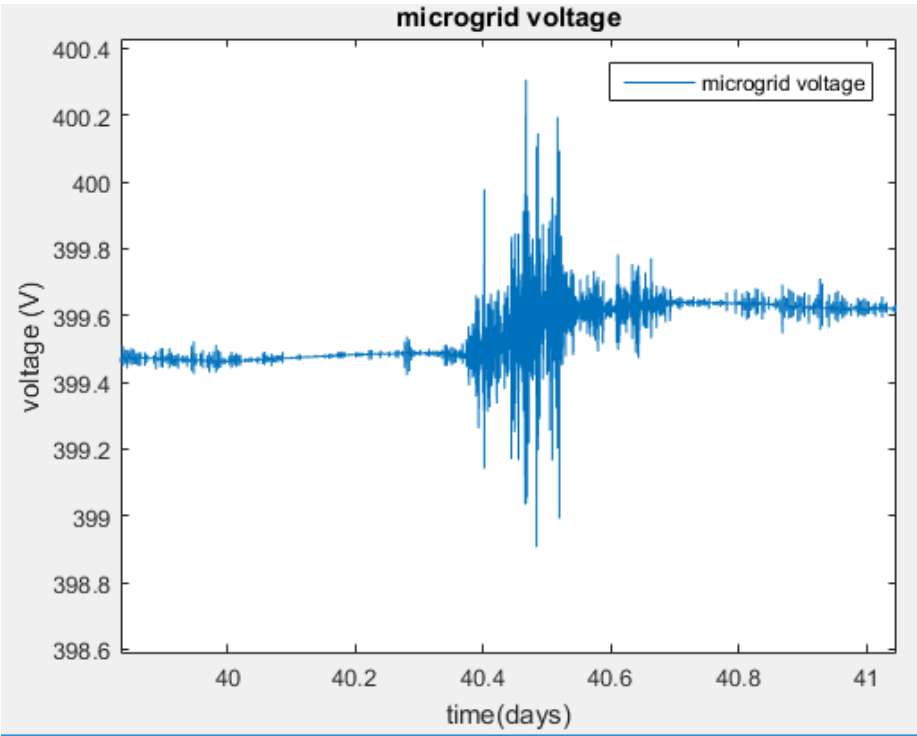


Figure 104: Microgrid node voltage in Lithium-ion on January the 9th.

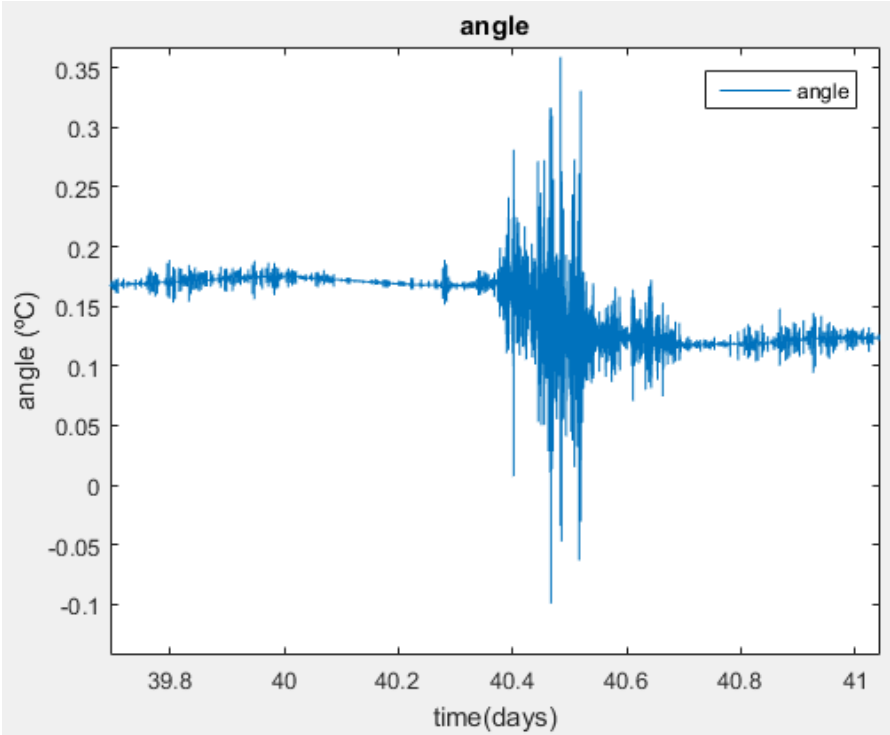


Figure 105: Voltage angle phase in microgrid node in Lithium-ion on January the 9th

Conclusions and future works

Conclusions

A two month simulation of two different batteries has been presented in this work. A case study of a residential grid which demands 56.29 MWh and it is supported by photovoltaic generation able to provide 47.68 MWh has been shown. When these two systems are working together it is possible to see that 37,60 MWh of total energy flows from the distribution grid into the residential grid and 28,99 MWh flows from the residential grid into the distribution grid as a reverse flow. Simulation has been produced the two months where PV generators produce less electrical energy, so it seems that PV generators are also well-scaled for the requirements of the microgrid.

It is possible to see that the two batteries can contribute to reduce power consumption that crosses common couple point. Power capacity of both of them has been chosen for a battery that is able to store only one full day power requirements because it is what it has been considered as a good trade-off between size and power support. Results of both batteries are presented below:

- i) Vanadium-redox battery case has a power flow of 18,72 MWh. from the distribution grid into the microgrid and a reverse flow of 2,57 MWh. It means that power required from the microgrid is less than the half that it would required if that battery would not exists. It is important to mention that this battery has some operative power requirements (power pumps) that could increase losses systems if they are not well scaled to the application requirements.
- ii) Lithium-ion battery case has 13,76 MWh. of power flow from the distribution grid into the microgrid and a reverse power flow of 5,09 MWh. It means a power reduction of 75%. That battery also has a better efficiency than vanadium one.

Future works

It has been a hard work of nearly a year to do this TFM so some of the difficulties found on it are presented blow. So if someone continues with a similar work could know which problems should they have to face on.

Vanadium-redox battery model: One of the main advantages of that type of battery is that it self-refrigerates by moving its electrolytes. It has no sense to put so much effort in energy balances as it has been done in that work and do not put any on pumps management that could contribute so much on efficiency and voltage variations of that battery than temperature by itself. It is a battery that seems difficult to model because it requires something more than an equivalent circuit.

Lithium-ion model: There are many different types of lithium-ion batteries and that battery has a main difference compared to Vanadium one. Power and capacity could not be decoupled, which means that the case of application should be known before choosing it to not over

dimensioned one of these battery characteristics. Hysteresis voltage curve could be interesting to include for adjusting some power losses this battery has.

Case study: A phasor diagram of the transformer has been included. It looks like it complicates the model while the only variable that is not despicable is transformer power losses that could be obtained with the nominal resistance of it.

Simulations: Case study simulations cover two months with one second time step. Some variables change in periods of seconds as it is the case of OCV and some variables take periods of minutes or hours; this is the case of SOC. It is important to know which of these variables are important. It is possible that time steps durations of minutes could be considered acceptable and easier to model.

Bibliography

- [1] T. Z. Q. Xu, "Fundamentals models for flow batteries," *Sciencedirect*, pp. 40-49, 2015.
- [2] B. R. M. D. M. L. Ali Jokar, "Review of simplified Pseudo-two-Dimensional models of lithium-ion," *Sciencedirect Journal of Power Sources 327*, pp. 44-55, 2016.
- [3] M. G. M. K. F. H. I. G. R. M. M. Mykhaylova, "An elementary 1-dimensional model for a solid state," *Sciencedirect Journal of the Mechanics and Physics of Solids* , pp. 1-15, 2018.
- [4] V. K. Ingemar Kaj, "Modeling battery cells under discharge using kinetic and," *Sciencedirect Applied Mathematical Modelling 40* , pp. 7901-7915, 2016.
- [5] J. F. M. Z. Z. Y. Tao Wang, "Dynamic control strategy for the electrolyte flow rate of vanadium redox," *Sciencedirect Applied Energy 227*, pp. 613-623, 2018.
- [6] M. Taragna, "http://www.ladispe.polito.it/corsi/MIC/material/LEFSI_I.pdf," [Online].
- [7] A. U. A. U. P. S. Alberto Berrueta, "A comprehensive model for lithium-ion batteries: From the physical," *Sciencedirect Energy 124*, pp. 286-300, 2018.
- [8] Y. Y. A. T. L.H. Saw, "Electro-thermal characterization of Lithium Iron Phosphate cell," *Sciencedirect Energy conversion and management*, pp. 367-377, 2014.
- [9] R. X. ,. T. M. L. S. M. M. S.-K. Zhongbao Wei, "Online monitoring of state of charge and capacity loss for vanadium redox," *Sciencedirect Journal of Power Sources 402*, pp. 252-262, 2018.
- [10] L. W. L. W. C. L. Wenjie Zhang, "An improved adaptive estimator for state-of-charge estimation of lithiumion batteries," *Sciencedirect Journal of Power Sources*, pp. 422-433, 2018.
- [11] M. M. M. J. P. M. P. N. R. J. T. G. Q. L. Adam Z. Weber, "Redox flow batteries: a review," 2011.
- [12] S. T. J. B. M. S.-K. Ao Tang, "Thermal modeling and simulation of the all-vanadium redox flow battery.," *Sciencedirect*, pp. 165-176, 2011.
- [13] M. I. J. Z. M. Y. S. Z. W. Binyu Xiong, "State of Charge Estimation of Vanadium Redox Flow," *IEEE TRANSACTIONS ON SUSTAINABLE ENERGY, VOL. 8, NO. 4*, pp. 1658-1667, 2017.
- [14] J. B. M. S.-K. Ao Tang, "Studies on pressure losses and flow rate optimization in vanadium," *Sciencedirect Journal of Power Sources 248*, pp. 154-162, 2014.
- [15] J. M. M. Skyllas-Kazacos, "Vanadium redox flow batteries for medium- and large scale energy storage," in *Advances in Batteries for Medium and Large-Scale Energy Storage*, University of

New South Wales (Australia), Woodhead Publishing Series in Energy, 2015, pp. 329-386.

- [16] D. G. D. N. P. V. P. Rachel Carnegie, "Utility Scale Energy Storage Systems," State Utility Forecasting Group , United States, 2013.
- [17] R. D.-L. M. C. G. P. Ghassan Zubia, "The lithium-ion battery: State of the art and future perspectives," *Sciencedirect Renewable and Sstainable Energy Review* 89, pp. 292-308, 2018.
- [18] R. G. D. W. A. B. J. M. Elham Hosseinzadeh, "A systematic approach for electrochemical-thermal modelling of a large," *Sciencedirect Journal of power sources* 382, pp. 77-94, 2018.
- [19] K. S. Hariharan, "A coupled nonlinear equivalent circuit e Thermal model for lithium ion cells," *Sciencedirect Journal of Power Sources*, pp. 171-176, 2013.
- [20] M. N. N. T. H. C. H. S. S. A. S. A. J. Michael Schimpea, "Energy efficiency evaluation of a stationary lithium-ion battery container," *ciencedirect Applied Energy* 210, pp. 211-229, 2018.
- [21] [Online]. Available:
http://ocw.uniovi.es/pluginfile.php/5422/mod_resource/content/1/Cat%C3%A1logo%20transformadores%20ABB.pdf.
- [22] J. B. P. S. L. M. Julio Pascual, "Energy management strategy for a renewable-based residential," vol. *Applied Energy*, no. 158, 2015.
- [23] Y. Z. F. G. K. Y. Q. J. Chuang Qi, "Mathematical model for thermal behavior of lithium ion battery pack under overcharge.," *Sciencedirect International Journal of Heat and Mass Transfer* 124, pp. 552-563, 2018.
- [24] J. Z. Y. S. Z. W. Binyu Xiong, "State of Charge Estimation of Vanadium Redox Flow," *IEEE TRANSACTIONS ON SUSTAINABLE ENERGY, VOL. 8, NO. 4*, pp. 1658-1667, 2017.

++++